

2011

Biochemical and genetic insights into asukamycin biosynthesis

Zhe Rui

Louisiana State University and Agricultural and Mechanical College, zrui2@tigers.lsu.edu

Follow this and additional works at: https://digitalcommons.lsu.edu/gradschool_dissertations

Recommended Citation

Rui, Zhe, "Biochemical and genetic insights into asukamycin biosynthesis" (2011). *LSU Doctoral Dissertations*. 2028.
https://digitalcommons.lsu.edu/gradschool_dissertations/2028

This Dissertation is brought to you for free and open access by the Graduate School at LSU Digital Commons. It has been accepted for inclusion in LSU Doctoral Dissertations by an authorized graduate school editor of LSU Digital Commons. For more information, please contact gradetd@lsu.edu.

BIOCHEMICAL AND GENETIC INSIGHTS INTO ASUKAMYCIN BIOSYNTHESIS

A Dissertation

Submitted to the Graduate Faculty of the
Louisiana State University and
Agricultural and Mechanical College
in partial fulfillment of the
requirements for the degree of
Doctor of Philosophy

in

The Department of Biological Sciences

by
Zhe Rui
B.S., Zhejiang University, P. R. China, 2006
May 2011

ACKNOWLEDGEMENTS

First and foremost, I would like to express my sincere gratitude to my former major advisor Dr. Tin-Wein Yu, for his constant support and steadfast patience throughout my entire PhD study. His enthusiasm and meticulousness towards science have not only set a great example, but also guided me to become a devout believer in natural product engineering. My most enjoyable time in this research is the discussion session with him, where I have learned tremendously about logical thinking and scientific research development. In addition to a great mentor, he has been a true friend always available and ready to help.

I am very fortunate to have Dr. Marcia Newcomer as my current major advisor. She has provided exceptional support, both mentally and financially, for me to accomplish these projects in the past year. I am grateful to her precious protein chemistry class, where I established a strong background for my biosynthetic research from the enzymology aspect.

I am grateful to my committee members, Dr. Sue Bartlett, Dr. Huangen Ding, Dr. Fareed Aboul-ela, and Dr. Thomas Gillis for their patient instruction, kind help, and constructive advices.

I would like to thank my lab members, Jeffery West, Mozzy Saboori, Hassan Hashem, Kaori Fujikawa, Waleed Elsegeiny, and Mike Dicharry for their support and useful discussions.

This dissertation was supported by NIH Research Grant CA76461 and Louisiana State Economic Development Assistantship.

I am deeply thankful to my parents and uncle Guojun for being continuously and unconditionally supportive of my career, for their care and attention. I am also indebted to my girlfriend Weishi Kong. It is her love, devotion and encouragement that have made this achievement possible and meaningful.

TABLE OF CONTENTS

ACKNOWLEDGEMENTS	ii
LIST OF TABLES	iv
LIST OF FIGURES	iv
ABSTRACT.....	vii
CHAPTER ONE: GENERAL INTRODUCTION	1
CHAPTER TWO: IDENTIFICATION AND CHARACTERIZATION OF THE ASUKAMYCIN BIOSYNTHETIC GENE CLUSTER	21
CHAPTER THREE: FORMATION OF THE ASUKAMYCIN LOWER CHAIN.....	32
CHAPTER FOUR: ASSEMBLY OF THE ASUKAMYCIN UPPER CHAIN	41
CHAPTER FIVE: ASUKAMYCIN C ₅ N MOIETY FORMATION	52
CHAPTER SIX: POST-ASSEMBLY OXYGENATION OF PROTOASUKAMYCIN.....	60
CHAPTER SEVEN: A TYPE TWO THIOESTERASE AND OTHER ASUKAMYCIN BIOSYNTHETIC GENES.....	68
CHAPTER EIGHT: SUMMARY AND FUTURE PROSPECT	77
CHAPTER NINE: MATERIALS AND METHODS.....	88
REFERENCES	102
APPENDIX: PERMISSIONS.....	117
VITA.....	118

LIST OF TABLES

Table 1.1 Structures of manumycin family metabolites.	4
Table 2.1 Deduced functions of ORFs in the asukamycin biosynthetic gene cluster.....	25
Table 4.1 Summary of observed ^1H -NMR and ^{13}C -NMR of B8	45
Table 6.1 NMR connectivities in 4-hydroxyprotoasukamycin (D1).	64
Table 7.1 Fatty acid composition of <i>S. nodosus</i> wild type strain and the <i>asuC15</i> mutant..	73
Table 9.1 Exact mass of asukamycin and its derivatives.....	91
Table 9.2 Oligonucleotide primers used for the mutant constructions and Lambda-Red recombinations.	94

LIST OF FIGURES

Figure 1.1 Molecular structure of manumycin A, asukamycin, and congeners	3
Figure 1.2 Classification of manumycins... ..	7
Figure 1.3 3,4-AHBA derived natural products.....	12
Figure 1.4 Biosynthetic origin of asukamycin.....	12
Figure 1.5 CHC-CoA derived natural products.. ..	14
Figure 1.6 Examples of natural products containing C ₅ N moiety	16
Figure 1.7 C ₅ and Shemin pathways for the 5-ALA formation	17
Figure 1.8 Previously proposed dioxygenase mechanism for asukamycin biosynthesis based on the formation of Vitamin K oxide and LL-C10037 α	19
Figure 2.1 Open reading frames identified in the asu cluster.. ..	24
Figure 2.2 Assembly of two cosmids with overlapping inserts	27
Figure 2.3 HPLC analysis of the <i>S. nodosus</i> WT and the <i>S. lividans</i> K4-114 transformants.....	28
Figure 2.4 Construction of pART1391	29
Figure 3.1 HPLC analysis of the <i>asuA1</i> and <i>asuA3</i> mutants	34
Figure 3.2 Proposed structures of E1 and E3/E4	35
Figure 3.3 HPLC detection of 3,4-AHBA in the <i>asuA2</i> , <i>asuC11C12</i> , and <i>asuC13</i> mutants.....	36
Figure 3.4 HPLC analysis of the <i>asuA2</i> , <i>asuC11C12</i> , and <i>asuC13</i> mutants	37
Figure 3.5 Proposed biosynthetic pathway of asukamycin lower chain.....	40
Figure 4.1 HPLC analysis of the <i>asuB1</i> , <i>asuC3C4</i> mutants, and the <i>S. nodosus</i> wild type strain.....	43
Figure 4.2 HPLC detection of A8 , B8 , and C8 in the <i>asuB1</i> and <i>asuC2</i> mutants.....	44
Figure 4.3 Molecular structures of A8 , B8 , and C8	44
Figure 4.4 Proposed biosynthesis pathway of CHC-CoA in <i>S. nodosus</i> subsp. <i>asukaensis</i>	48

Figure 4.5 Comparison of biosynthetic pathways of asukamycin upper chain, R1128A, and fatty acids.	49
Figure 4.6 Proposed upper chain assemblies of the asukamycin congeners (A2-A7).....	51
Figure 5.1 Sequence alignment of AsuD2 with other 2-oxoamine synthases... ..	54
Figure 5.2 TLC analysis and bioassay of the AsuD1-D3 enzymes	55
Figure 5.3 HPLC analysis of the <i>asuD1</i> , <i>asuD2</i> , and <i>asuD3</i> mutants.	57
Figure 5.4 The proposed C ₅ N moiety biosynthetic pathway and the coexisting C ₅ pathway..	59
Figure 6.1 Reactions catalyzed by PHBD, PheA1/A2, and LimB.....	61
Figure 6.2 HPLC analysis of the <i>asuE1-E3</i> mutants	63
Figure 6.3 Structures of C1-C5 and D1-D5	65
Figure 6.4 A comparison of two-step monooxygenase and one-step dioxygenase mechanisms for the respective asukamycin and vitamin K oxide biosynthesis..	66
Figure 6.5 The proposed function of MmyO in methylenomycin A biosynthesis	67
Figure 7.1 Proposed functions of type II thioesterases (TEII).....	70
Figure 7.2 HPLC analysis of the <i>asuC15</i> mutant and the <i>S. nodosus</i> wild type strain.....	71
Figure 7.3 Fatty acid profiles generated by GC-MS analysis.....	72
Figure 7.4 The proposed function of AsuC6	76
Figure 8.1 Proposed asukamycin biosynthetic pathway	79
Figure 8.2 Structures of manumycin metabolites from <i>S. nodosus asukaensis</i> , <i>S. parvulus</i> T ü64, and <i>S. griseoflavus</i> T ü2880..	84
Figure 8.3 Confirmed or postulated asukamycin analogs obtained by feeding the <i>asuA3</i> or <i>asuA1</i> mutants with diverse aromatic precursor	87
Figure 9.1 Southern blots of thirteen constructed mutants.	95

ABSTRACT

Asukamycin, a member of the manumycin family metabolites, is an antimicrobial and potential antitumor agent isolated from *Streptomyces nodosus* subsp. *asukaensis*. The entire asukamycin biosynthetic gene cluster was cloned, assembled and expressed heterologously in *Streptomyces lividans*. Bioinformatic analysis and mutagenesis studies elucidated the biosynthetic pathway at the genetic and biochemical level. Four gene sets, *asuA-D*, govern the formation and assembly of the asukamycin building blocks, a 3-amino-4-hydroxybenzoic acid (3,4-AHBA) core component, a cyclohexane ring, two triene polyketide chains and a 2-amino-3-hydroxycyclopent-2-enone (C₅N) moiety to form the intermediate protoasukamycin. AsuE1 and AsuE2 catalyze the conversion of protoasukamycin to 4-hydroxyprotoasukamycin, which is epoxidized at C5-C6 by AsuE3 to the final product, asukamycin. Branched acyl CoA starter units, derived from Val, Leu and Ile, can be incorporated by the actions of the polyketide synthase KSIII AsuC3/C4 as well as the cellular fatty acid synthase FabH to produce the asukamycin congeners A2-A7. In addition, the type II thioesterase AsuC15 limits the cellular level of ω -cyclohexyl fatty acids and likely maintains homeostasis of the cellular membrane.

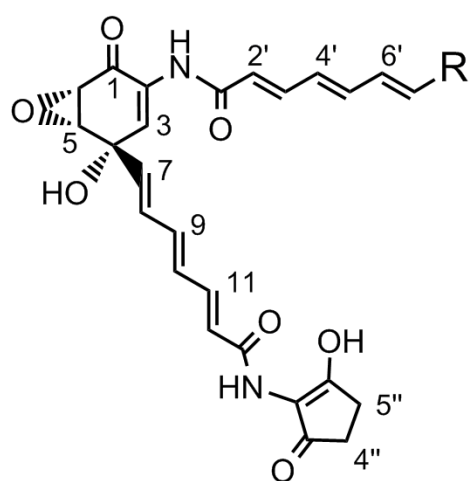
CHAPTER ONE:
GENERAL INTRODUCTION

Discovery of Manumycin Metabolites

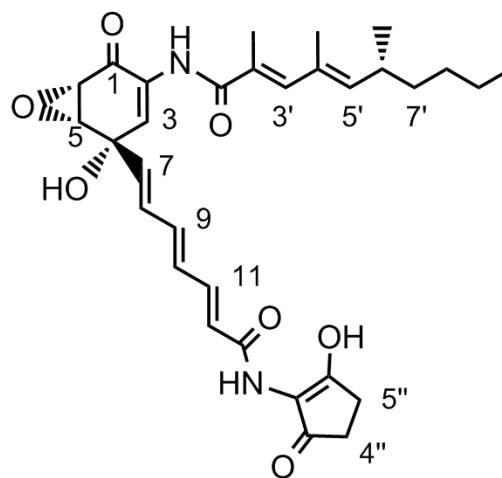
The manumycin family of metabolites contains 34 members, and continues to expand due to the ongoing discovery of novel natural products. The first member, manumycin A, was isolated from *Streptomyces parvulus* T ü 64 in 1963 [1]. Revealed by Zeeck group, the chemical structure of manumycin A features two polyketide chains (Fig. 1.1) [2]. The “lower” *trans* triene chain starts with a 2-amino-4-hydroxy-5,6-epoxycyclohex-2-enone (mC₇N) core and terminates into a five-membered ring, 2-amino-3-hydroxycyclopent-2-enone (C₅N) moiety; the “upper” one consists of methyl branched polyketide, amide-linked to the mC₇N core. The stereochemistry of this compound was first presented by Thiericke group [3, 4], and later revised by Taylor and co-workers [5].

Asukamycin (**A1**) was discovered in the fermentation culture of *Streptomyces nodosus* subsp. *asukaensis* by Omura et al. in 1976 (Fig. 1.1) [6]. Elucidated by Omura and Floss groups, asukamycin shares the entire lower chain with manumycin A, while it differs at the upper one, a *trans* triene polyketide initiated with a characteristic cyclohexane moiety [7, 8]. Soon after the discovery of asukamycin, twenty-one novel manumycin compounds including the type II form of colabomycin D and manumycin D were subsequently identified during 1980s and 1990s (Table 1). These type II manumycins contain a hydroxyethylene group to replace the epoxy moiety at the C5-C6 position of the mC₇N core. Scrutinizing the metabolic profile of *S. nodosus*, Floss and colleagues have identified six more asukamycin congeners, manumycin G (**A2**), El-1511-5 (**A3**), U-56,407 (**A4**), manumycin E (**A5**), asukamycin F (**A6**), asukamycin G (**A7**), plus five type II asukamycins, **B1-B5** (Fig. 1.1) [6, 9, 10]. In the same study, a series of unnatural asukamycin analogs, containing various cyclic ring structures to substitute the cyclohexane moiety were

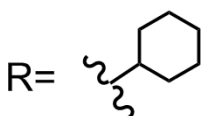
obtained through the feeding experiments with the variable ring-sized alicyclic carboxylates in *S. nodosus* (Table 1).



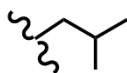
Asukamycin and congeners



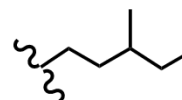
Manumycin A



A1



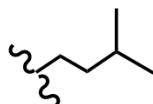
A4



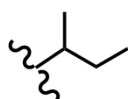
A7



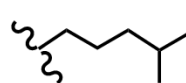
A2



A5



A3



A6

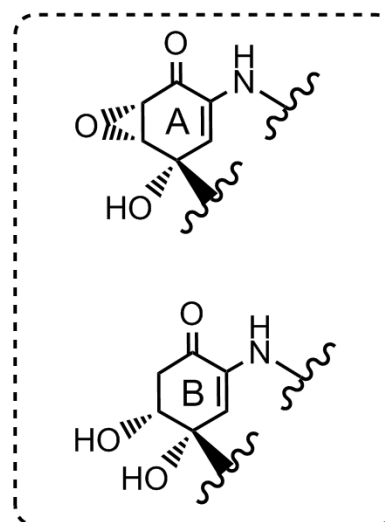


Figure 1.1 Molecular structure of manumycin A, asukamycin, and congeners. Type I and II metabolites are grouped according to the main core units of A and B, respectively.

Table 1.1 Structures of manumycin family metabolites.

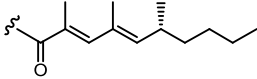
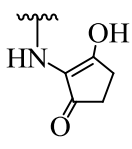
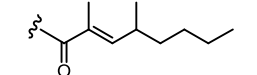
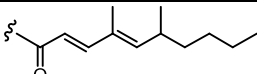
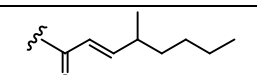
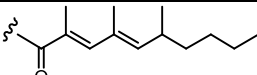
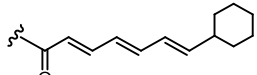
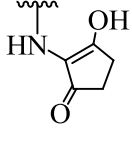
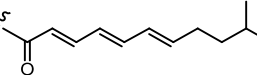
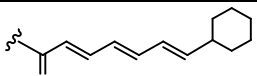
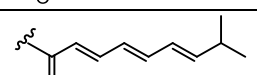
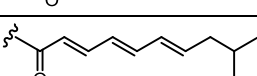
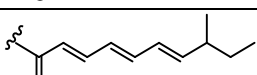
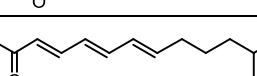
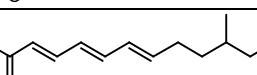
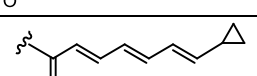
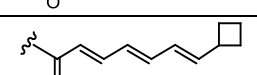
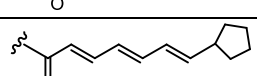
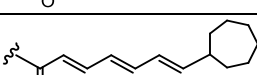
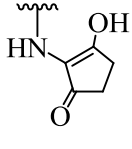
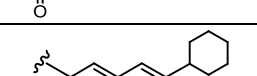
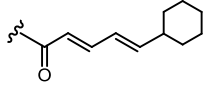
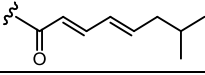
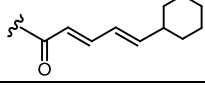
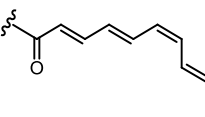
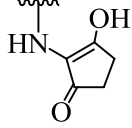
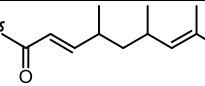
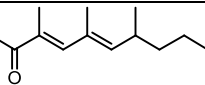
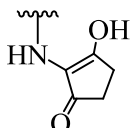
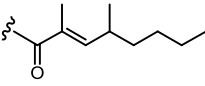
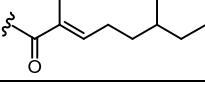
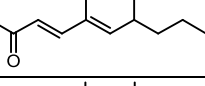
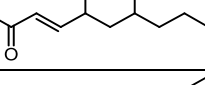
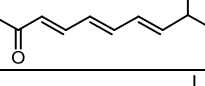
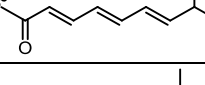
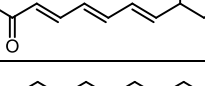
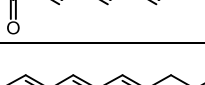
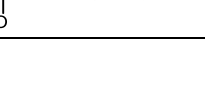
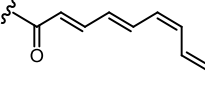
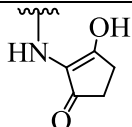
Compounds	Stereochemistry	R ₁	R ₂	References
Type Ia				
Manumycin A	4 <i>S</i> , 5 <i>R</i> , 6 <i>S</i> *			[2-4, 11, 12]
Manumycin B	4 <i>S</i> , 5 <i>R</i> , 6 <i>S</i> *			[11-14]
Manumycin C	4 <i>S</i> , 5 <i>R</i> , 6 <i>S</i>			[11-14]
EI-1625-2	4 <i>S</i> , 5 <i>R</i> , 6 <i>S</i> *			[14-17]
Compound	not determined		-OH	[18]
Asukamycin (A1)	4 <i>S</i> , 5 <i>R</i> , 6 <i>S</i>			[6-8, 10, 19-21]
Manumycin E (A5)	4 <i>S</i> , 5 and 6 not determined			[10, 22, 23]
Manumycin F	4 <i>S</i> , 5 and 6 not determined			[22, 23]
Manumycin G (A2)	4 <i>S</i> , 5 and 6 not determined			[10, 17, 22, 23]
U-56, 407 (A4)	4 <i>S</i> , 5 <i>R</i> , 6 <i>S</i>			[10, 24, 25]
EI-1511-5 (A3)	4 <i>S</i> , 5 <i>R</i> , 6 <i>S</i>			[10, 14-17]
Asukamycin F (A6)	Possibly 4 <i>S</i> , 5 <i>R</i> , 6 <i>S</i>			[10]
Asukamycin G (A7)	Possibly 4 <i>S</i> , 5 <i>R</i> , 6 <i>S</i>			[10]
Cyclopropyl-asukamycin	Possibly 4 <i>S</i> , 5 <i>R</i> , 6 <i>S</i>			[10]
Cyclobutyl-asukamycin	Possibly 4 <i>S</i> , 5 <i>R</i> , 6 <i>S</i>			[10]
Cyclopentyl-asukamycin	Possibly 4 <i>S</i> , 5 <i>R</i> , 6 <i>S</i>			[10]
Cycloheptyl-asukamycin	Possibly 4 <i>S</i> , 5 <i>R</i> , 6 <i>S</i>			[10]
Alisamycin	4 <i>R</i> , 5 <i>S</i> , 6 <i>R</i>			[26-29]

table continued

<i>Ent</i> -alisamycin	4 <i>S</i> , 5 <i>R</i> , 6 <i>S</i>			[14-17]
EI-1511-3	4 <i>S</i> , 5 <i>R</i> , 6 <i>S</i>			[14-17]
Nisamycin	4 <i>R</i> , 5 <i>S</i> , 6 <i>R</i>		-OH	[30-33]
Type Ib				
Colabomycin A	4 <i>S</i> , 5 <i>R</i> , 6 <i>S</i>			[34-36]
Type Ic				
U-62, 162	not determined		-OH	[37]
Type IIa				
Manumycin D	4 <i>S</i> , 5 <i>R</i>			[11, 13]
TMC-1A	4 <i>S</i> , 5 <i>R</i>			[11]
TMC-1B	4 <i>S</i> , 5 <i>R</i>			[11]
TMC-1C	4 <i>S</i> , 5 <i>R</i>			[11]
TMC-1D	4 <i>S</i> , 5 <i>R</i>			[11]
Asukamycin A-II (B1)	Possibly 4 <i>S</i> , 5 <i>R</i>			[9]
Asukamycin B-II (B2)	Possibly 4 <i>S</i> , 5 <i>R</i>			[9]
Asukamycin C-II (B3)	Possibly 4 <i>S</i> , 5 <i>R</i>			[9]
Asukamycin D-II (B4)	Possibly 4 <i>S</i> , 5 <i>R</i>			[9]
Asukamycin E-II (B5)	Possibly 4 <i>S</i> , 5 <i>R</i>		[9]	
Type IIb				
Colabomycin D	4 <i>S</i> , 5 <i>R</i>			[36]

Structure and Classification

Manumycin metabolites were categorized into two classes based on the structure of the mC₇N core moiety (Fig. 1.2). While the type I manumycins contain an oxirane at the C5-C6 position, a ring-opened hydroxyethylene was adopted by the type II compounds, which are likely originated from their type I counterparts through an enzymatic /or non-enzymatic path (Fig. 1.2). For example, the crude extract of asukamycin (**A1**) can be gradually reduced to the asukamycin A-II (**B1**) under room temperature. To the type I form of manumycins, the mC₇N core mostly displays a 4*S*, 5*R*, 6*S* stereochemistry except for nisamycin and alisamycin, exhibiting a 4*R*, 5*S*, 6*R* configuration. Notably, the mC₇N configuration was incorrectly assigned as a 4*R*, 5*R*, 6*S* for manumycin A, manumycin B and EI-1625-2 in an early study. As manumycin A revealed an opposite pattern of the optical rotation and CD spectrum compared with that of the synthesized *ent*-(+)- manumycin A, the chirality of manumycin A has been revised to 4*S*, 5*R*, 6*S*. In this study, we have identified two new classes besides type I and II manumycins, the proto-type (**C1-C5**) and the 4-hydroxyproto-type (**D1-D5**), featuring with an aromatic and a hydroxyquinol cores, respectively (see chapter 6).

Based on the chain length and the degree of saturation of the lower polyketide chain, the type I manumycins are further divided into three subgroups. Type Ia, Ib, and Ic feature the corresponding *trans* triene, tetraene, and saturated polyketides. The majority of manumycin compounds belong to the type Ia subfamily, while colabomycin A and U-62,162 are the only reported type Ib and Ic manumycins, respectively. Correspondingly, a majority of the type II manumycins belong to the type IIa subgroup with one exception of the unique IIb member, colabomycin D. Besides, most manumycins contain a lower polyketide chain amide-linked with

a C₅N moiety except for nisamycin and U-62,162, carrying a free carboxylic group without the C₅N moiety attached.

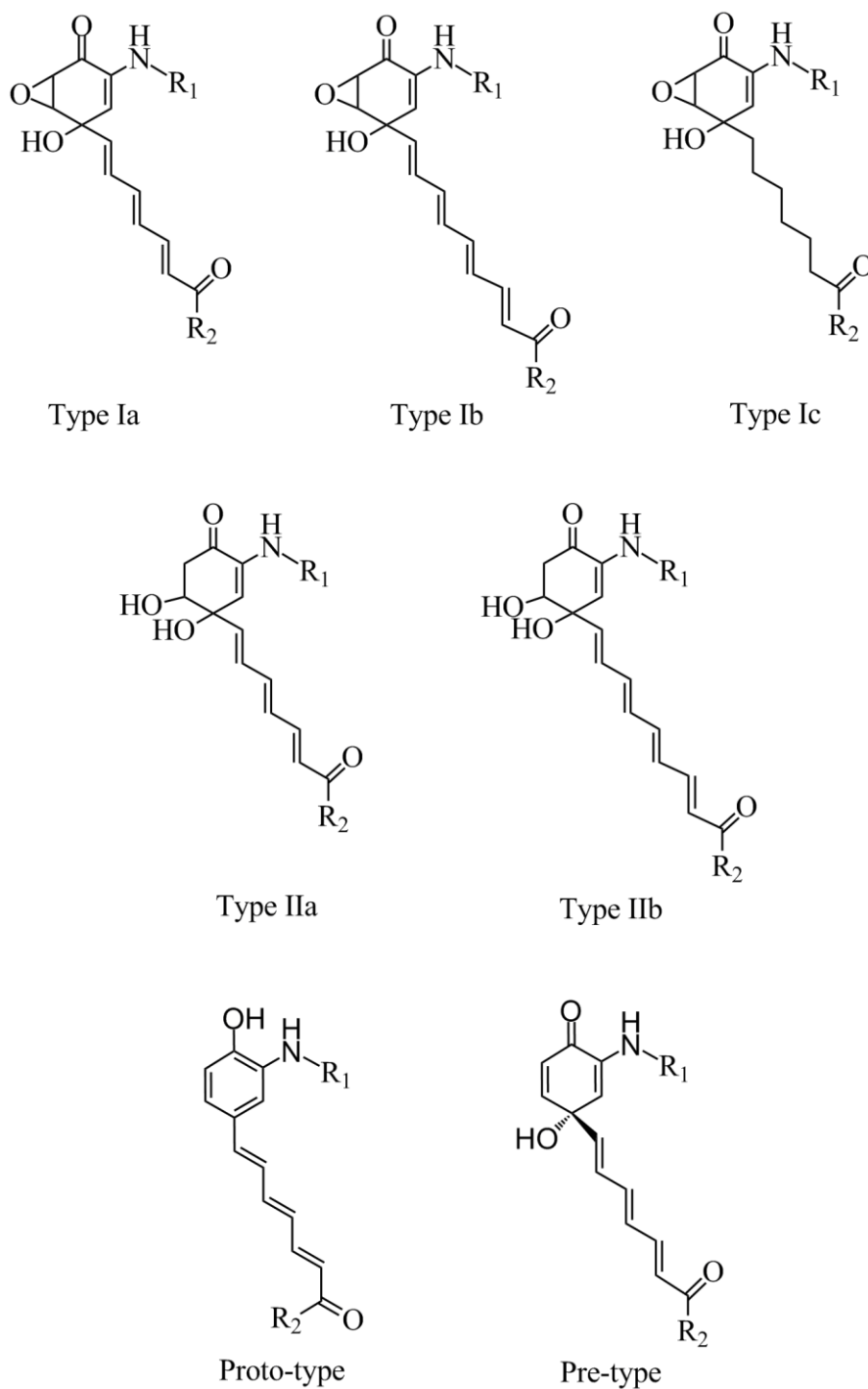


Figure 1.2 Classification of manumycins. The proto-type and the pre-type compounds are discussed in chapter 6.

Biological Activity

Antimicrobial Activity

Manumycin metabolites have been identified mostly through the antibiotic screening based on their broad antimicrobial actions including the antibacterial (Gram-positive), anticoccidial, and antifungal activities [38]. Manumycin A also exhibits the insecticidal activity [39]. Although the detailed mechanism has yet been fully understood, the epoxyquinol moiety of the mC₇N core likely plays an essential role for these antimicrobial activity, as the type II manumycins, TMC-1A-D and manumycin D, failed to show the effectiveness against the Gram-positive or Gram-negative bacteria [11]. Interestingly, nisamycin, lacking a C₅N moiety, displayed 6-fold higher antibacterial potency than its C₅N-containing analog, alisamycin. This observation indicated that the presence of the C₅N moiety might not be critical in view of the biological activity [33]. Furthermore, the derivatives of nisamycin with an amide-linkage to an alkane, a cycloalkane, or an arene also reduced its antimicrobial activity.

Anticancer Activity

Manumycin compounds are known for the anticancer function against various tumors *in vitro* and *in vivo* [38]. Manumycin A has been proved to inhibit the progression of the human fibrosarcoma HT1080 tumor cells in the transplanted mice [40]. Two other studies showed that the human pancreatic cancer was significantly suppressed *in vivo* by the manumycin A treatment without having apparent hepatotoxicity [41, 42]. In addition, manumycin A also displayed the antiangiogenesis ability in mice transplanted with the hypoxic Anaplastic thyroid cancer (ATC) cells, likely by limiting the vascular endothelial growth factor [43, 44]. A triple drug “cocktail”, manumycin A, combretastatin A4 phosphate (CA4P), and paclitaxel developed by Yeung and

co-workers, assured a great promise in the treatment of several ATC cell lines without showing a significant toxicity in mice [43, 45, 46].

Despite the elusive mechanism behind these anticancer activities, some manumycin metabolites seem to elicit the cell death through the inhibition of the RAS farnesyltransferase (FTase). RAS FTase catalyzes the linkage between a farnesyl pyrophosphate and the C-terminal Cys residue of RAS, an essential modification step to anchor the RAS to the cellular membrane for its function. As a binary enzyme switching between the active and inactive form, RAS protein is a key player to regulate the cell growth and malignant transformation. The mutation of *ras* oncogene frequently results in its consistent activation, which is associated with 30% to 50% of lung and colon carcinomas and up to 90% of human pancreatic cancers. Thus, one chemotherapeutic treatment for these cancers is to suppress the RAS activity by inhibiting the RAS FTase [47]. For example, manumycin A has been shown to slow down the growth of human hepatoma cell line via inhibiting the Ras activity [48]. Moreover, manumycin A, B, and C specifically inhibit the FTase activity but not the closely-related geranylgeranyltransferase (GGTase), which allows the normal cell to survive by bypassing the FTase deficiency through GGTase [40, 49]. Due to a high potency against the tumor cells but a low cytotoxicity towards the normal cells, these compounds hold great promise in the chemotherapeutic application.

Besides the inhibition of RAS FTase, manumycin A can trigger the cell death through some FTase-independent pathways. One study showed that manumycin A caused the death of the breast cell lines and thyroid cells by induction of the reactive oxygen species (ROS), such as nitric oxide ($\text{NO}\bullet$) and superoxide anion ($\bullet\text{O}_2^-$), triggering the downstream caspase-independent dsDNA breakages [50]. Another report claimed that manumycin A stimulated apoptosis of lymphoid tumor and myeloma cell lines due to the caspase-dependent ROS induction [51]. Most recently, the manumycin family compounds have been confirmed to suppress the oncogenesis by

inhibiting the I κ B kinase β (IKK β) activity, possibly through a covalent dimerization of IKK β [52]. These findings provided more information on how the cancer cells were killed by the manumycin compounds.

Inhibition of Interleukin-1 β Converting Enzymes

Interleukin-1 β converting enzymes cleave the inflammatory cytokines, interleukin-1 β and interleukin 18, to generate the active form of peptides to trigger the inflammatory cascade. Manumycin metabolites, EI-1511-3, -5, EI-1625-2, manumycin A, B, G, U-56,407, and *ent*-alisamycin, reveal not only the inhibitory activity against interleukin-1 β converting enzymes, but also suppress the secretion of interleukin-1 β [16, 53]. Notably, the inhibition of the interleukin-1 β secretion but not for the interleukin-1 β converting enzymes is no longer sustained, once the lower polyketide and a C₅N moiety of these manumycin compounds were removed.

Inhibition of Acetylcholinesterase

Recently, manumycin A, B and C were found to serve as a specific acetylcholinesterase (AChE) inhibitor, which might lead to potential drug development for Alzheimer's disease treatment [54]. Found in the neuromuscular junctions and cholinergic synapses of the central nervous system, AChE catalyzes the degradation of the neurotransmitter, acetylcholine (ACh), to give choline and acetate to terminate the synaptic transmission. Thus, the AChE inhibitor can boost the cholinergic synapse activity via the increasing ACh availability. Manumycin A, B and C could inhibit the AChE comparable to the commercial available Tacrine (Cognex®, 1993) but with much better specificity, as these three compounds did not exhibit any inhibitory activity on butyrylcholinesterase (BuChE), which causes Tacrine's major hepatotoxic side effects during therapeutic treatment. The epoxide of the mC₇N core likely plays an essential role, as manumycin D, the type II form of manumycin A, failed to inhibit the AChE activity.

Biosynthetic Study

The biosynthetic study of manumycin compounds has been focusing on manumycin A and asukamycin. These two compounds may reflect the biosynthesis of other family member, as a majority of the manumycin metabolites share an identical lower triene polyketide, primed with an mC₇N core and ended up with a C₅N ring. A rational biosynthetic route has been proposed in according to a series of chemical feedings, while little biochemical or genetic data was available before this study except for the cloned 5-aminolevulinic acid synthase (ALAS) gene published by Petricek group [21].

mC₇N Core

The mC₇N core moiety of manumycin metabolites arises from 3-amino-4-hydroxybenzoic acid (3,4-AHBA) instead of 3-amino-5-hydroxybenzoic acid (3,5-AHBA), the common building block for ansatrienin A, rifamycin B and mitomycin C [55]. Feeding labeled 3,4-AHBA, Zeeck group has first isolated the 64-3,4-AHBA₂, a proto-type of manumycin A in the culture of *S. parvulus* T ü 64 [56, 57]. Gould and co-workers proposed that 3,4-AHBA is the real precursor of manumycin compounds [58], and Floss group further confirmed this speculation through a successful feeding of 3,4-AHBA to asukamycin and manumycin A [19]. In addition to manumycins, 3,4-AHBA is also a biosynthetic precursor for 4-hydroxy-3-nitrosobenzamide and grixazone found in *Streptomyces murayamaensis* and *Streptomyces griseus*, respectively (Fig. 1.3) [58, 59].

Polyketide Chains and the Cyclohexane Moiety

Feeding experiments with either [1-¹³C]-acetate or [2-¹³C]-acetate indicated that the lower and upper trienes were built up using three malonyl CoA extenders through the polyketide condensations (Figure 1.4) [60]. The polyketide-derived biosynthesis was also supported by the

effusive incorporation of $[1-^{13}\text{C}, ^{18}\text{O}]$ -acetate at C-13 and C-1' position in asukamycin. Despite these, it is unclear whether a multi-domain type I or an iterative type II polyketide synthases (PKS) with discrete functional units is involved in the chain assembly.

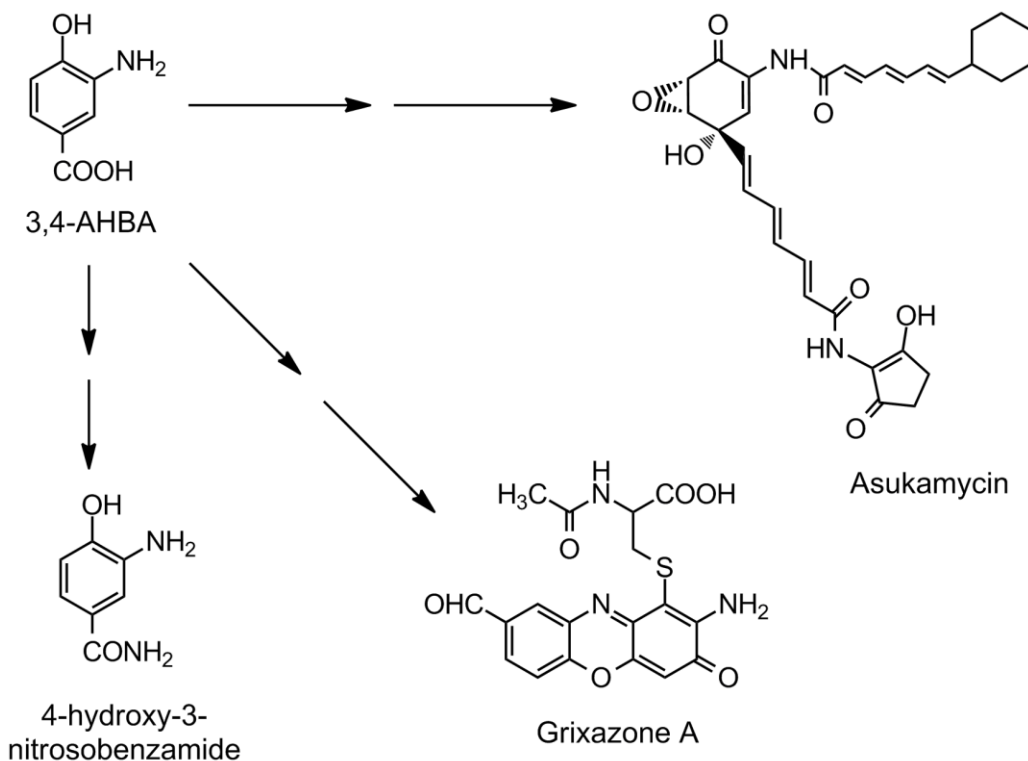


Figure 1.3 3,4-AHBA derived natural products. 3,4-AHBA is the common precursor of manumycins, grixazones, and 4-hydroxy-3-nitrosobenzamide.

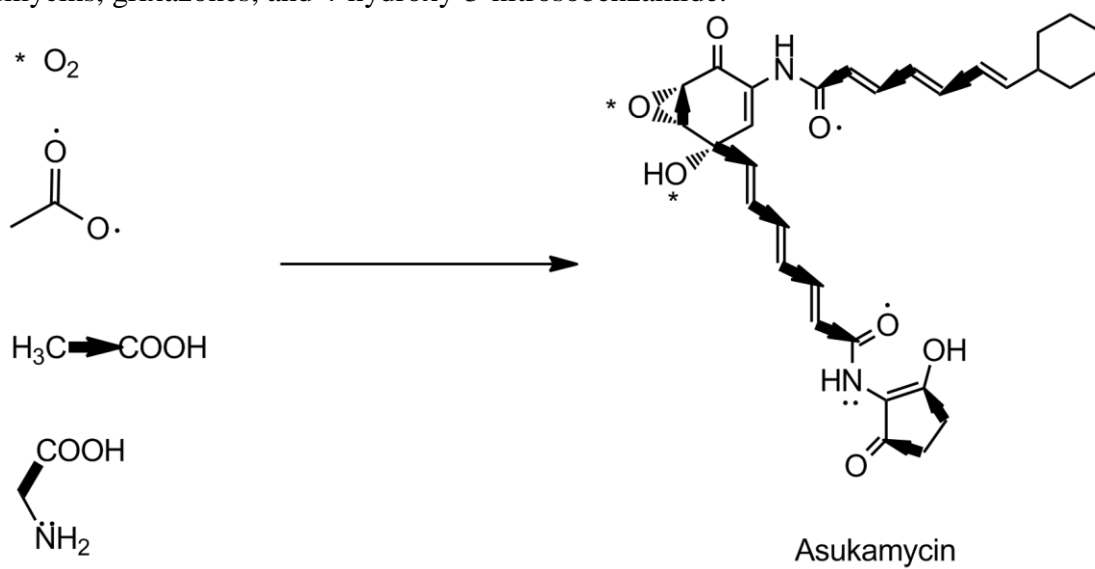


Figure 1.4 Biosynthetic origin of asukamycin.

Feeding pattern of labeled glycerol demonstrated that the origin of the cyclohexane moiety, CHC-CoA, is derived from shikimic acid [60]. In fact, this cyclohexane moiety has been widely found in other natural products, such as ansatrienin [61], doramectin [62], phoslactomycin [63], all of which were proved to arise from the shikimate pathway via the chemical feeding and genetic studies (Fig. 1.5). A gene set, *ansJKLM/chcA*, involved in the CHC-CoA biosynthesis of ansatrienin has been well characterized in *Streptomyces collinus* [62]. Additionally, Floss and co-workers has managed to generate a series of novel manumycin compounds, such as cyclopropyl-, cyclobutyl-, cyclopentyl- and cycloheptyl-asukamycin by feeding with various ring sizes of carboxylates to *S. nodosus* (Table 1.1).

Alternatively, the CHC-CoA can also be recruited to form ω -cyclohexyl fatty acids as a part of cellular membrane components in *S. nodosus* subsp. *asukaensis* (Fig. 1.5) [10]. Notably, the incorporation of CHC-CoA to give cyclohexyl fatty acids also occurs in other microorganisms, including the *Alicyclobacillus acidocaldarius* and the ansatrienin producer *S. collinus* [62, 64]. As the membrane fluidity and permeability are strongly determined by the fatty acid composition, the biosynthetic regulation of each fatty acid component is crucial for membrane homeostasis in bacteria [65, 66]. The content of ω -cyclohexyl fatty acids, a byproduct generated during the peak period of asukamycin biosynthesis, is maintained to be as low as 3% [10]. This implies that the organism has a control mechanism to balance the metabolic flux between the production of membrane fatty acids and asukamycin.

The C₅N Moiety

The lower polyketide chain of asukamycin terminates with a 2-amino-3-hydroxycyclopent-2-enone (C₅N) moiety, an enol tautomer of the 2-aminocyclopentanediol. This nitrogen-containing five membered cyclic ring also serves as a structural component in many other natural products, such as reductionimycin, moenomycin A, virustomycin A,

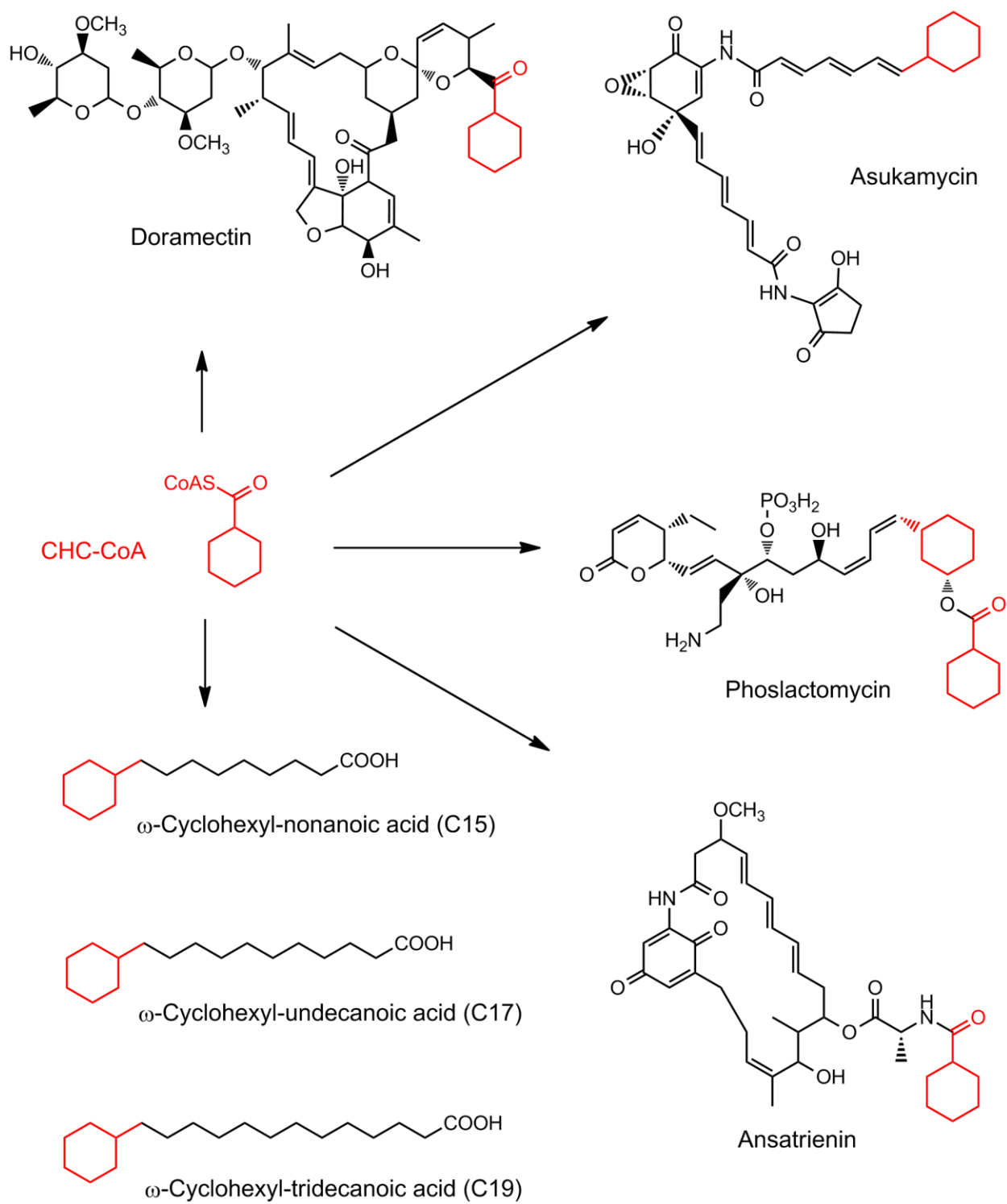


Figure 1.5 CHC-CoA derived natural products.

bafilomycin B1, ECO-02301, ECO-0501, and the majority of manumycin metabolites (Fig. 1.6) [21, 67-72]. Feeding experiments illustrated that a glycine and a succinyl-CoA are the building blocks for this C₅N moiety (Fig. 1.4) [60, 73]. Moreover, the labeled 5-aminolevulinate (5-ALA) was found to be incorporated in a low efficiency to the reductionmycin biosynthesis of *Streptomyces xanthochromogenus*, implying that 5-ALA could be a close precursor of the cyclic C₅N structure.

5-ALA is an essential precursor for the assembly of tetrapyrrole, which is further converted to hemes, chlorophylls, billins and corrinoids in many organisms [74]. Two biosynthetic routes have been described to form this primary metabolite (Fig. 1.7). In plants and many bacteria, 5-ALA arises from a glutamate-tRNA through the C₅ pathway, which requires the consecutive actions of a glutamyl-tRNA^{Glu} reductase (Gtr) and a glutamate-1-semialdehyde 2,1-aminomutase [75]. To animals, fungi, and some other bacteria, the 5-ALA formation is governed by the Shemin pathway, where the 5-ALA synthase catalyzes the condensation between a glycine and a succinyl-CoA to give 5-ALA [75]. *S. nodosus* subsp. *asukaensis* employs the C₅ pathway to form 5-ALA, as the growth of the *gtr* mutant highly relies on the addition of 5-ALA to the culture [21].

Encoding a putative 5-ALA synthase to catalyze the condensation between a glycine and a succinyl-CoA, the cloned *hemA-asuA* (herein named as *asuD2*) is essential for the asukamycin biosynthesis, as the *asuD2* mutant failed to produce asukamycin in *S. nodosus* [21]. Interestingly, neither the accessible C₅ pathway can compensate the *asuD2* deficiency to continue the production of asukamycin; nor the AsuD2 is capable of providing a sufficient 5-ALA to sustain the survival of the *gtr* mutant (Fig. 1.7). These seemingly contradictory observations implied that AsuD2 might have an unknown or additional functional activity compared with other characterized 5-ALA synthases.

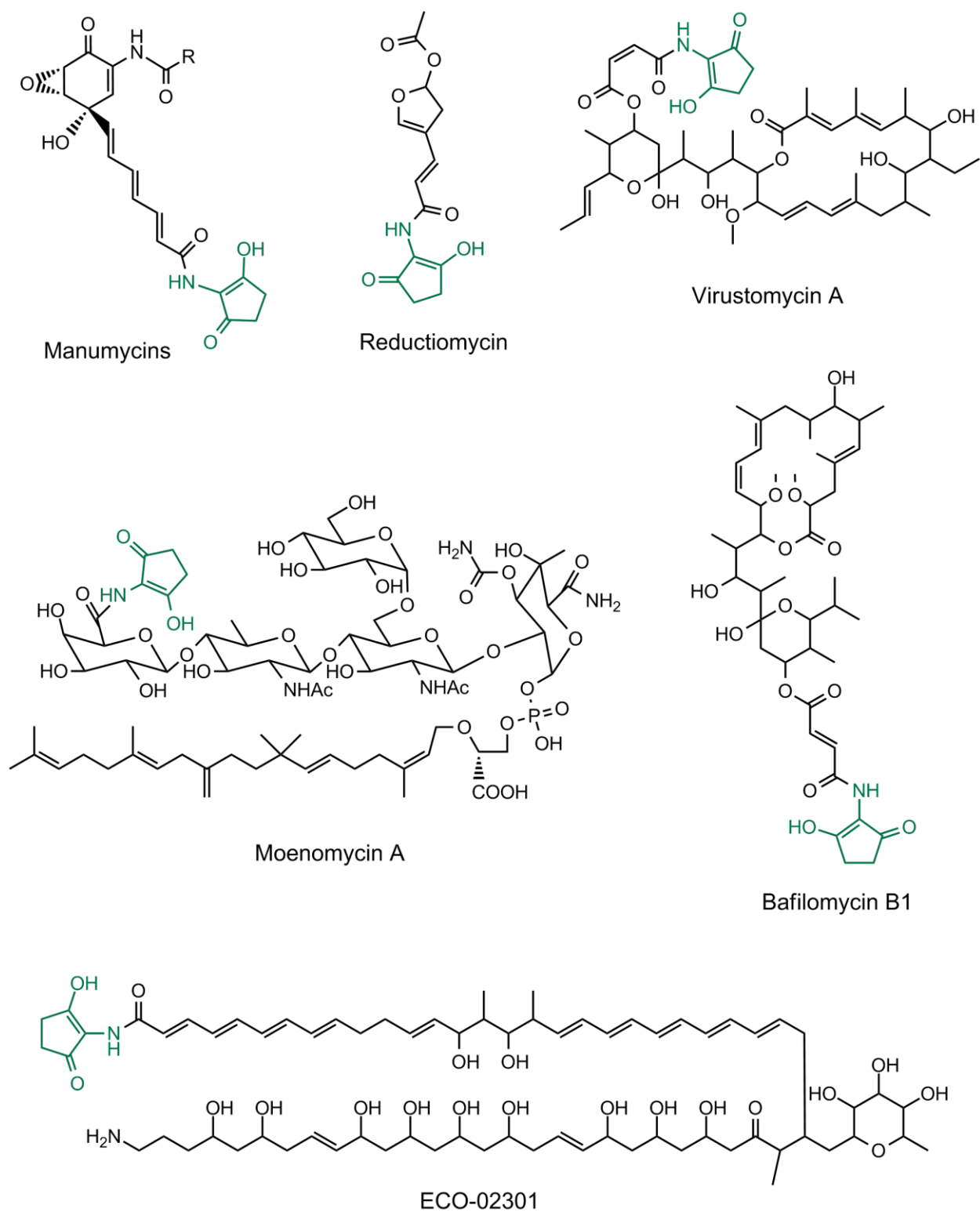


Figure 1.6 Examples of natural products containing C₅N moiety. The C₅N moieties are indicated in green.

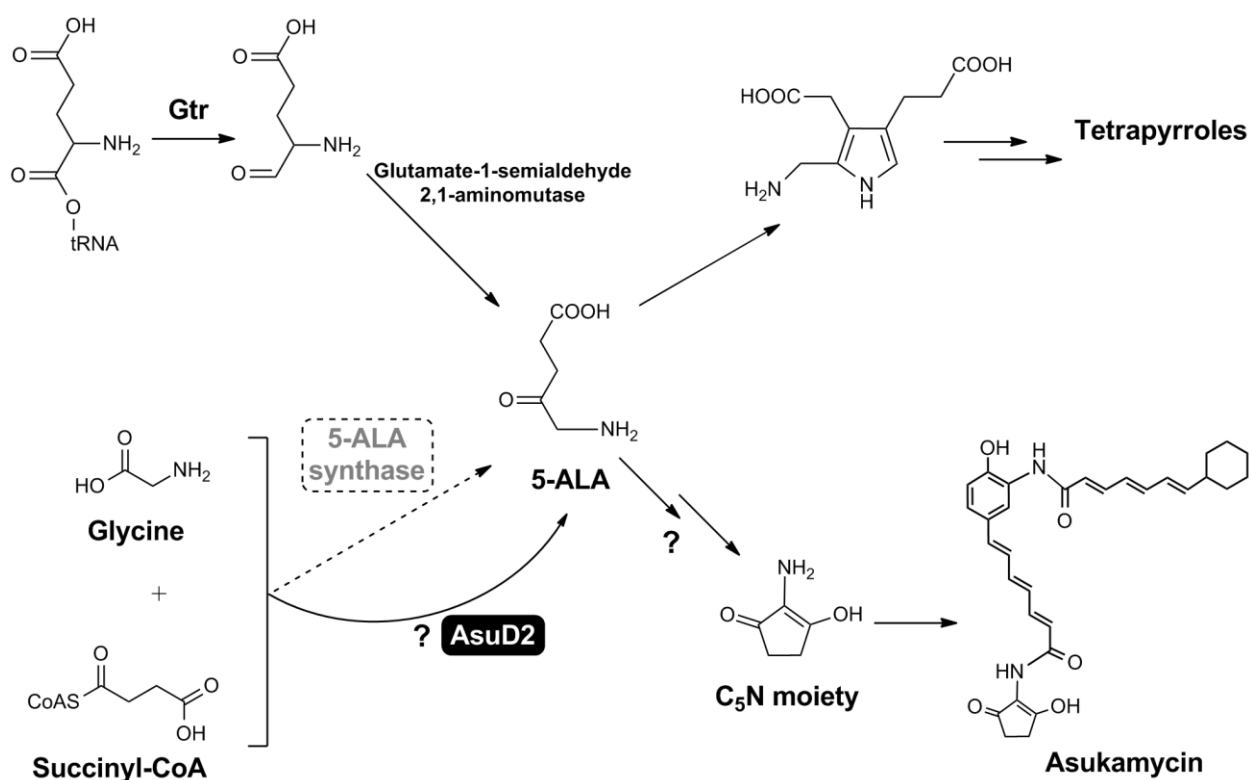


Figure 1.7 C₅ and Shemin pathways for the 5-ALA formation. The question marks indicate the dubious steps. The dashed arrow and enzyme indicate the standard 5-ALA synthase that might not be present in *S. nodosus*.

To date, the mechanism behind the intramolecular cyclization of the C₅N moiety remains to be clarified. Besides, the amino group of C₅N moiety is mostly acylated through an amide bond to a polyenoic acid component of polyketide, with the exception of moenomycin A (Fig. 1.6). The amide-forming enzyme committed in this step is still unknown. Due to the stability issues, there has yet been a successful feeding experiment using a C₅N or its derivatives such as 2-amino-3-hydroxycyclopent-2-enone, or 2-amino-3-hydroxycyclopent-2-enone hydrochloride (Hu Y., Floss H., unpublished).

The Oxygenation of Protoasukamycin to Form Asukamycin

The two oxygen atoms, positioned in the C4 hydroxyl group and the C5-C6 epoxy group, had been proved to arise from the atmosphere O₂ through the feeding experiment (Fig. 1.4) [76].

Notably, all the isolated manumycin metabolites from each individual producing organism feature a unique stereochemistry with either all 4*S*, 5*R*, 6*S* or all 4*R*, 5*S*, 6*R*. For example, both *S. parvulus* and *S. nodosus* generate an identical 4*S*, 5*R*, 6*S* core of manumycins and asukamycins, while alisamycin and nisamycin, characterized with a 4*R*, 5*S*, 6*R* configuration, are solely found in *Streptomyces* K106. These observations strongly suggested that the oxygenation does not occur spontaneously, and likely requires the involvement of enzymes.

The ¹³C-labeled feeding study has shown that protoasukamycin **C1** is the precursor of asukamycin **A1** in *S. nodosus* subsp. *asukaensis* [20]. The structure analysis indicates that the 2-amino-4-hydroxy-5,6-epoxycyclohex-2-enone core of asukamycin bears a resemblance with the epoxyquinone moiety of the Vitamin K-2,3-epoxide and LL-C10037R, in which the epoxide oxygen atom is recruited from the atmosphere O₂ through the action of a dioxygenase dihydrovitamin K epoxidase and a 2,5-dihydroxyacetanilide epoxidase respectively (Fig. 1.8) [9, 20, 38, 77-80]. Nevertheless, the ¹⁸O₂ feeding has specified that the hydroxyl and the epoxide oxygen atoms positioned at the C4 and C5-C6 positions of manumycin A were incorporated independently from the air oxygen, possibly through a two-step oxygenation mechanism in *S. parvulus* Tü 64 [76].

Research Objects

1. Identification of the Asukamycin Biosynthetic Genes

- (1) To find the conserved gene probes to identify the *asu* genes.
- (2) To clone and sequence the *asu* genes from a cosmid library.
- (3) To functionally express the entire *asu* cluster in a heterologous strain.
- (4) To justify a minimal set of the *asu* gene cluster.

2. Genetic and Biochemical Studies of the *asu* Genes

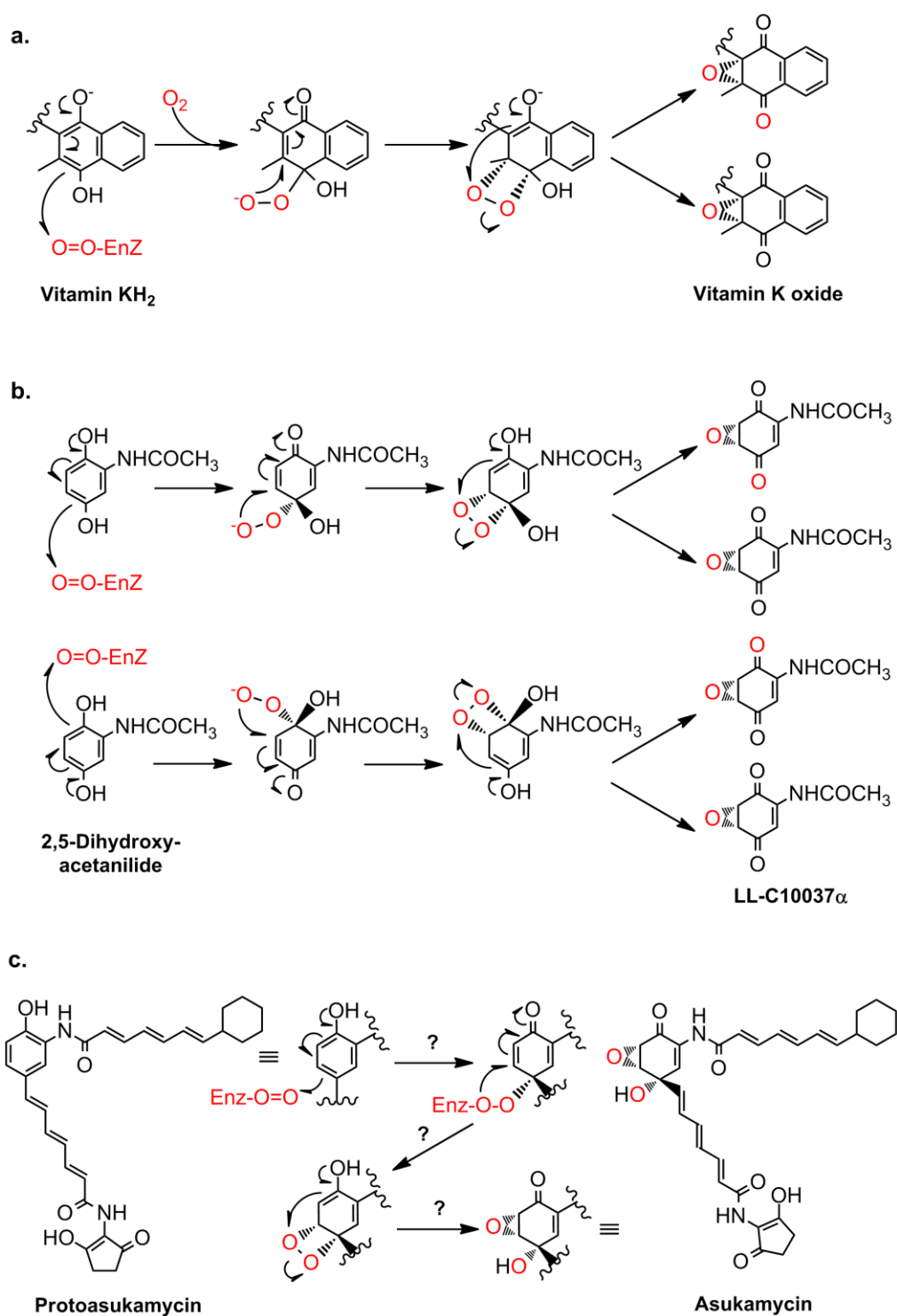


Figure 1.8 Previously proposed dioxygenase mechanism for asukamycin biosynthesis based on the formation of Vitamin K oxide and LL-C10037 α .

- (1) Genes involved in the biosynthesis of the 3,4-AHBA core.
- (2) Genes responsible for the C₅N moiety formation.
- (3) Genes in control the assembly of the upper and lower triene polyketides.
- (4) Genes acting on the formation of two amide bond linkages.
- (5) Genes governing the oxygenation of protoasukamycin to give asukamycin.

3. Characterization of the Asukamycin Biosynthetic Pathway.

- (1) To explore the novel intermediates and pathway related products.
- (2) To determine the timing for the assembly of the building blocks.
- (3) To dissect the biosynthetic routes for asukamycin and its congeners.
- (4) To investigate the interaction between the formations of asukamycin and the cellular fatty acids.
- (5) To assess and revise the current biosynthetic model.

CHAPTER TWO:

**IDENTIFICATION AND CHARACTERIZATION OF THE ASUKAMYCIN
BIOSYNTHETIC GENE CLUSTER**

Introduction

Owing to the accumulated genetic and biochemical data, the biosynthetic genes for a natural product can be targeted from the genomic library using a DNA probe, designed and amplified based on a conserved protein involved in the assembly of a similar structural moiety. For example, genes coding for TDP-D-glucose 4,6-dehydratase and halogenase were used to fish the biosynthetic gene clusters of kanamycin and kutzneride, respectively [81, 82]. As secondary-metabolite biosynthetic genes tend to be clustered in prokaryotes, the identification of one gene could lead to the revealing of the entire gene cluster in its vicinity.

Asukamycin contains several characteristic structural moieties, such as a cyclohexane group, a C₅N ring, an mC₇N core, and two triene polyketides. Due to the specificity problem of the polyketide synthases (PKS), it could be difficult to pinpoint the dedicated genes for the triene formation, particularly in the presence of many irrelevant PKSs involved in the biosynthesis of other secondary polyketide metabolites. The genes responsible for the formation of a unique cyclohexane group can be targeted by the gene set, *ansJKLM/chcA*, which had been proved to govern the CHC-CoA assembly in ansatriene biosynthesis [62]. To target the C₅N moiety, we can choose either the *asuD2*, the only gene reported to condense the glycine and succinyl-CoA precursors in the asukamycin biosynthesis.

Results

Identification and Cloning of the Asu Cluster

To identify the asukamycin biosynthetic gene cluster, a cosmid genomic library of *S. nodosus* subsp. *asukaensis* was constructed and screened with two ³²P-labelled DNA probes. Encoding the 1-cyclohexenylcarbonyl CoA reductase involved in the assembly of cyclohexane moiety for the ansatrienin biosynthesis in *Streptomyces collinus*, the *chcA* identified two

cosmids, 2B9 and 10D6, which revealed a 1.8 kb overlapping region of the cloned DNA inserts [62]. Encoding a 2-oxoamine synthase for the C₅N moiety formation of asukamycin, the *asuD2* only hybridized with cosmid 10D6 [21]. As cosmid 10D6 was picked out by both probes, we predicted that the overlapping 10D6 and 2B9 likely covers large part of the asukamycin biosynthetic gene cluster. Thus, these two cosmids were mapped and sequenced to disclose a total combined 63,922 bp of DNA inserts (GeneBank accession No. GQ926890). DNA sequence analysis revealed 36 potential open reading frames, tentatively assigned as the *asu* genes, encoding for the gene products potentially involved in the asukamycin biosynthesis and regulatory activities (Fig. 2.1 and Table 2.1).

Heterologous Expression of the Asu Cluster

DNA analysis has preliminarily allocated the crucial genes required for the compilation of the building blocks (*asuA-E* groups), such as the 3,4-AHBA, the cyclohexanyl carboxylate and the 2-amino-3-hydroxy-cyclopent-2-enone (C₅N) components, the upper and lower polyketide chains assembly, and the post-assembly oxygenation of the protoasukamycin. Also proposed were the genes tentatively involved in the regulation (*asuR*) and the exportation of the newly formed asukamycin metabolites outside the cells (*asuMI*). To confirm that the cloned region contained all the genes in control of the biosynthesis, regulation and self-immunity, a series of heterologous expression experiments were conducted in the asukamycin nonproducing *Streptomyces lividans* K4-114. Because neither of the cloned cosmids carried the full gene sets mentioned above, we intended to reassemble the cosmids 2B9 and 10D6 into one single clone.

To combine two large DNA fragments, the conventional digestion/ligation cloning strategy has several shortcomings. For example, the choice of a unique cloning restriction site can be limited, and the large ligation products can also lead to low transformation efficiency. To

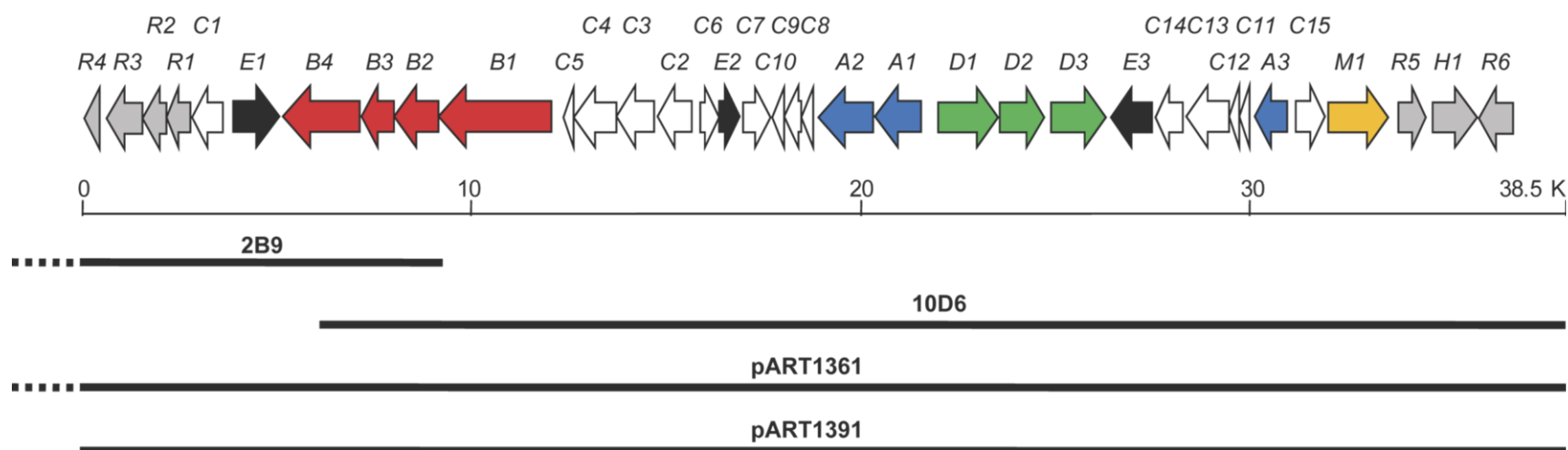


Figure 2.1. Open reading frames identified in the *asu* cluster. The putative genes were divided into eight groups based on the functional characterization. Group A: 3,4-AHBA biosynthesis and adenylation; Group B: CHC-CoA biosynthesis; Group C: polyketide chain assembly; Group D: C₅N moiety biosynthesis; Group E: oxygenation; Group R: transcriptional regulation; AsuM1: efflux protein. The relative genomic regions and overlapping inserts of three cosmid clones 2B9, 10D6, pART1361, and pART1391 are indicated with bold lines.

Table 2.1 Deduced functions of ORFs in the asukamycin biosynthetic gene cluster.

Protein	aa	Homolog (Accession No.)	Identified or Proposed Function
AsuA1	372	GriH (YP_001825760.1)	3,4-AHBA synthase
AsuA2	471	ACMS I (AAD30111.1)	3,4-AHBA carboxyl group adenylation
AsuA3	278	GriI (BAF36651.1)	Condensation of ASA and DHAP
AsuB1	983	PlmJK (AAQ84158.1)	EPSP synthase/CHC-CoA ligase
AsuB2	394	PlmL (AAQ84159.1)	Acyl-CoA dehydrogenase
AsuB3	277	ChcA (AAC44655.1)	1-cyclohexenylcarbonyl CoA reductase
AsuB4	667	PlmM (AAQ84161.1)	2,4-dienoylCoA reductase
AsuC1	219	Sfp (pdb 1QR0)	Phosphopantetheinyl transferase
AsuC2	269	GdmF (AAO06919.1)	Arylamine N-acyltransferase
AsuC3	338	ZhuH (pdb 1MZJ)	Asukamycin ketosynthase III
AsuC4	361	ZhuH (pdb 1MZJ)	Asukamycin ketosynthase III
AsuC5	84	ZhuG (AAG30194.1)	Asukamycin KSIII associated ACP
AsuC6	151	PaaI (P76084)	Thioesterase
AsuC7	234	Sco1815 (pdb 2NM0)	Ketoreductase
AsuC8	152	HadC (NP_215151.1)	Acyl dehydratase
AsuC9	150	HadB (YP_001281933.1)	Acyl dehydratase
AsuC10	94	Putative ORF	Unknown
AsuC11	91	ZhuN (AAG30201.1)	KSI/II associated ACP
AsuC12	87	AcmACP (AAD30112.1)	3,4-AHBA carrier protein
AsuC13	397	FabF(pdb 2GQD)	Asukamycin ketosynthase I/II
AsuC14	240	FabF (pdb 2GQD)	Asukamycin ketosynthase I/II
AsuC15	260	RifR (pdb 3FLB)	Type II thioesterase
AsuR1	242	GerE (pdb 1FSE)	Transcriptional regulation
AsuR2	191	TetR family protein	Transcriptional regulation
AsuR3	307	Membrane protein	Transcriptional regulation
AsuR4	141	DNA-binding protein	Transcriptional regulation
AsuR5	254	FarR3 (BAG74713.1)	Transcriptional regulation
AsuH1	384	Putative ORF	Unknown
AsuR6	280	GerE (pdb 1FSE)	Transcriptional regulation
AsuE1	407	PHBH (pdb 1YKJ)	Protoasukamycin 4-hydroxylase
AsuE2	185	PheA2 (pdb 1RZ0)	Flavin Reductase
AsuE3	371	LimB (Q9EUT9.1)	4-hydroxyprotoasukamycin epoxidase
AsuD1	531	NovL (AAF67505.1)	Amide synthase
AsuD2	409	MoeC4 (ABJ90148.1)	2-oxoamine synthase
AsuD3	468	MoeA4 (ABJ90146.1)	5-aminolevulinate CoA ligase
AsuM1	512	EmrB (YP_001507963.1)	Asukamycin exporter

bypass these difficulties, the λ -Red recombination system has been developed [83-87]. This *in vivo* recombinant system includes three key proteins, Bet, Exo, and Gam, in which Gam stabilizes the transformed linear DNA by inhibiting the RecBCD exonuclease, and Bet/Exo promote homologous recombination [88]. Taking advantage of the innate merit of the two shared DNA segments of 2B9 and 10D6, the pOJ446 vector and the overlapping 1.8 kb inserts region, we further simplified the established λ -RED recombination system by skipping the conventional PCR cloning and multiple “stitching” processes, and assembled two cosmids in a single step [84-86, 89] (Fig. 2.2). 2B9 and 10D6 were linearized by the unique cut restriction enzymes SpeI and XbaI, respectively. The linearized cosmids are unable to replicate, while the circular recombinant clones resulted from two cosmids will propagate and form colonies under the apramycin antibiotic selection. The resulting cosmid, pART1361, was introduced into the *S. lividans* K4-114 by conjugation from the *E. coli* strain.

Carrying the pART1361, the *S. lividans* transformant produced the brightly yellowish metabolites, which displayed an inhibitory effect against *Staphylococcus aureus*. HPLC analysis detected a group of compounds with an identical UV absorption spectrum and the similar solvent mobility as the asukamycin metabolites **A1-A7** observed in *S. nodosus* subsp. *asukaensis* (Fig. 2.3). The production of asukamycin and congeners **A1-A7** were further confirmed by a high-resolution LC-MS. In the meantime, the ω -cyclohexyl fatty acids were also detected at 7.8% in the *S. lividans* K4-114 by GC-MS. Notably, the productivity of asukamycin was more stable and persistent in *S. lividans* K4-114 in comparison with its natural host *S. nodosus* subsp. *nodosus*, possibly due to the imposed apramycin antibiotic selection.

In pART1361, located on one end of the insertion were many ORFs related to the primary metabolic functions of *Streptomyces* species but unlikely involved in the asukamycin biosynthesis. To further justify the boundaries of *asu* cluster, we eliminated this 25.4 kb region

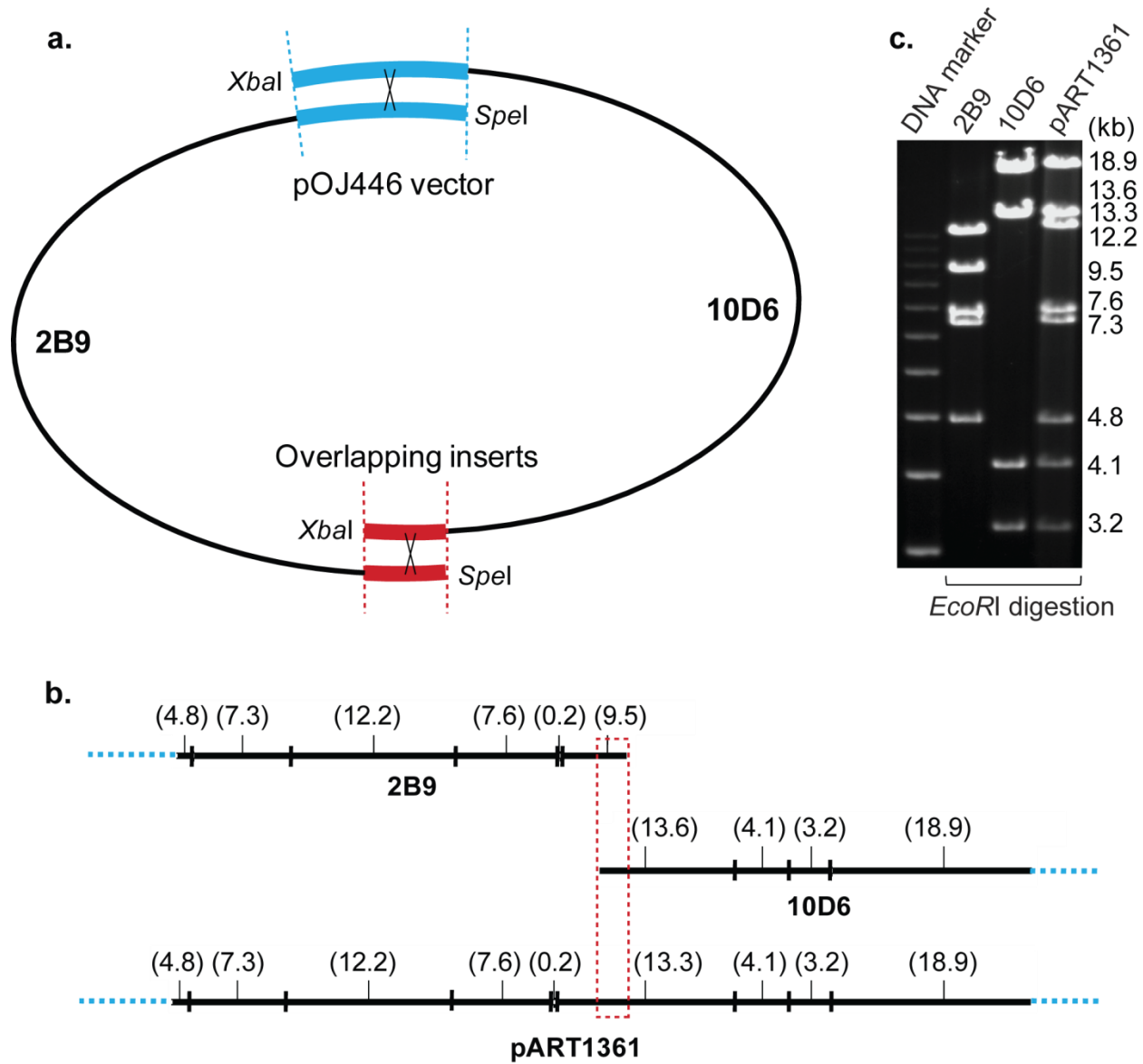


Figure 2.2 Assembly of two cosmids with overlapping inserts. **a**, cosmids 2B9 and 10D6 were linearized by *SpeI* and *XbaI*, respectively. Homologous recombination occurred at two overlapping insert and vector regions, indicated by heavy lines. **b**, the restriction map of 2B9, 10D6 and pART1361. The inserts are shown with solid lines. The *EcoRI* fragment sizes are indicated (kb). **c**, comparison of the *EcoRI* digestion patterns by DNA gel electrophoresis.

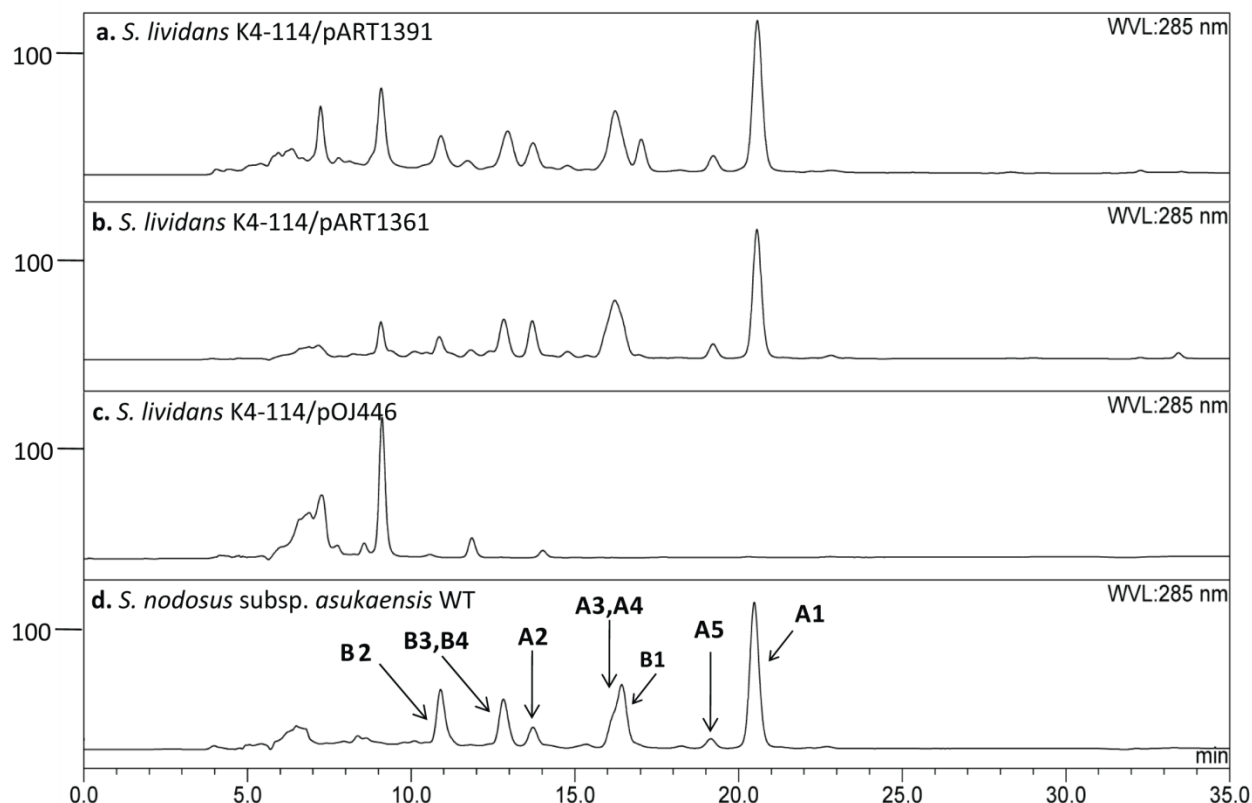


Figure 2.3 HPLC analysis of the *S. nodosus* WT and the *S. lividans* K4-114 transformants. Twenty μ L of crude culture extract of the *S. lividans* K4-114/pART1391 (a), the *S. lividans* K4-114/pART1361 (b), the control *S. lividans* K4-114/pOJ446 (c), and the *S. nodosus* subsp. *asukaensis* wild type strain (e). The arrows identify the peaks of asukamycin **A1** and related metabolites, **A2-A5**, **B1-B4**. The x axis indicates the time (min); y axis indicates the absorbance abundance (mAu).

by replacing it with the spectinomycin resistance gene to give a pART1391. The HPLC, high-resolution MS, and bioassay further supported that *S. lividans* K4-114/pART1391 was fully capable of producing asukamycin **A1** and its congeners **A2-A7**. These expression results indicate that the cloned 36 *asu* genes in pART1391 are sufficient for the asukamycin production.

Discussion

The chemical structure of asukamycin features two triene polyketide chains locked on a 3,4-AHBA-originated mC_7N core. The lower chain ends with a C_5N structural moiety, while the upper one starts with a cyclohexane head group. From the sequence analysis, four major groups

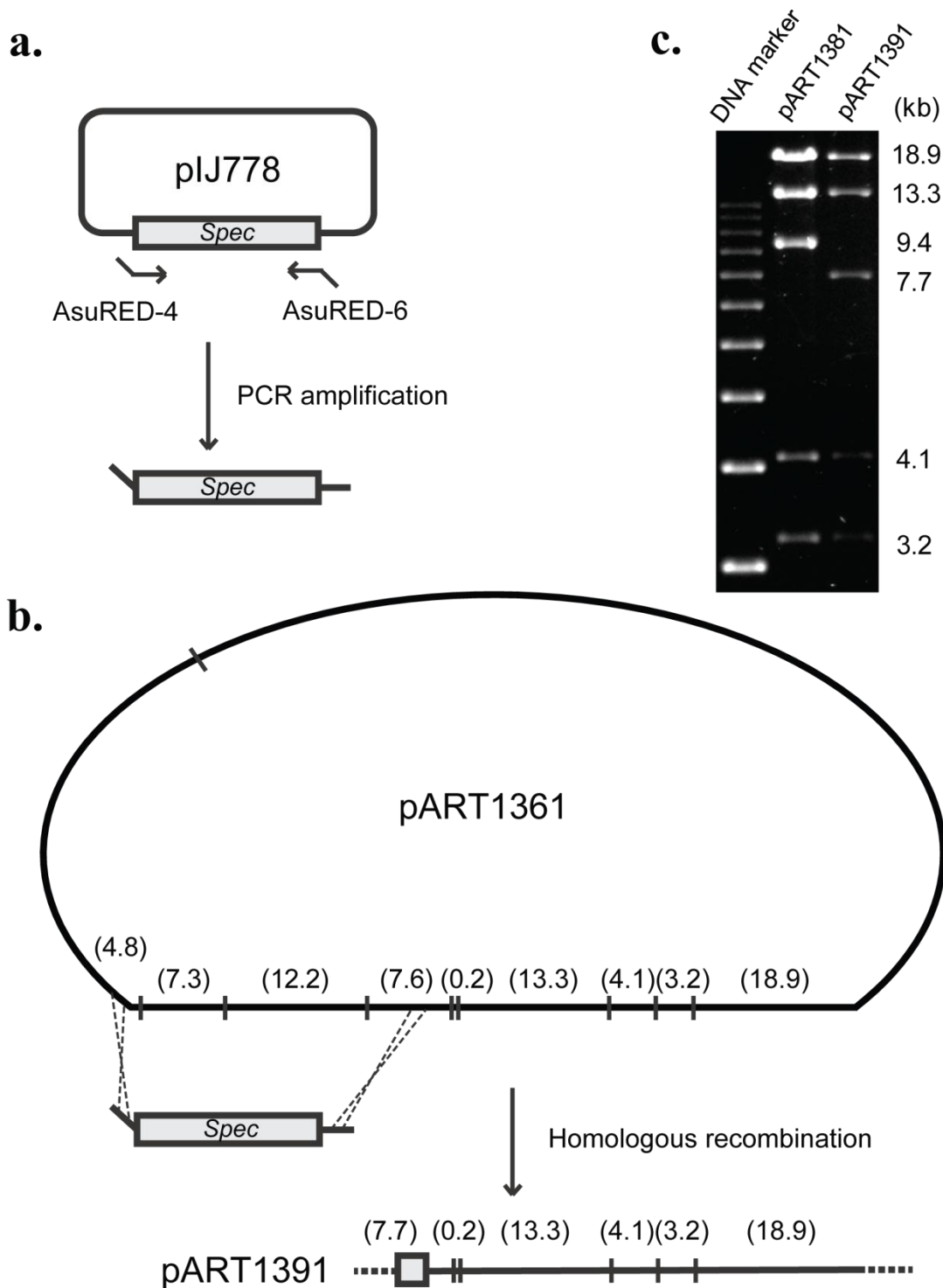


Figure 2.4 Construction of pART1391. **a**, spectinomycin resistance gene cassette (*spec*) was PCR amplified from pIJ778 using primers AsuRED-4 and -6. **b**, the λ -RED based recombination was conducted to replace the 25.4 kb insert region of pART1361 with a *spec* cassette to create pART1391. The predicted *EcoRI* digestion fragments are indicated (kb). **c**, comparison of the *EcoRI* digestion pattern by DNA gel electrophoresis. Note: Lane pART1381 indicates another pART1361 derived cosmid clone which is not related to this study.

of the *asu* genes were proposed to be involved in the structural assembly, including the *asuA* for the biosynthesis and activation of 3,4-AHBA, the precursor of the mC₇N core, the *asuB* for the conversion of shikimate to form CHC-CoA, the *asuD* for the C₅N formation, and the *asuC* group for the lower and upper polyketide chain assembly (Fig. 2.1). Besides, the sequenced genomic region also covers the putative regulatory genes and an exporter coding gene. The identification and the subsequent functional expression of the *asu* cluster provided a platform for the further investigation of these biosynthetic genes.

Heterologous expression of the entire gene cluster is not only a strategy to confirm the putative biosynthetic genes, but also an ideal approach to delineate the boundaries, justify the sufficiency, and set a stage for engineering of the targeted gene cluster. However, the frequently encountered difficulty is that the intact cluster is not accommodated by one clone from the genomic library. For example, cosmid 2B9 and 10D6, together but not one of the two, encompasses all the *asu* genes. To add or trim large genomic DNA regions on a cosmid clone, the λ -Red recombination system has been well developed due to the simplicity and high fidelity compared with the conventional molecular cloning [83-87]. Recently, Bachmann group developed a method to combine two overlapping cosmids, which required three times of λ recombinations and a single unique restriction site in the overlap region [85]. Besides, a redundant DNA “scar” sequence was also added in the resulting cosmid.

In this study, taking advantage of the innate merit of the two shared DNA segments, the vector and the overlapping inserts region, we further simplified this system by skipping the conventional PCR cloning and multiple “stitching” processes, and assembled two cosmids in a single step (Fig. 2.2). The target cosmids can be linearized by the restriction enzyme digestion, as a majority of commercial cosmid vectors carry multiple rare cut restriction sites such as XbaI and SpeI on the pOJ446. The linearized cosmids are unable to replicate, while the circular

recombinant clones resulted from two cosmids will propagate and form colonies under the antibiotic selection. This straight-forward recombination approach is particularly useful to examine the competence of the cloned genes, and provide a convenient platform for the further gene manipulations. In this study, the productivity of asukamycin was found more consistent in the *S. lividans* K4-114 introduced with the recombinant pART1361 than its natural producer *S. nodosus* subsp. *asukaensis*, possibly due to the antibiotic selection pressure. As to be mentioned in later chapters, a reliable yield of the novel intermediate 4-hydroxylprotoasukamycin **D1** was also detected in the *S. lividans* K4-114 carrying the pART1361E3, which was further generated from pART1361 based on the straight-forward λ -Red PCR strategy by replacing the *asuE3* with a spectinomycin resistance gene.

CHAPTER THREE:
FORMATION OF THE ASUKAMYCIN LOWER CHAIN

Results

3,4-AHBA Formation

Feeding experiments demonstrated that the mC₇N core structure is resulted from the precursor 3,4-AHBA in the asukamycin biosynthesis [19, 58]. Two genes in the cloned *asu* cluster, *asuA1* and *asuA3*, are closely related to the *griH* and *griI* involved in the grixazone biosynthesis in *Streptomyces griseus* [59]. GriI catalyzes an aldol condensation using *L*-aspartate-4-semialdehyde (ASA) and dihydroxyacetone phosphate (DHAP) to form a putative intermediate 2-amino-4,5-dihydroxy-6-one-heptanoate-7-phosphate, which could be further converted to 3,4-AHBA by GriH, an intra-molecular cyclase. Notably, the *griH* and *griI* locate side-by-side in the genome of *S. griseus*, while the *asuA1* and *asuA3* separate apart from each other by eight additional ORFs. To confirm their roles in 3,4-AHBA formation of asukamycin, we constructed two mutants by disrupting the corresponding *asuA1* and *asuA3*. Neither 3,4-AHBA nor asukamycin were detected in these mutants (Fig. 3.1). The asukamycin production can be further restored with the addition of 3,4-AHBA in both mutant cultures. Moreover, LC-MS analysis revealed a small amount of the novel products, **E1** and **E3/E4**, which possess a C₅N moiety amide-linked with the triene upper chains corresponding to **A1** and **A3/A4**, respectively (Fig. 3.2).

Activation of 3,4-AHBA

Previous feeding studies indicated that the lower polyketide chain assembly begins on 3,4-AHBA as a starter building block [60]. According to several polyketide/polypeptide biosynthetic systems that employ AMP-linked aroyl starters [90-92], 3,4-AHBA is presumably activated via adenylation and then tethered to a specific aroyl carrier protein (ArCP) for the downstream chain extensions. Located immediately downstream of the *asuA1*, the *asuA2* is

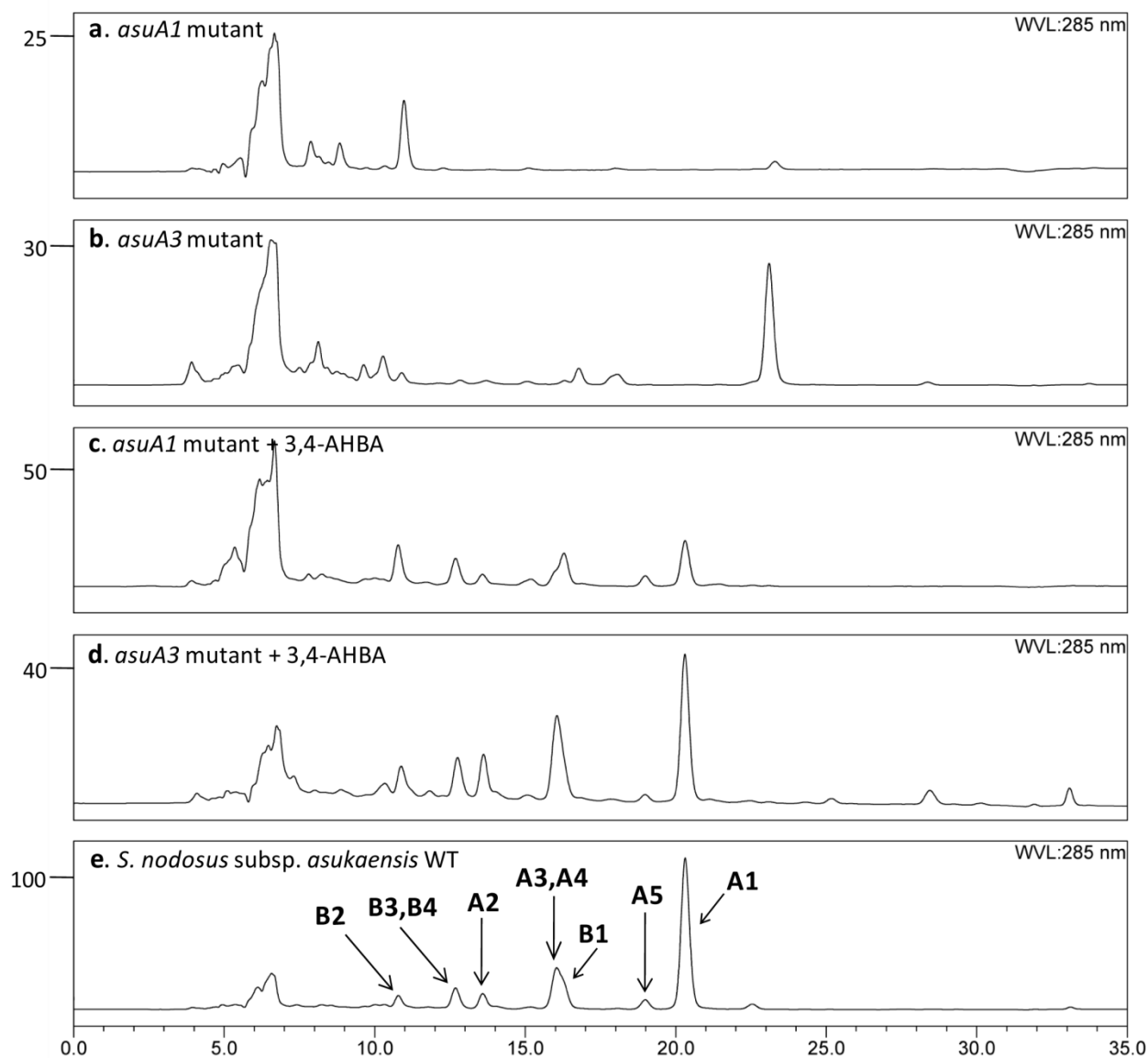


Figure 3.1 HPLC analysis of the *asuA1* and *asuA3* mutants. Twenty μL of crude culture extract of the *asuA1* mutant (a), the *asuA3* mutant (b), the *asuA1* mutant supplemented with 3,4-AHBA (c), the *asuA3* mutant supplemented with 3,4-AHBA (d), and the *S. nodosus* subsp. *asukaensis* wild type strain (e). The arrows identify the peaks of asukamycin **A1** and related metabolites, **A2-A5**, **B1-B4**. The x axis indicates the time (min); y axis indicates the absorbance abundance (mAu).

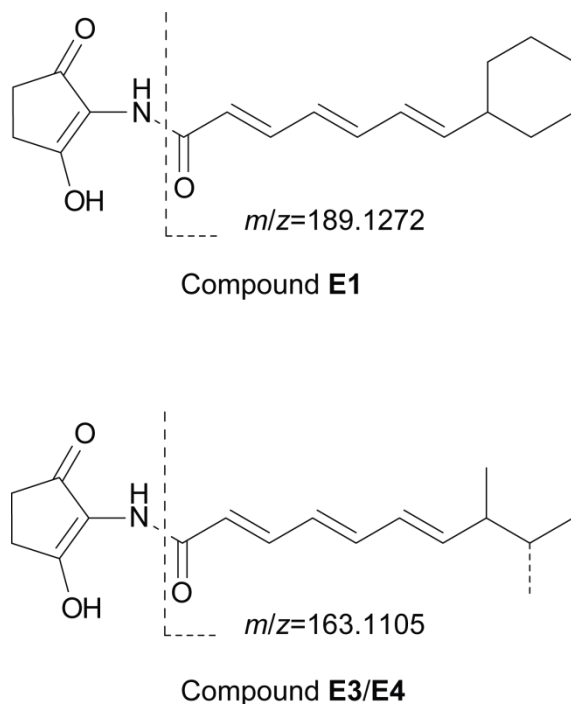


Figure 3.2 Proposed structures of E1 and E3/E4. The exact mass of **E1** is 301.1670 (calculated for $C_{18}H_{23}NO_3$, 301.1678; mass error, 3.30 ppm) with a fragment 189.1272 (calculated for $C_{13}H_{17}O$, 189.1279). The exact mass of **E3/E4** is 275.1501 (calculated for $C_{16}H_{21}NO_3$, 275.1521; mass error, 7.58 ppm) with a fragment 163.1105 (calculated for $C_{11}H_{15}O$, 163.1123).

homologous to the coding gene for the actinomycin synthetase I (ACMS I), which initiates the actinomycin formation in *Streptomyces chrysomallus* by activating 4-methyl-3-hydroxyanthranilate (4-MHA) in the presence of ATP [90]. To examine the function of AsuA2, we constructed a mutant by replacing *asuA2* with an apramycin resistant cassette. The *asuA2* mutant failed to produce asukamycins, but accumulated 3,4-AHBA through HPLC analysis (Fig. 3.3). The detected 3,4-AHBA also could complement the asukamycin production of the 3,4-AHBA-deficient *asuA1* mutant upon co-culturing (Fig. 3.4). Located seven ORFs upstream of the *asuA2*, the *asuC11* and *asuC12* both belong to the gene family coding for the acyl carrier protein (ACP). AsuC12 is distinctly related to AcmACP, a specific ArCP of the actinomycin pathway, which escorts the priming molecule 4-MHA-AMP to the peptide synthase AcmII for chain initiation [90]. The mutant in which both *asuC11* and *asuC12* were truncated showed a

similar phenotype as the *asuA2* mutant, i.e., 3,4-AHBA accumulation and no asukamycin production (Fig. 3.3 and 3.4).

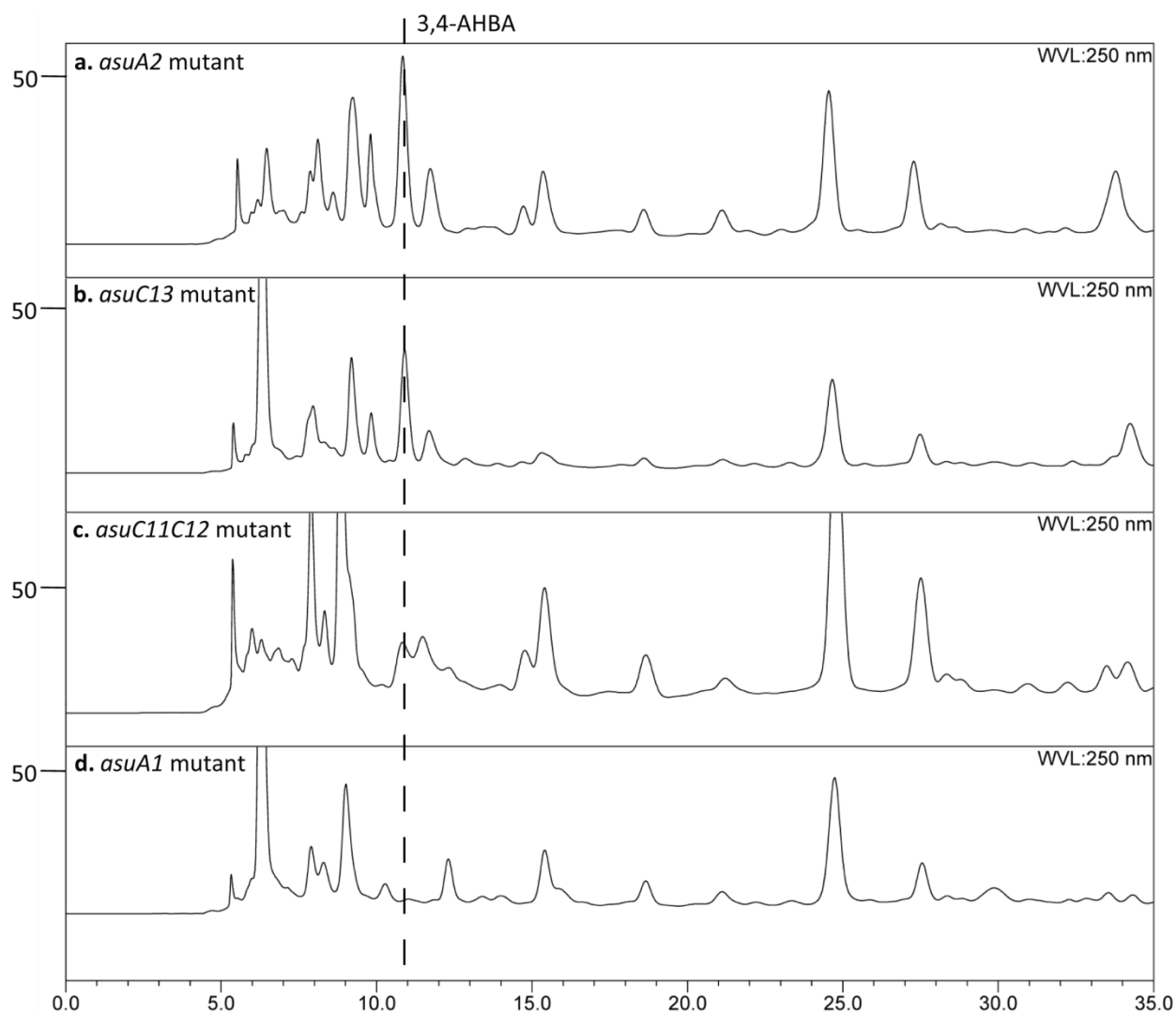


Figure 3.3 HPLC detection of 3,4-AHBA in the *asuA2*, *asuC11C12*, and *asuC13* mutants. 200 μ L of crude culture extract from the aqueous layer of the *asuA2* mutant (a), the *asuC13* mutant (b), the *asuC11C12* mutant supplemented (c), and the control group, *asuA1* mutant (d). The dash line identifies the peaks of 3,4-AHBA. The x axis indicates the time (min); y axis indicates the absorbance abundance (mAu).

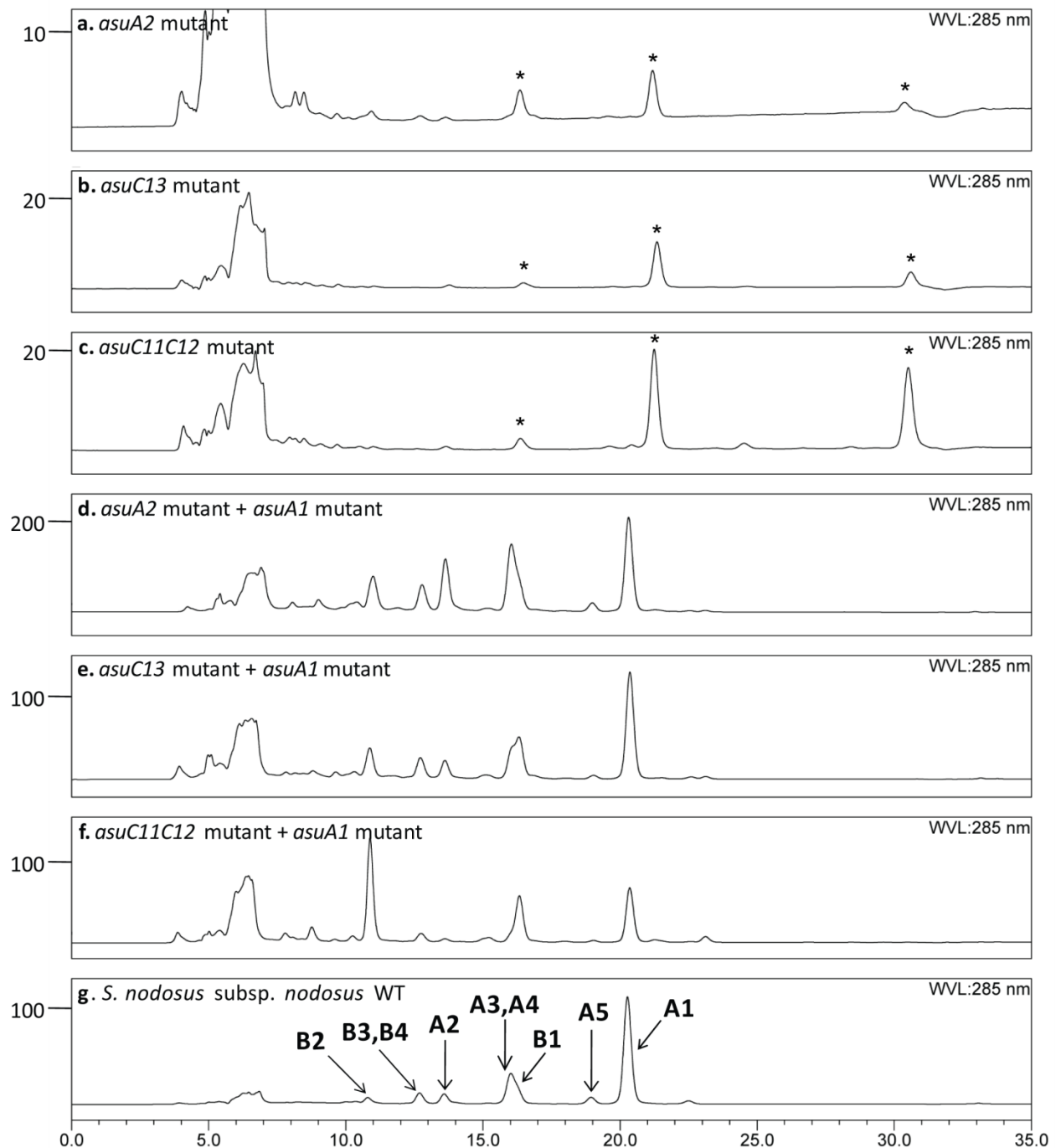


Figure 3.4 HPLC analysis of the *asuA2*, *asuC11C12*, and *asuC13* mutants. Twenty μL of crude culture extract of the *asuA2* mutant (a), the *asuC13* mutant (b), the *asuC11C12* mutant (c), the *S. nodosus* subsp. *asukaensis* wild type strain (g), and 100 μL crude co-culture extract of the *asuA2* and the *asuA1* mutant (d), the *asuC13* and the *asuA1* mutant (e), the *asuC11C12* and the *asuA1* mutant (f).

Assembly of Lower Polyketide Chain

Positioned next to the *asuC12*, the *asuC13* has strong similarity to a group of genes encoding for the type II iterative fatty acid/polyketide synthases (FAS/PKS) [93, 94]. Besides featuring a putative Cys¹⁵¹-His²⁸⁵-His³²² catalytic triad, AsuC13 also holds several conservative hydrophobic residues, which have been depicted to form a pocket to accommodate the ongoing acyl intermediate in the bacterial fatty acid synthases [95-97]. As the constructed *asuC13* mutant failed to produce asukamycins and accumulated 3,4-AHBA, similar to the *asuA2* and *asuC11C12* mutants, AsuC13 was confirmed to be a KSI/II polyketide synthase involved in the lower polyketide chain assembly (Fig. 3.3 and 3.4). Notably, trace amounts of **E1** and **E3/E4** were also found in this mutant culture as observed in the *asuA1* and *asuA3* mutants. Immediately downstream of *asuC13*, the *asuC14* encodes a protein homologous to AsuC13, except for a truncated N-terminus and lacking the characteristic Cys-His-His catalytic triad. Coincidentally, this uncommon *asuC13/asuC14* gene pair, in which an intact polyketide synthase gene accompanies a partially truncated partner, is also present in the uncharacterized gene clusters from the genomic sequencing projects of *Streptomyces hygroscopicus* (ZP_05513707-8) and *Salinispora arenicola* (YP_001535964-5 and YP_001537504-5). So far, the AsuC14 function remains unknown.

Two additional reactions, a β -keto reduction and a dehydration, are required in the formation of the lower triene polyketide. Sequence analysis revealed that only one set of genes, the *asuC7-C9*, could fulfill these anticipated functions in the cloned *asu* cluster. AsuC7 displays a high homology to several polyketide ketoreductases (KR), including the bacterial FabG proteins, the SCO1815 from *Streptomyces coelicolor*, and the MabA from *Mycobacterium tuberculosis* [98, 99]. Two putative dehydratase genes *asuC8* and *asuC9* were found downstream of *asuC7*. AsuC9 contains a typical hydratase motif with the catalytic residues Asp³⁷-X(4)-His⁴²

and is closely related to the HadB, which forms a heterodimer with either the HadA or HadC to act on the compilation of the long chain mycolic acids in *M. tuberculosis* H37Rv [100-103]. Coincidentally, AsuC8 is highly related to both HadA and HadC. As *asuC7* and *asuC8,C9* are the only genes in the cluster which could be involved in β -keto reduction and dehydration of the polyketide, we suggest that they operate in the assembly of the lower as well as the upper *trans* triene chains (to be discussed in the following chapter).

Discussion

3,4-AHBA is a common precursor for several natural products, such as manumycin A-C, grixazones, and 4-hydroxy-3-nitrosobenzamide in the corresponding *Streptomyces parvulus*, *Streptomyces griseus*, and *Streptomyces murayamaensis*. These cloned biosynthetic genes, *asuA3* and *asuA1*, could serve as probes to fish other gene clusters for these 3,4-AHBA related metabolites. By using their homologous gene probes, *griI* and *griH*, Ohnishi and co-workers recently identified the 4-hydroxy-3-nitrosobenzamide biosynthetic gene cluster [104]. Moreover, the genome mining could further extend to a long list of *asuA3* and *asuA1* homologs deposited in GenBank to explore the 3,4-AHBA related natural products.

The results indicate that 3,4-AHBA is activated by AsuA2 to form an acyl-AMP, subsequently loaded onto the aroyl carrier protein AsuC12 to initiate the lower polyketide assembly (Fig. 3.5). Construction of the lower polyketide chain likely requires a set of type II polyketide synthetic enzymes including the KSI/II AsuC13,C14, the KR AsuC7 and the DH AsuC8,C9, based on the sequencing and mutagenic analysis (Fig. 3.5). AsuC13 and AsuC14 are most likely responsible for the initiation and two further rounds of polyketide chain extensions, as the lower chain biosynthesis was abolished in the *asuC13* mutant. The presence of *asuC14* might not be coincidental. AsuC13 and AsuC14 could function together to constrain the growing

triene structures and control the polyketide chain length. Further studies on other manumycin biosynthetic genes should provide more clues on the function of *asuC14*. Since the *asuC11* is potentially organized in the same transcription unit with the *asuC12-C14*, AsuC11 ACP could be involved in the second and the third rounds of lower chain polyketide extensions.

Interestingly, governing the lower chain biosynthesis, *asuA1-A3* and *asuC11-C14* are discretely located, while their homologs in *S. hygroscopicus*, ZP_05513702-8, are organized in a seven-gene cluster, and likely function in a sequential order, suggesting that asukamycin biosynthesis has evolved through multiple horizontal gene transfer events and possibly an extensive genomic rearrangement in *S. nodosus* subsp. *asukaensis*.

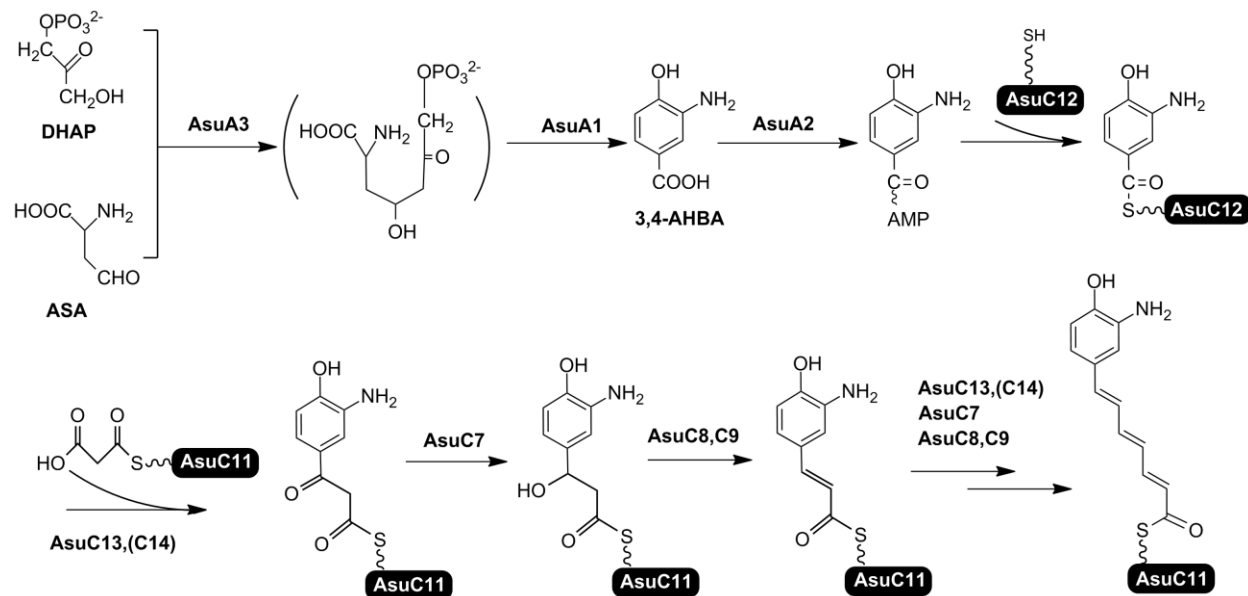


Figure 3.5 Proposed biosynthetic pathway of asukamycin lower chain.

CHAPTER FOUR:
ASSEMBLY OF THE ASUKAMYCIN UPPER CHAIN

RESULTS

Cyclohexylcarbonyl-CoA Formation

Unlike other manumycins, the formation of the asukamycin upper polyketide chain starts with cyclohexylcarbonyl-CoA (CHC-CoA), which is derived from the primary metabolite, shikimic acid [60]. Four clustered genes, *asuB1-B4*, are homologous to two independent gene sets, *ansJKLM/chcA* from the ansatrienin producer *S. collinus* and *plmJKLM/chcA* from the phoslactomycin producer *Streptomyces* sp. HK-803, which are involved in CHC-CoA biosynthesis [62, 105]. All these CHC-CoA biosynthetic genes are organized in the same order in these three strains. Notably, AsuB1 and PlmJK are likely bifunctional proteins which contain an N-terminal 5-enolpyruvylshikimate-3-phosphate synthase (EPSP synthase) domain as well as a cyclohexanecarboxylate-CoA ligase domain at C-terminus. However, these functional activities are carried out by two separated protein products AnsJ and AnsK in *S. collinus*. Constructed by gene disruption, the *asuB1* mutant failed to produce asukamycin, but levels of the previously identified asukamycin congeners **A2-A7** were increased three-fold compared with those of the wild type strain (Fig. 4.1). LC-MS analysis further identified three new compounds **A8**, **B8** and **C8** (Fig. 4.2 and 4.3). The NMR analysis of **B8** revealed a **B1**-like structure except that the upper polyketide chain was replaced by an acetyl group (Table 4.1). Based on the molecular weight, compounds **C8** and **A8** are likely the proto- and type I-form of **B8**, respectively. These products probably resulted from an increasingly buildup of the 3,4-AHBA-lower chain-ACP intermediate. Besides, GC-MS analysis revealed that the cellular level of ω -cyclohexyl fatty acids were at 7.8% in the *S. lividans* K4-114/pART1391 but not in the control strain carrying an empty vector, suggesting the included *asuB1-B4* are sufficient for the CHC-CoA assembly.

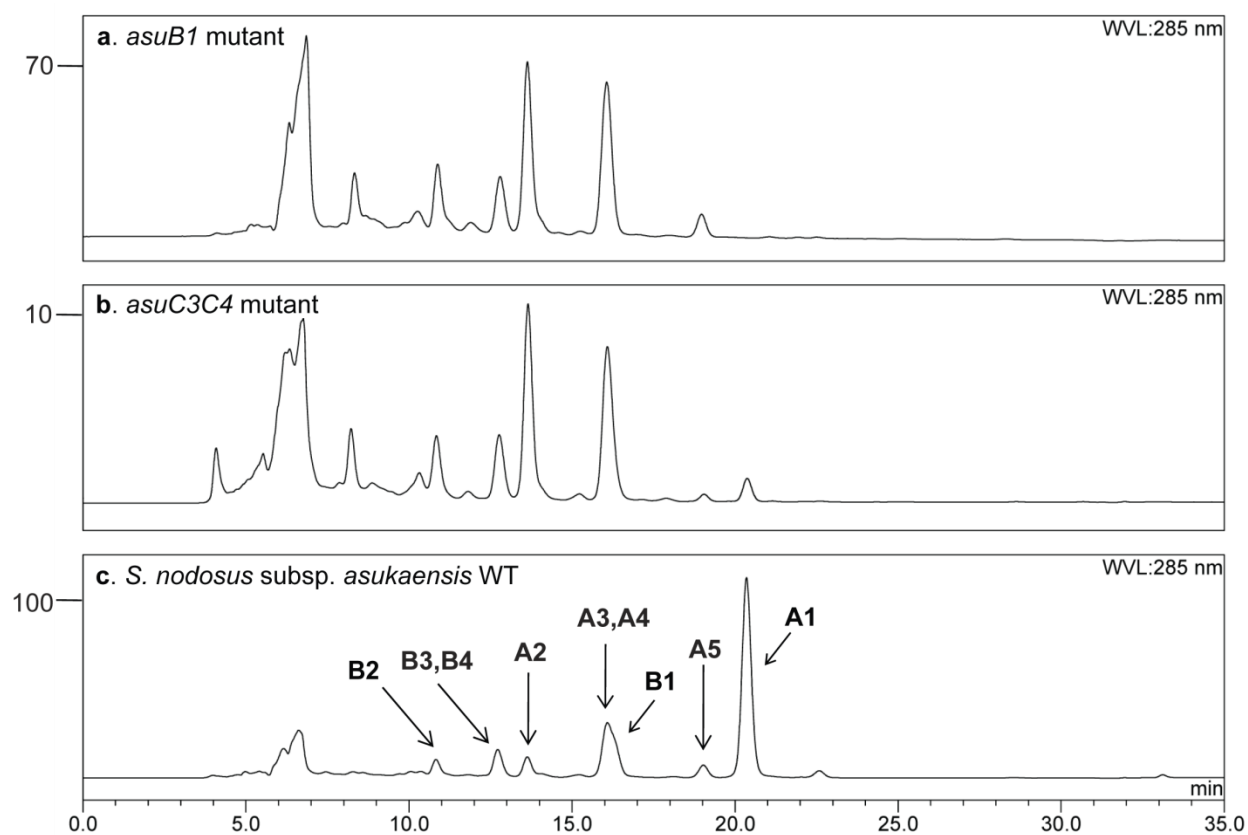


Figure 4.1 HPLC analysis of the *asuB1*, *asuC3C4* mutants, and the *S. nodosus* wild type strain. Twenty μ L of crude culture extract of the *asuB1* mutant (a), the *asuC3C4* mutant (b), and the *S. nodosus* subsp. *asukaensis* wild type strain (c). The arrows identify the peaks of asukamycin **A1** and related metabolites, **A2-A5**, **B1-B4**. The y axis indicates the absorbance abundance (mAu). Panel **b** was calculated based on a 10X injection amount.

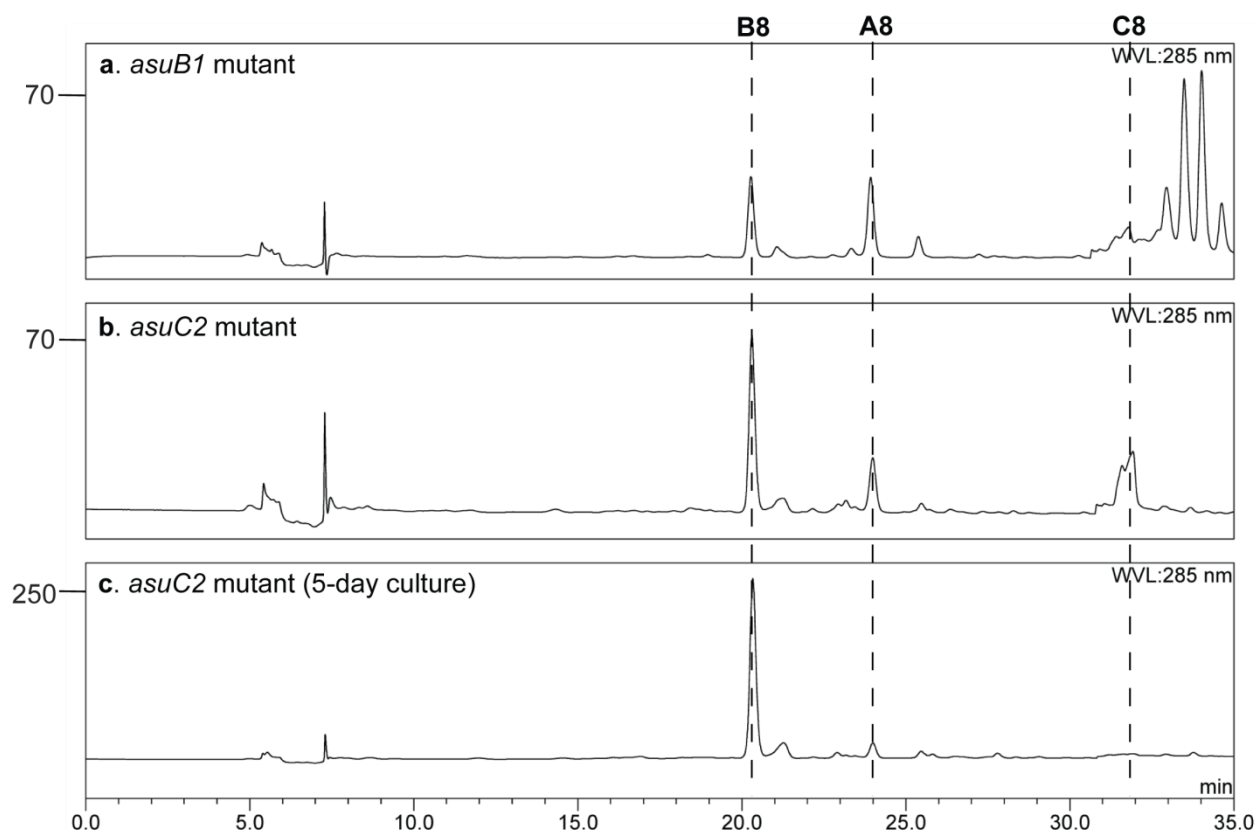


Figure 4.2 HPLC detection of A8, B8, and C8 in the *asuB1* and *asuC2* mutants. Twenty μL of crude culture extract of the *asuB1* mutant (a) and the *asuC2* mutant (b). An old culture of *asuC2* mutant was shown in panel c. The dash lines identify the peaks of A8, B8, and C8. The y axis indicates the absorbance abundance (mAu).

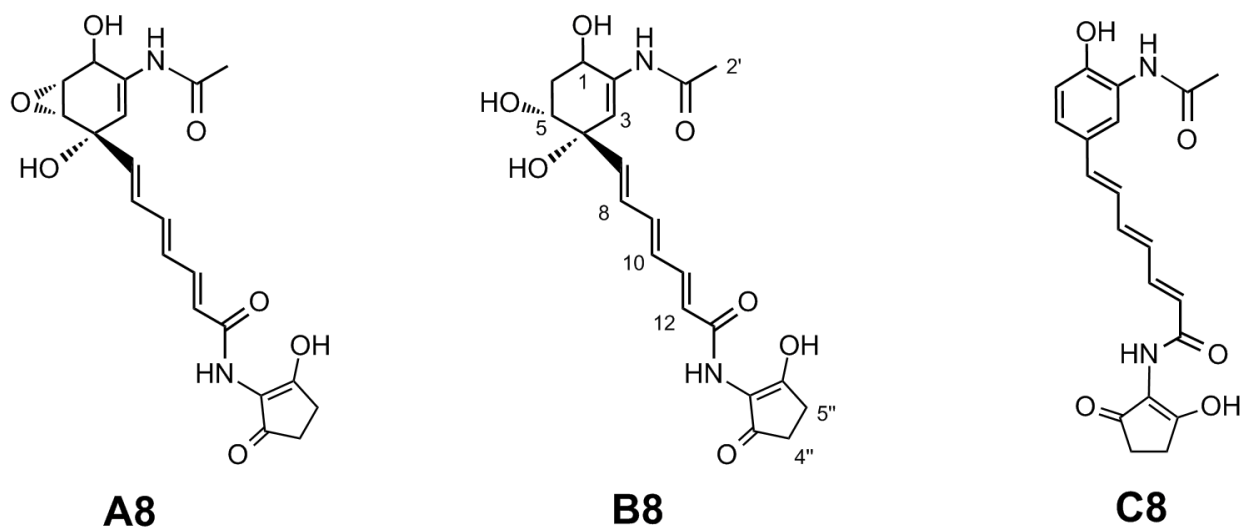


Figure 4.3 Molecular structures of A8, B8, and C8.

Table 4.1 Summary of observed ^1H -NMR and ^{13}C -NMR of B8.

Position	δ_{C} (ppm)	δ_{H} (ppm)
1	192.6	--
2	130.8	--
3	129.6	7.27 (d, $J=7.8$)
4	73.0	--
5	71.3	3.85 (m)
6ax	40.1	2.71 (dd, $J=16.8, 3.2$)
6eq		2.59 (dd, $J=16.5, 6.07$)
7	138.4	6.12 (d, $J=15.2$)
8	131.5	6.43 (dd, $J=14.9, 11.5$)
9	138.8	6.67 (dd, $J=15.1, 10.9$)
10	129.5	6.47 (dd, $J=15.2, 11.0$)
11	140.3	7.12 (dd, $J=15.0, 11.5$)
12	124.5	6.38 (d, $J=15.0$)
13	165.0	--
1'	169.5	--
2'	23.9	1.90 (s)
1''		--
2''		--
3''		--
4''		
5''		
NH-14		8.91 (s)
NH-O'		8.88 (s)

Note: ^{13}C -NMR and ^1H -NMR signals for C1''- C5'' are undetectable in DMSO- d^6 due to the coalescence phenomena.

Assembly of the Upper Polyketide Chain

To initiate fatty acid or polyketide biosynthesis, acyl-CoA starters are recruited and condensed with a (methyl)-malonyl-ACP by the action of fatty acid synthases FabH or the polyketide synthases III (KSIII). This is distinct from the action of KSI/II, joining two ACP-bound acyl substrates in the subsequent chain extensions in many microorganisms [93, 94]. The adjacent *asuC3* and *asuC4* are homologous to numerous genes encoding bacterial FabHs and KSIIIs including the *zhuH* of *Streptomyces*. sp. R1128 [106, 107]. Both *AsuC3* and *AsuC4* feature a putative CoA binding site and a conserved Cys-His-Asn catalytic triad, which is crucial for the nucleophilic acyl substitution. As *AsuC3* and *AsuC4* are highly similar to each other, we assume that they might act together as a heterodimer to condense the CHC-CoA and malonyl-ACP to give a 3-cyclohexyl-3-oxopropanoyl-ACP intermediate for the downstream polyketide chain assembly. Interestingly, a double mutation of *asuC3* and *asuC4* did not completely eliminate the asukamycin production. The *asuC3C4* mutant retained 0.9% asukamycin **A1** and 30.0% congeners **A2-A7** relative to the wild type strain yield (Fig. 4.1), possibly due to a functional complementation by the cellular FabH involved in the fatty acid biosynthesis. *AsuC5*, presumably organized in the same transcription unit with *asuC3,C4*, is a *zhuG* homolog [108]. As *ZhuG* acts together with *ZhuH* to initiate the assembly of the antitumor polyketide R1128 [108], *AsuC5* may play a crucial role in the beginning round of asukamycin upper chain assembly. So far, the KSI/II gene(s) required for the second and third round extensions of the upper chain remain to be identified.

Attachment of the Upper Polyketide Chain

Asukamycin contains two amide bonds, the linkage between the upper chain and the mC₇N core, and the bridge tethering the C₅N moiety to the lower polyketide chain. Coincidentally, two putative amide synthase genes, the *asuD1* and *asuC2*, were detected in the cloned cluster.

Sited together with the *asuD2* and *asuD3* and possibly sharing the same transcription unit, the *asuD1* is likely involved in the C₅N moiety biosynthesis (see the following chapter), while the *asuC2* was detected immediately upstream of the *asuC3-C5*, presumably organized in the same transcription unit. AsuC2 is homologous to the family of *N*-acyltransferases, which contains the arylamine *N*-acetyltransferase (NAT 1), Asm9, and RifF from the corresponding *Mesorhizobium loti* MAFF303099, *Actinosynnema pretiosum* subsp. *auranticum*, and *Amycolatopsis mediterranei* S699 [109-112]. An *asuC2* disrupted mutant was constructed to confirm its involvement in the attachment of the upper chain to the 3-amino group of the 3,4-AHBA primed polyketide intermediate. The production of asukamycins **A1-A7** was completely blocked in the *asuC2* mutant. Instead, the *N*-acetylated compounds **A8**, **B8** and **C8** were accumulated, as observed in the *asuB1* mutant (Fig. 4.2 and 4.3). In view of the functional deficiency of *asuC2*, these shunt products presumably resulted from the action of a cellular arylamine *N*-acetyltransferase, commonly found to detoxify arylamine or arylhydroxylamine metabolites [113, 114].

Discussion

The *asuB* gene set likely governs the conversion of shikimic acid to give CHC-CoA, the polyketide starter of asukamycin upper chain, as their homologous genes in *S. collinus*, *ansJKLM/chcA*, were confirmed to be essential for the same conversion by mutation experiments. Despite that, only the AsuB3 homolog, ChcA, has been proved to catalyze three independent reactions *in vitro*, including reductions of 1-cyclohexenylcarbonyl CoA, 5-hydroxy-1-cyclohexenylcarbonyl CoA, and 4,5-dihydroxy-1,5-cyclohexadienylcarbonyl CoA (Fig. 4.4) [115]. In these steps, ChcA reduces α , β -double bonds of either an enoyl or dienoyl CoA substrate with the same stereochemistry pattern: *anti* fashion with addition of solvent hydrogen

to the *si* face of the α -carbon. Besides, the mutation and *in vitro* studies demonstrated that the non-clustered ChcB, a ubiquitous Δ^1, Δ^2 enoyl CoA isomerase in *Streptomyces*, is required for the perultimate step in the CHC-CoA formation.

Sequence analysis indicated that AsuB1 is a bifunctional protein, where the C-terminal domain is similar to a number of acyl-CoA ligases, implying the role of incorporating a CoA to the carboxyl group of shikimate [116]. The N-terminal (1-424aa) domain of AsuB1 shows a relatively weak similarity with the well-characterized EPSP synthase involved in the conversion of shikimate to form chorismate. Rather than a real EPSP synthase functioning to conjugate PEP to the shikimate 3-phosphate, AsuB1 may play a role in the 1,4-*anti* elimination of shikimate or shikimate 3-phosphate (Fig. 4.4) [62, 116]. Although AsuB2 and AsuB4 are homologous to an acyl-CoA dehydrogenases and an oxidoreductase, respectively, the exact function of these two enzymes remain to be determined.

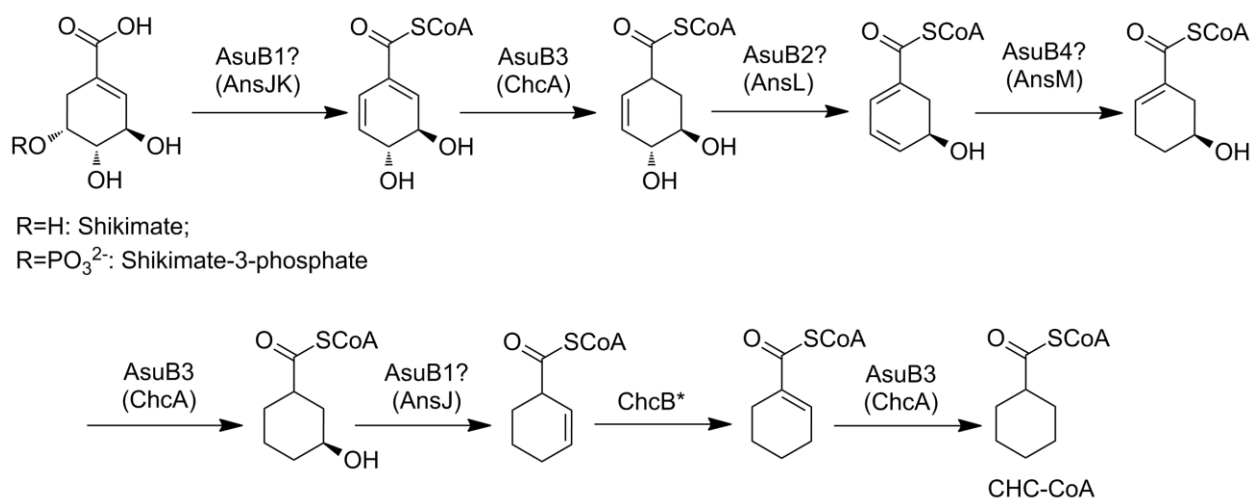


Figure 4.4 Proposed biosynthesis pathway of CHC-CoA in *S. nodosus* subsp. *asukaensis*.

Related homologous enzymes are indicated in brackets. The question marks indicate the unverified roles of the essential enzymes.

For the assembly of asukamycin upper polyketide, AsuC3,C4 likely initiate the condensation between CHC-CoA and malonyl-ACP, resembling the bacterial FabH and other KSIIIs, which are directly primed with an acyl-CoA (Fig. 4.5). In the *asuC3,C4* mutant most asukamycin **A1** production was abolished, and levels of the congeners **A2-A7** were also reduced compared to the wild-type. This reflects a possible involvement of the cellular fatty acid synthase FabH, which displays a substrate preference distinct from AsuC3,C4, priming preferentially with branched chain acyl-CoAs rather than CHC-CoA, to give a higher yield of **A2-A7** relative to **A1** [10].

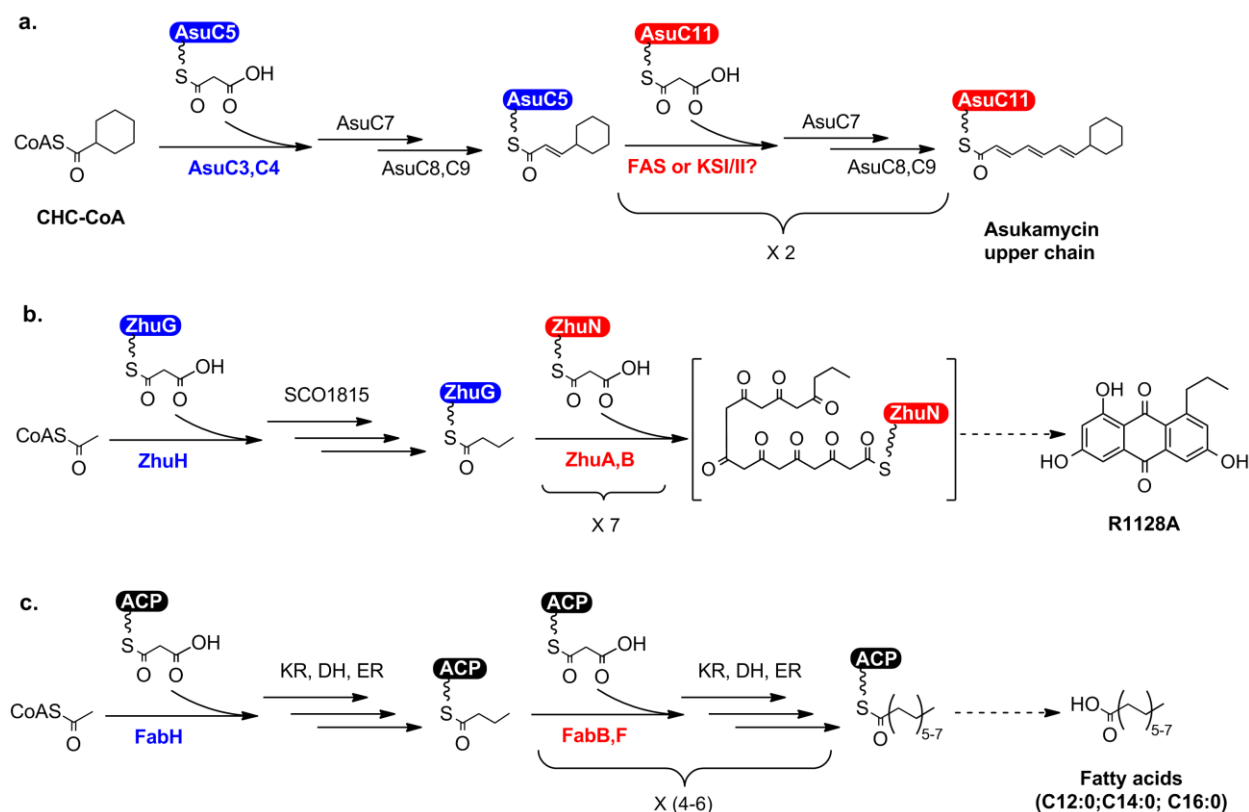


Figure 4.5 Comparison of biosynthetic pathways of asukamycin upper chain, R1128A, and fatty acids. The ACPs are in capsules. Enzymes dedicated in the first condensation are shown in blue; the ones responsible for the iterative extensions are indicated in red.

The involvement of AsuC3,C4 in the second and third chain elongations is less likely, as FabH catalyzes only the first condensation step and passes the resulting 3-ketoacyl-ACP directly to another enzyme complex for further reductions and chain elongations. Given that **E1** and **E3/E4** were found in the *asuC13* mutant, the only recognized KSI/II gene pair, *asuC13,C14*, may not play a crucial role in the upper chain assembly, although both the upper and lower polyketide chains of asukamycin share an identical triene structure. It seems that an unidentified polyketide KSI/II is required to act together with the KR AsuC7 and DH AsuC8,C9 to carry out the upper triene polyketide extension. We also cannot rule out the involvement of a cellular FabB/F-like fatty acid synthase, as the successful heterologous expression in *S. lividans* implies that a common KSI/II or FASI/II can fulfill the functional role of this unidentified β -keto condensation enzyme.

The formation of **A1-A4** only differs at the priming step of the upper polyketide chain. Instead of CHC-CoA starter, **A2-A4** employ the branched acyl-CoA thioesters, the corresponding 2-methylpropionyl-CoA, 2- and 3-methylbutanoyl-CoA, which are predominantly used for fatty acid synthesis in *Streptomyces* (Fig. 4.6) [10]. These starters, 2-methylpropionyl-CoA, 2- and 3-methylbutanoyl-CoA, are derived from the corresponding branched-chain amino acids, valine, leucine, and isoleucine. In the *asuB1* mutant, the absence of CHC-CoA abolished the entire **A1** production and redirected the biosynthetic flux to **A2-A4**. Since **A2-A4** formation was ten-fold higher in this mutant than in the *asuC3,C4* mutant, the majority of **A2-A4** upper polyketide initiation is likely performed by the KSIII AsuC3,C4, and only a minor fraction of **A2-A4** production in the *asuB1* mutant as well as the wild type strain is contributed by the FabH activity. The relatively small amount of **A5-A7** production could result from an action of the primary FAS complex to give 4-methylpentanoyl-, 5- and 4-methylhexanoyl-ACP intermediates. These ACP-tethered thioesters could be directly recruited by an unidentified KSI/II or FASI/II to

perform three additional elongations and introduce the characteristic triene in analogy with the **A1-A4** upper chain biosynthesis. These observations are in agreement with the involvement of FabH and suggest a physiological cross-talk between polyketide and fatty acid biosynthesis.

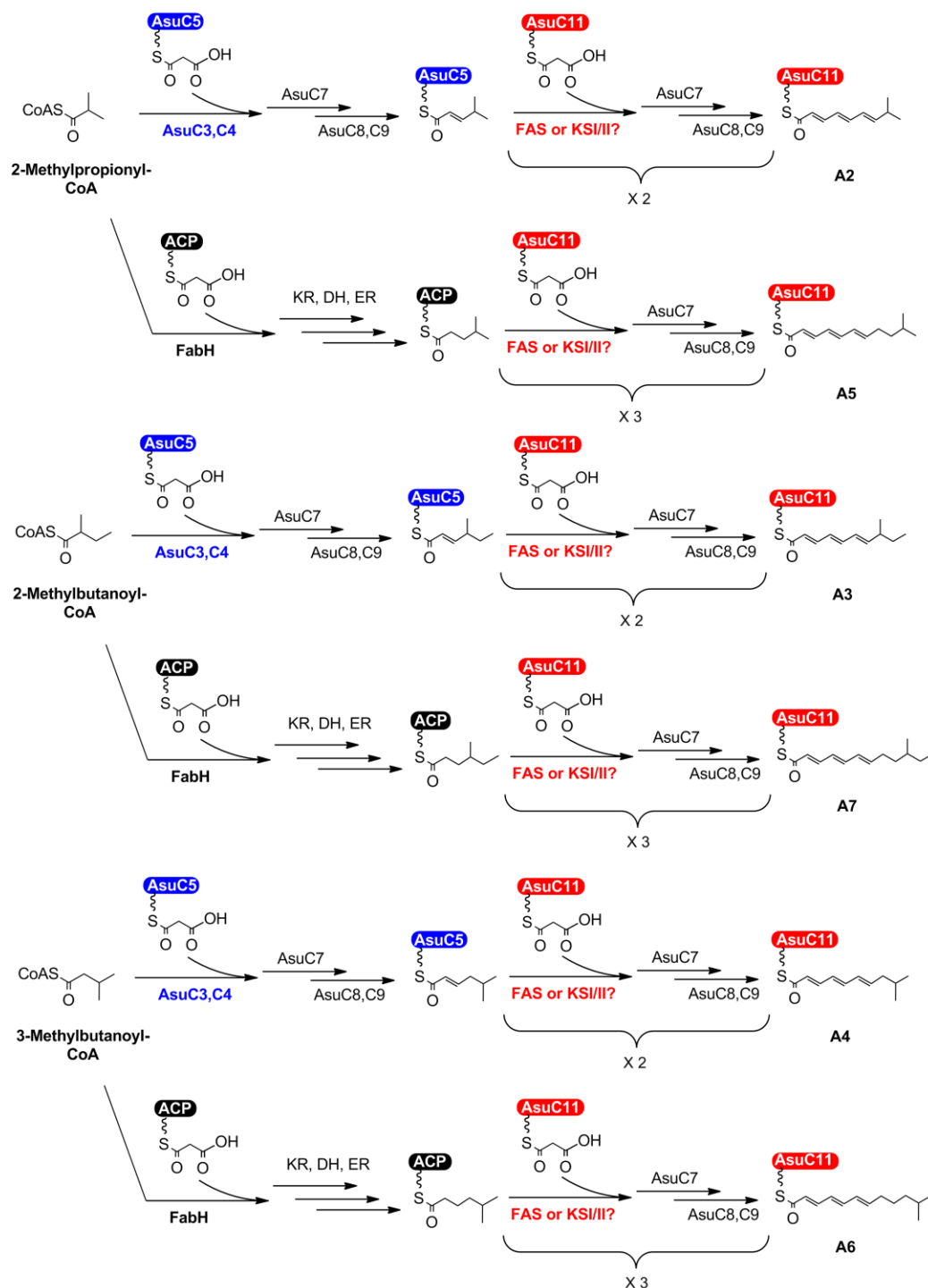


Figure 4.6 Proposed upper chain assemblies of the asukamycin congeners (A2-A7).

CHAPTER FIVE:
ASUKAMYCIN C₅N MOIETY FORMATION

Results

Three gene sets have been studied for the C₅N moiety formation, including the ones for moenomycin A, ECO-02301, and ECO-0501 from the corresponding *Streptomyces ghanaensis*, *Streptomyces aizunensis* NRRL B-11277, and *Amycolatopsis orientalis* [69, 70, 117]. Each carries three highly conserved genes encoding for a 5-aminolevulinate (5-ALA) synthase-like enzyme, an acyl-CoA ligase, and an amide synthase. To the *asu* cluster, three adjacent genes, *asuD1*, *asuD2*, and *asuD3*, were found and appeared to share a common transcription unit (Fig. 2.1).

Previously identified as HemA-AsuA, AsuD2 belongs to the family of pyridoxal phosphate (PLP)-dependent 2-oxoamine synthases, including 5-ALA synthase, FUM8, *L*-serine palmitoyltransferase (SPT) and 8-amino-7-oxononanoate synthase (AONS), which catalyze the decarboxylative condensation between an amino acid and an acyl-CoA in the assembly of corresponding 5-ALA, fumonisin, ceramide-sphingolipid, and biotin [21, 118-121]. The gene disrupted *asuD2* mutant failed to produce the asukamycin products, nevertheless the asukamycin productivity was recovered by reintroducing an expression plasmid pALS4 carrying the *asuD2* [21]. Unexpectedly, the asukamycin production could not be complemented by the existing C₅ pathway, or recovered by adding exogenous 5-ALA to the *asuD2* mutant culture, which implied that AsuD2 functions differently from the well-known 5-ALA synthase in the Shemin pathway to produce 5-ALA in many organisms (Fig. 1.7).

Despite high overall sequence similarity, AsuD2 possesses a Ser83 instead of a strictly invariant Thr83 of the 5-ALA synthase subgroup (Fig. 5.1). To examine the essentiality of this residue for the enzymatic activity, Petricek group constructed a pALS4-S83T with a S83T replacement in *asuD2*, which failed to restore the asukamycin production in the *asuD2* mutant

(Fig. 5.2). Surprisingly, the pALS4-S83T complemented a 5-ALA-deficient *gtr* mutant of *S. coelicolor*, which could only grow with 5-ALA supplementation.

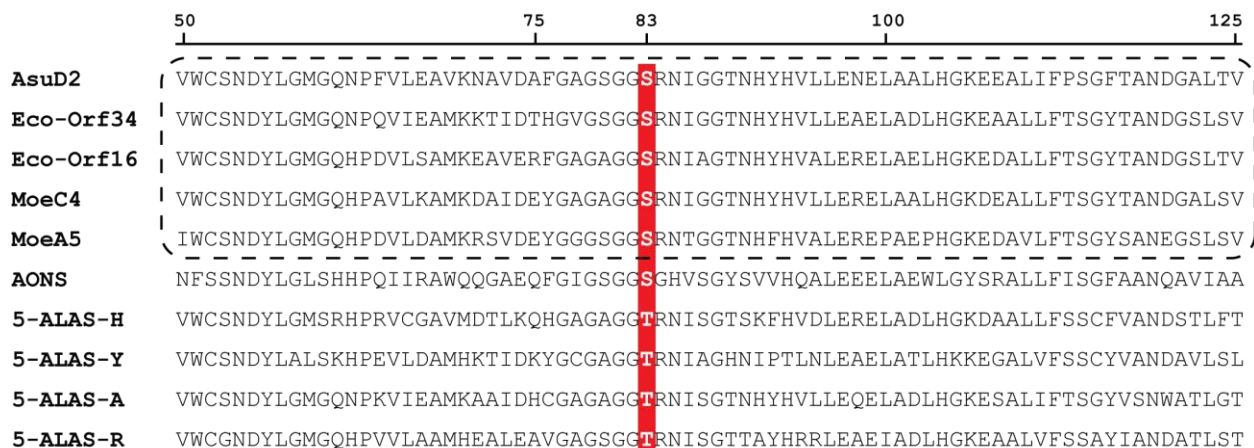


Figure 5.1 Sequence alignment of AsuD2 with other 2-oxoamine synthases. The Ser⁸³ or Thr⁸³ positions are highlighted in red. Sequences of enzymes involved in the C₅N moiety assembly are boxed. The ruler above indicates positions of amino acid residues relative to AsuD2. The enzymes functions/accession number/original strains: AsuD2 (asukamycin/AAO62615/*S. nodosus*); Eco-Orf34 (Eco-02301/AAAX98209/*S. aizunensis*); Eco-Orf16 (Eco-0501/ABM47017/*Amycolatopsis orientalis*); MoeC4 (Moenomycin A/ABJ90148/*S. ghanaensis* ATCC 14672); MoeA5 (Moenomycin A/ ABJ90153/*S. ghanaensis* ATCC 14672); AONS (8-amino-7-oxononanoate/pdb1BS0/*E. coli*); 5-ALAS-H (5-ALA/NP_000679/*Homo sapiens*); 5-ALAS-Y (5-ALA/ NP_010518/*Saccharomyces cerevisiae*); 5-ALAS-A (5-ALA/NP_355550/*Agrobacterium tumefaciens*); 5-ALAS-R (5-ALA/CAA37857/*Rhodobacter capsulatus*)

AsuD3, an acyl-CoA ligase, is proposed to act on the C₅N ring formation, since disruption of the homologous *moeA4* in *Streptomyces ghanaensis* led to accumulation of a moenomycin A analog lacking the C₅N moiety [117]. Located immediately upstream of *asuD2*, the *asuD1* is closely related to a group of amide synthase genes, including the *simL* and *novL* for the biosynthesis of simocyclinones and novobiocin in *Streptomyces antibioticus* Tü 6040 and *Streptomyces spheroides* NCIB 11891, respectively [122-124].

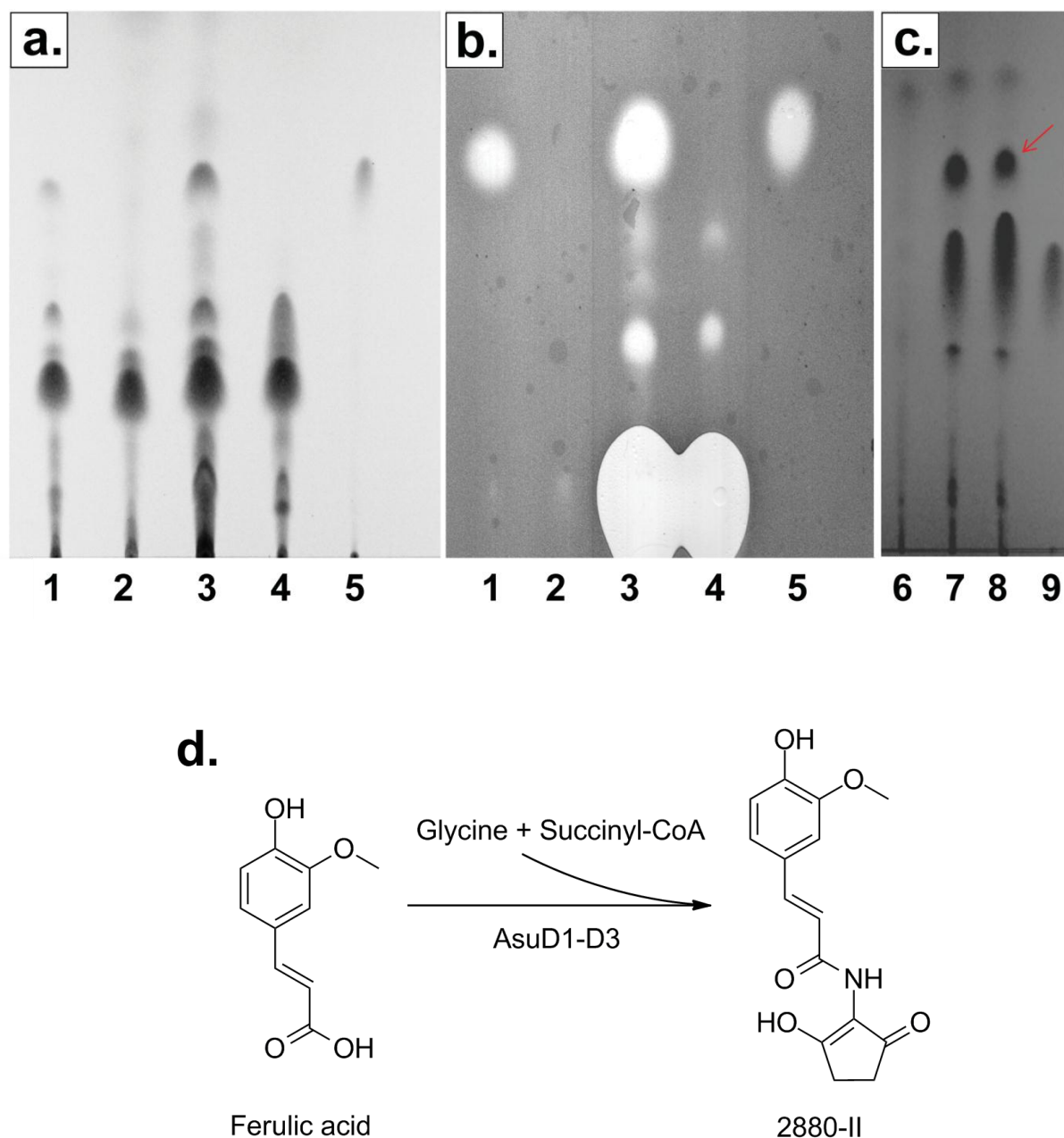


Figure 5.2 TLC analysis and bioassay of the AsuD1-D3 enzymes. **a.** and **c.** chromatograms visualized under UV 254 nm. **b.** the same TLC plate was further overlaid with *Bacillus subtilis* mixed with nutrient agar and incubated overnight at 37 °C. The red arrow shows the newly formed product 2880-II. Lane 1, the wild type strain; Lane 2, the *asuD2* mutant; Lane 3, the *asuD2* mutant/pALS4; Lane 4, the *asuD2* mutant/pALS4-S83T; Lane 5, standard asukamycin (10 µg); Lane 6, *S. lividans*/pAS9A1; Lane 7,8, *S. lividans*/pAS9A1 supplemented with ferulic acid (2.5 mg/ml); Lane 9, standard ferulic acid (10 µg). **d.** the conversion of ferulic acid to give 2880-II. *Communicated with Petricek group.

All the *asuD1*, *D2* and *D3* mutants failed to produce asukamycin, but accumulated a new set of metabolites, **A1a-A5a**, which were shown closely related to the corresponding **A1-A5** but with 95 Dalton less molecular weights, suggesting that the amide-linked C₅N moiety of **A1-A5** was replaced by a free carboxyl group in **A1a-A5a** (Fig. 5.3). The corresponding type II compounds, **B1a-B5a**, were also present in all three mutants. To confirm the *asuD1-D3* involvement in the C₅N moiety formation, the *asuD1-D3* operon was further cloned under the control of the constitutive *ermE** promoter and expressed in *S. lividans*. A novel brown metabolite was detected, but further attempts to characterize the compound have failed so far. Feeding ferulic acid to this strain, a new compound was obtained with a molecular weight of 290.097 (Fig. 5.2). MALDI-TOF MS-MS analysis of the TLC purified compound revealed an identical fragmentation pattern as the reported compound 2-(feruloylamino)-3-hydroxypent-2-enolone (2880-II) which possesses a C₅N moiety connected to the carboxyl group of ferulic acid [125]. 2880-II could not be formed if any one of the *asuD1*, *asuD2* or *asuD3* was omitted from the expression cassette.

Discussion

The *asuD1*, *D2*, and *D3* mutants revealed an identical set of accumulated products **A1a-A5a**, indicting their necessity for the assembly and attachment of the last piece of asukamycin building blocks, the C₅N moiety. The sufficiency of AsuD1-D3 for this process was also supported by the functional expression to convert ferulic acid into 2880-II in *S. lividans*. As a member of the 2-oxoamine synthases, the AsuD2 displays a high homology to the 5-ALA synthase, which is a dedicated enzyme in charge of the condensation of glycine and succinyl-CoA to form the 5-ALA, a primary metabolite and the possible precursor for the C₅N moiety [21, 67, 73]. However, as the AsuD2 and the HemA, a mammalian 5-ALA synthase, were unable to

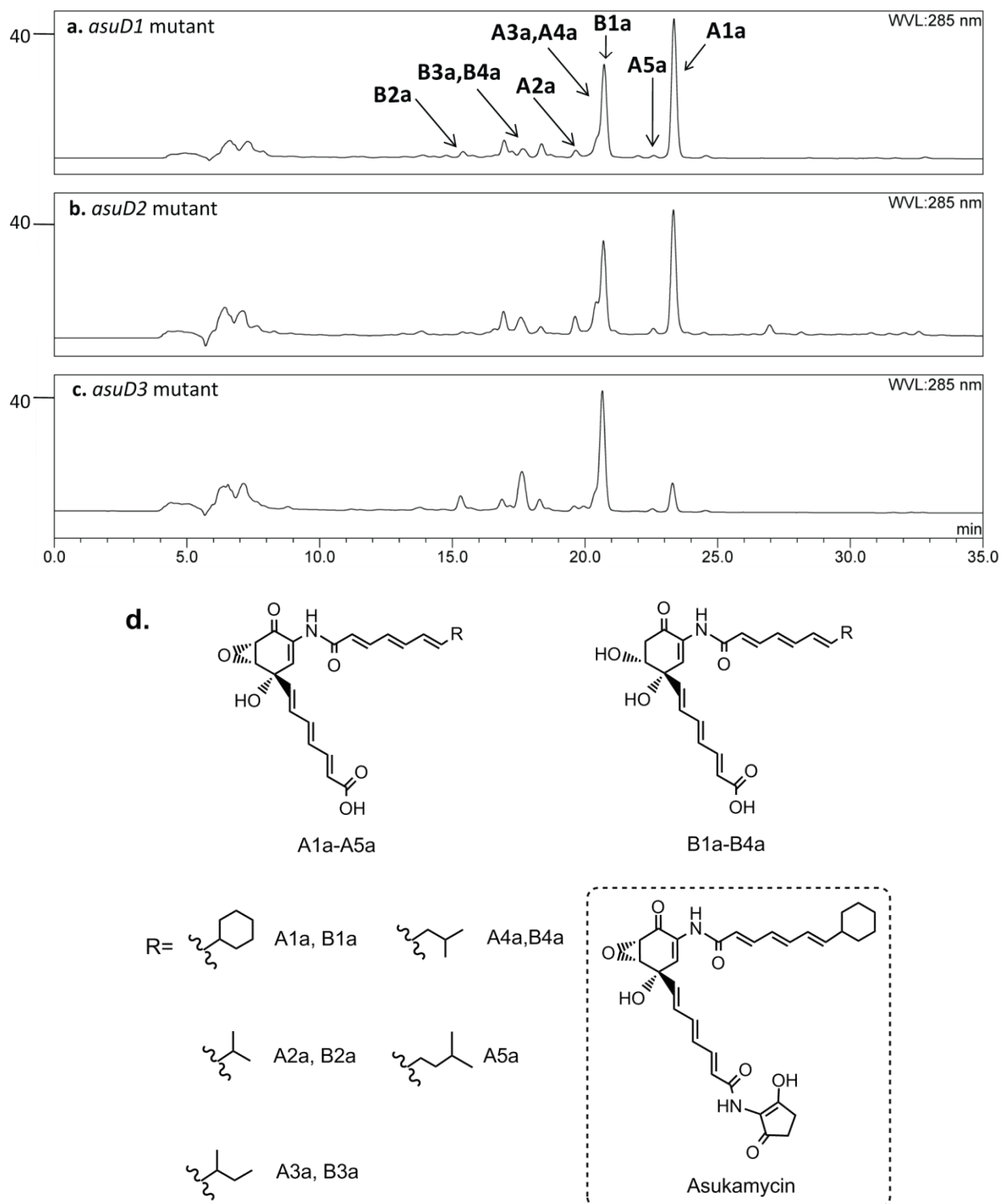


Figure 5.3 HPLC analysis of the *asuD1*, *asuD2*, and *asuD3* mutants. Twenty μL of crude culture extract of the *asuD1* mutant (a), the *asuD2* mutant (b), and the *asuD3* mutant (c). The arrows identify the peaks of A1a-A5a, B1a-B4a. The y axis indicates the absorbance abundance (mAu). Structures of A1a-A5a, B1a-B4a are shown in (d).

complement the functional activities of each other [21], AsuD2 could represent a new subfamily of enzymes that deviate from a valid 5-ALA synthase in the evolution. As the 2-oxoamine synthases catalyze the condensation between the C α of an amino acid and a CoA thioester, we suggest that AsuD2 could also perform the intra molecular C-C bond formation between the C α and C ϵ to give a C₅N ring structure. A nascent PLP-bound 5-ALA, or possibly the pre-decarboxylated intermediate, 2-amino-3-oxoadipate, could be carboxyl-activated by the action of the CoA ligase AsuD3, followed by cyclization catalyzed by AsuD2 (Fig. 5.4). The dual role of AsuD2 is also supported by the results of the heterologous expression of *asuD1-D3* to produce the C₅N unit in the absence of any other candidate cyclase gene in *S. lividans*. The amide synthase AsuD1 is responsible for the attachment of the C₅N unit to the carboxy-terminus of the lower chain. As all the assumed intermediates in this process are relatively unstable [20], AsuD1, D2 and D3 might work together to secure the formation of protoasukamycin.

Similar to other 2-oxoamine synthases, such as FUM8, SPT, and AONS that employ the amino acids containing bulky side-chain rather than glycine, AsuD2 bears a Ser83 in the position of the conserved Thr83 of 5-ALA synthase (Fig. 5.1). The distinct role of Ser83 in C₅N moiety formation was confirmed by expression of AsuD2-S83T, which failed to complement the *asuD2* mutant but restored the ability of 5-ALA formation in the *gtr* mutant of *S. coelicolor*. This point mutated AsuD2-S83T resembles an authentic 5-ALA synthase, which emerged as a serendipitous Shemin route to provide sufficient 5-ALA for the growth of *gtr* mutant. Revealed by the crystal structure of ALAS_{Rc} from *Rhodobacter capsulatus*, the side-chain methyl group of Thr83 interacts with the C α atom of the PLP-glycine intermediate (3.9 Å) at the active site [118]. In the presence of this methyl group of Thr83, amino acids other than glycine could not properly interact with the succinyl-CoA substrate, as the bulky side chain will confine the substrate binding capacity. On contrary, the Ser83 containing enzymes, including FUM8, SPT, and

AONS, are able to accommodate larger amino acids than glycine, such as alanine and serine. This not only provides another evidence for the cyclization function of AsuD2 proposed previously, but also implies the S83T mutation confines the substrate binding pocket, which facilitate the 5-ALA production but abolish the cyclization function of AsuD2.

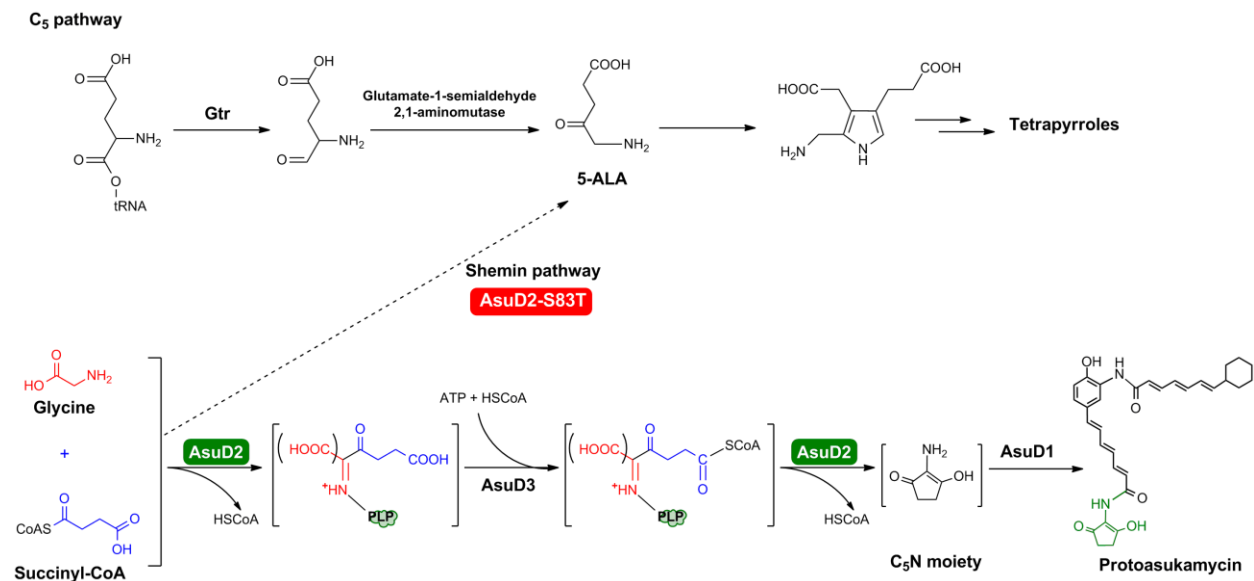


Figure 5.4 The proposed C₅N moiety biosynthetic pathway and the coexisting C₅ pathway. The dashed arrow indicates the serendipitous Shemin pathway triggered by AsuD2-S83T mutation. The AsuD2 (green) and AsuD2-S83T (red) are shown in capsules.

CHAPTER SIX:
POST-ASSEMBLY OXYGENATION OF PROTOASUKAMYCIN

Results

Growing *S. parvulus* Tü64 under an $^{18}\text{O}_2$ atmosphere has demonstrated that the hydroxyl and the epoxide oxygens at the C4 and C5-C6 positions of manumycin A originate from molecular oxygen, through either a dioxygenase mechanism or a two-step process (Fig. 1.8) [20, 76]. There was no closely related dioxygenase gene detected along the cloned cluster except that three distantly located genes, the *asuE1*, *asuE2* and *asuE3*, are likely involved in the oxygenation reaction(s). AsuE1 is homologous to the *p*-hydroxybenzoate hydroxylase (PHBH), which converts *p*-hydroxybenzoate to form 3,4-dihydroxybenzoate in *Pseudomonas aeruginosa* (Fig. 6.1) [126]. PHBH is also a bifunctional enzyme which revitalizes an oxidized FAD_{ox} to FAD_{red} in the presence of NAD(P)H and resume a next round of hydroxylation [127, 128]. Instead to produce asukamycin, the *asuE1* mutant was found to accumulate protoasukamycin **C1** and a series of protoasukamycin related congeners **C2-C5** in the fermentation cultural broth based on LC-MS analysis (Fig. 6.2).

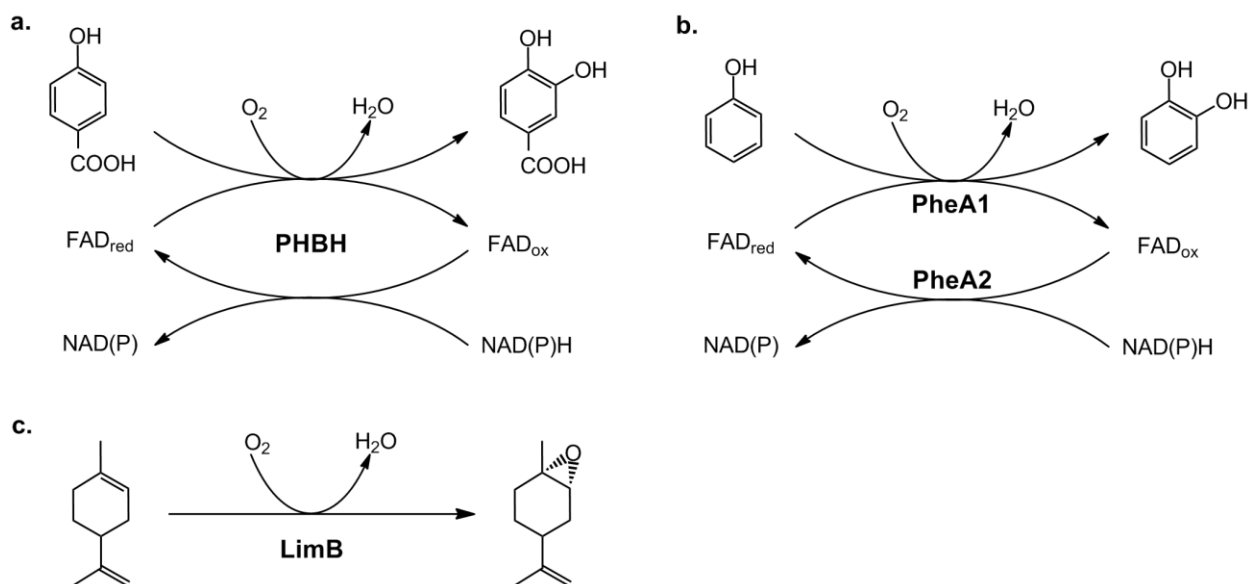


Figure 6.1 Reactions catalyzed by PHBD, PheA1/A2, and LimB.

AsuE2 is a homolog of the flavin reductase PheA2, which makes a FAD_{red} available to its hydroxylase partner PheA1 in the phenol hydroxylation in *Bacillus thermoglucosidasius* A7 (Fig. 6.1) [129]. Interestingly, a major amount of the protoasukamycin products **C1-C5** and a considerably lower yield of asukamycin **A1** were detected in the *asuE2* mutant (Fig. 6.2, 6.3). This result was rather unexpected and implied that the presence of the AsuE2 FAD reductase is required to support a full catalytic function of AsuE1, which is distinct to the bifunctional activity of PHBH.

The *asuE3* is highly related to the *limB*, encoding for a limonene 1, 2-monooxygenase, which opens the double bond of limonene and introduces an epoxide to form limonene-1, 2-epoxide in *Rhodococcus erythropolis* [130]. Neither asukamycin nor its congeners were detected in the *asuE3* mutant culture. Instead, a significant amount of a bright yellowish compound was accumulated and revealed a distinct retention time but with a similar UV absorption pattern of asukamycin **A1** by HPLC analysis (Fig. 6.2). A high resolution MS analysis suggested that one oxygen atom is missing in comparison with the asukamycin **A1**. ¹H-, ¹³C-, HMBC and HSQC NMR analysis of the purified compound pointed out that a signature alkene is positioned at C5 (152.5 ppm) and C6 (130.6 ppm) to replace the characteristic epoxide group of asukamycin **A1** (Table 6.1). This newly identified compound was assigned as 4-hydroxyprotoasukamycin **D1** (Fig. 6.3). Meanwhile, a group of 4-hydroxyprotoasukamycin related congeners **D2-D7** also presented in the fermentation culture based on the LC-MS analysis. **D1** was fed into the fermentation culture of the *asuA3* mutant and converted to asukamycin **A1**, which suggested that **D1** was indeed an intermediate and was further epoxidized by AsuE3 in the final biosynthetic step for asukamycin (Fig. 6.2).

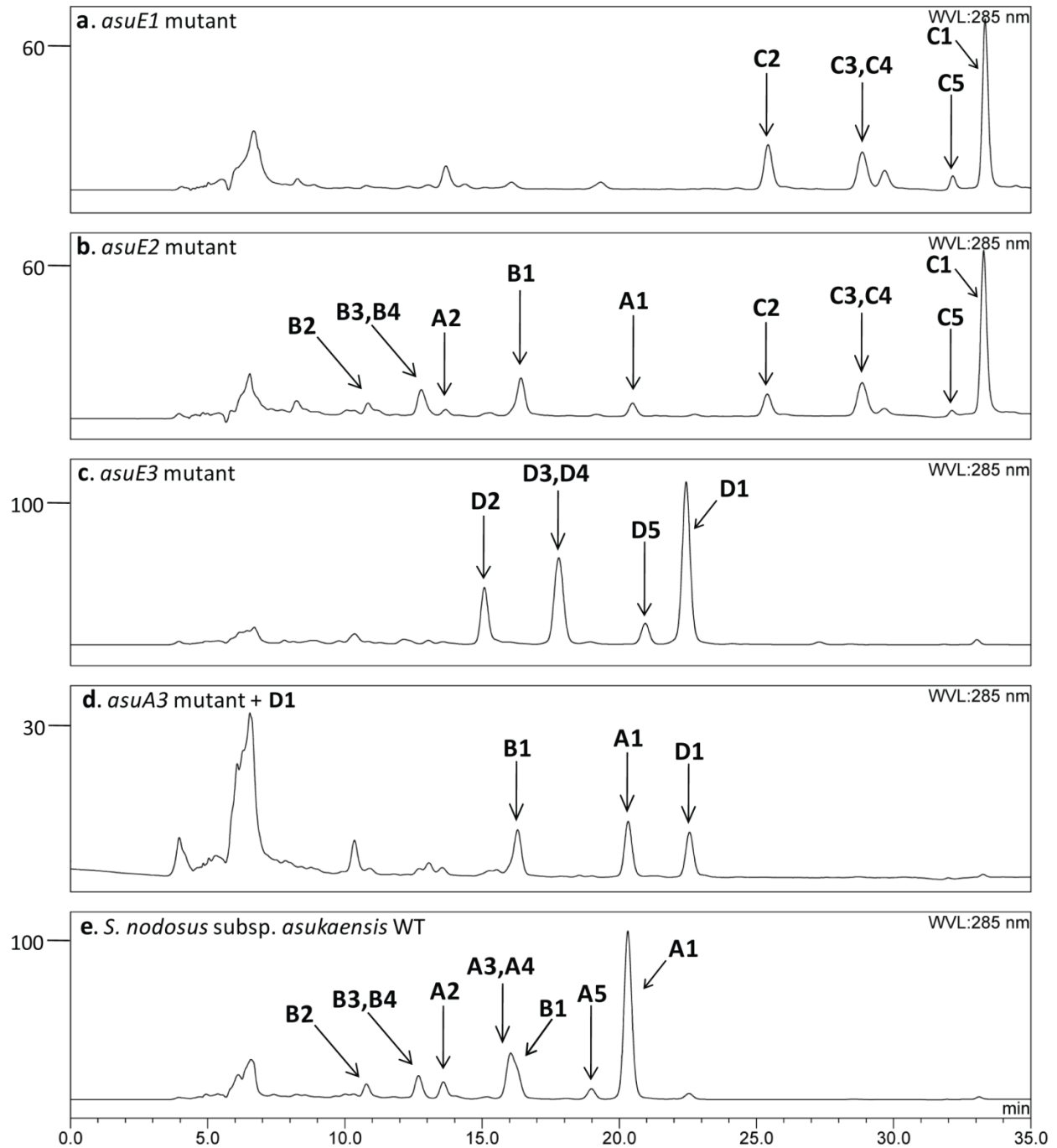


Figure 6.2 HPLC analysis of the *asuE1-E3* mutants. Twenty μ L of crude culture extract of the *asuD1* mutant (a), the *asuD2* mutant (b), and the *asuD3* mutant (c). Feeding *asuA3* mutant with pure D1 is shown (d). The arrows identify the peaks of A1-A5, B1-B4, C1-C5, D1-D5. The y axis indicates the absorbance abundance (mAu).

Table 6.1 NMR connectivities in 4-hydroxyprotoasukamycin (D1). NMR of **D1** acquired from 1J - and nJ -heteronuclear carbon-proton shift correlation methods (HSQC and HMBC).

Position	δ_C (ppm)	δ_H (ppm)	C,H-Coupling ^a
1	180.07	--	6-H, 0-NH, 5-H, 3-H
2	140.95	--	--
3	124.57	6.21 (d, $J=10.1$)	0-NH (w)
4	69.63	--	7-H, 3-H, 8-H, 5-H (w), 0-NH (w)
5	152.53	6.93 (dd, $J=10.0, 3.1$)	6-H, 7-H, 3-H (w)
6	130.64	7.62 (d, $J=2.95$)	5-H, 3-H, 7-H, 0-NH
7	137.64	5.80 (d, $J=15.5$)	6-H, 5-H, 3-H, 8-H, 9-H
8	131.12	6.48 (dd, $J=14.8, 11.8$)	9-H, 10-H
9	138.97	6.66 (dd, $J=14.8, 11.2$)	7-H, 8-H, 11-H
10	129.35	6.53 (dd, $J=15.37, 11.31$)	8-H, 11-H
11	141.23	7.07 (dd, $J=15.0, 11.6$)	10-H, 12-H
12	123.47	6.46 (d, $J=15.2$)	11-H, 10-H
13	164.94	--	14-NH
1'	164.94	--	0-NH, 2'-H
2'	123.85	6.51 (d, $J=15.2$)	3'-H, 4'-H
3'	141.23	7.15 (dd, $J=15.0, 11.6$)	2'-H, 4'-H, 5'-H
4'	128.53	6.30 (dd, $J=14.9, 11.7$)	3'-H, 2'-H, 6'-H
5'	140.59	6.63 (dd, $J=15.0, 10.9$)	3'-H, 6'-H, 7'-H
6'	127.67	6.18 (dd, $J=15.2, 10.9$)	4'-H, 5'-H
7'	144.84	5.90 (dd, $J=15.4, 7.0$)	5'-H, 9'/13'-H (w)
8'	40.46	2.08 (m)	6'-H, 7'-H, 9'/13'-H, 10'/12'-H
9',13'	32.10	1.70 (m), 1.09 (m)	10'/12'-H, 13'/9'-H, 7'-H, 11'-H
10',12'	25.39	1.26 (m), 1.68 (m)	11'-H, 9'/13'-H, 12'/10'-H
11'	25.60	1.13 (m), 1.63 (m)	10'/12'-H, 9'/13'-H
1''			
2''	113.57	--	
3''			
4''			
5''			
NH-14		9.20 (s)	
NH-0'		9.17 (s)	

^a. Indicated protons show connectivities to the given carbon attributed to 2J -, 3J - or weak 4J -coupling. (w) weak J -coupling.

^b. Coupling with 8'-H (2.08 ppm) was suppressed.

^c. ^{13}C -NMR and ^1H -NMR signals for C1'', C3'', C4'' and C5'' are undetectable in DMSO- d^6 .

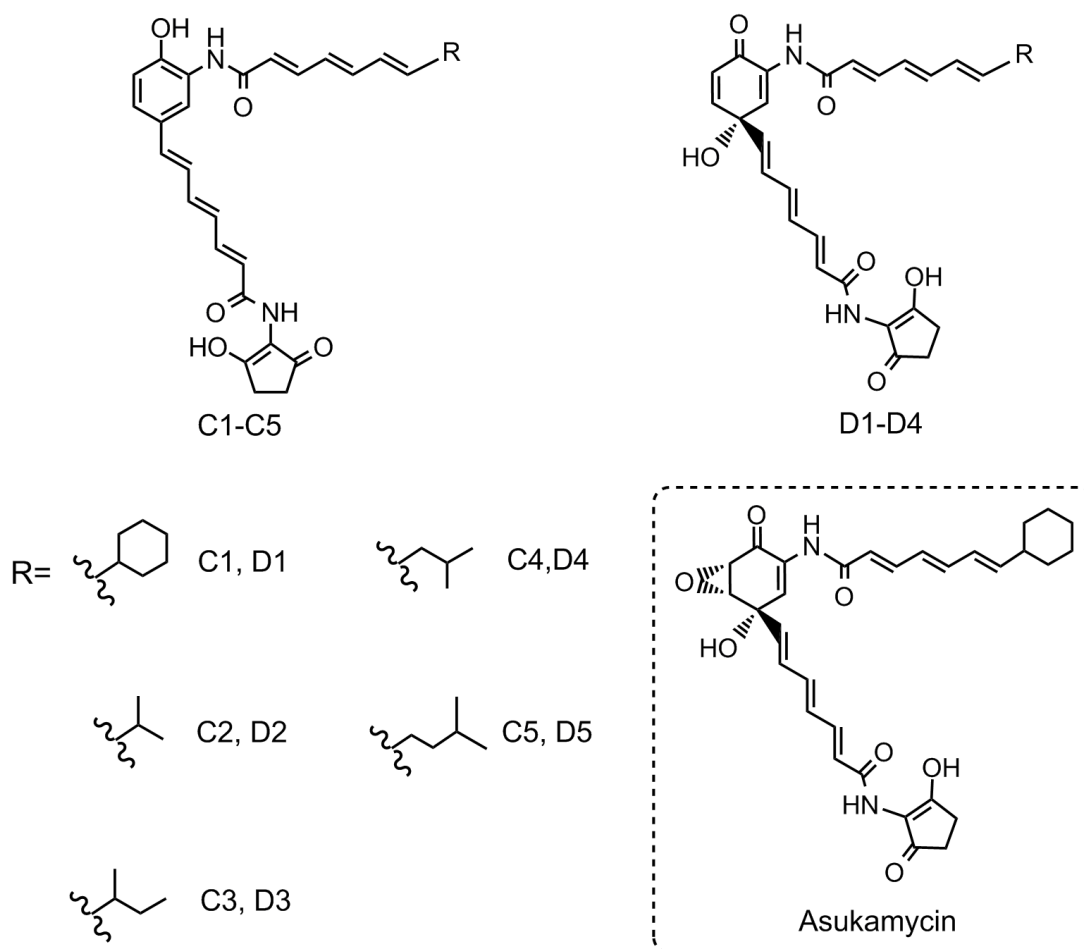


Figure 6.3 Structures of C1-C5, D1-D5.

Discussion

Both one-step dioxygenase and two-step monooxygenase mechanisms have been proposed for the epoxyquinol structure formation of the manumycin compounds [20, 38, 60]. The mutagenesis studies supported that the 4-hydroxyl group is introduced to protoasukamycin **C1** to give a 4-hydroxyprotoasukamycin intermediate **D1** through the actions of AsuE1 and AsuE2, and AsuE3 further introduces an epoxide to replace the C5,6-double bond of **D1** to form asukamycin **A1** (Fig. 6.4). The **C1** hydroxylation is catalyzed by AsuE1, whose full function requires the AsuE2 FAD reductase, possibly by using a reductive cofactor NAD(P)H. and the FAD reduction by AsuE2, possibly using a reductive cofactor NAD(P)H, is required for a full

function of AsuE1. Since the intermediate **D1** was not detected in the *asuE2* mutant, it is less likely that the AsuE3 epoxidation depends on the presence of AsuE2.

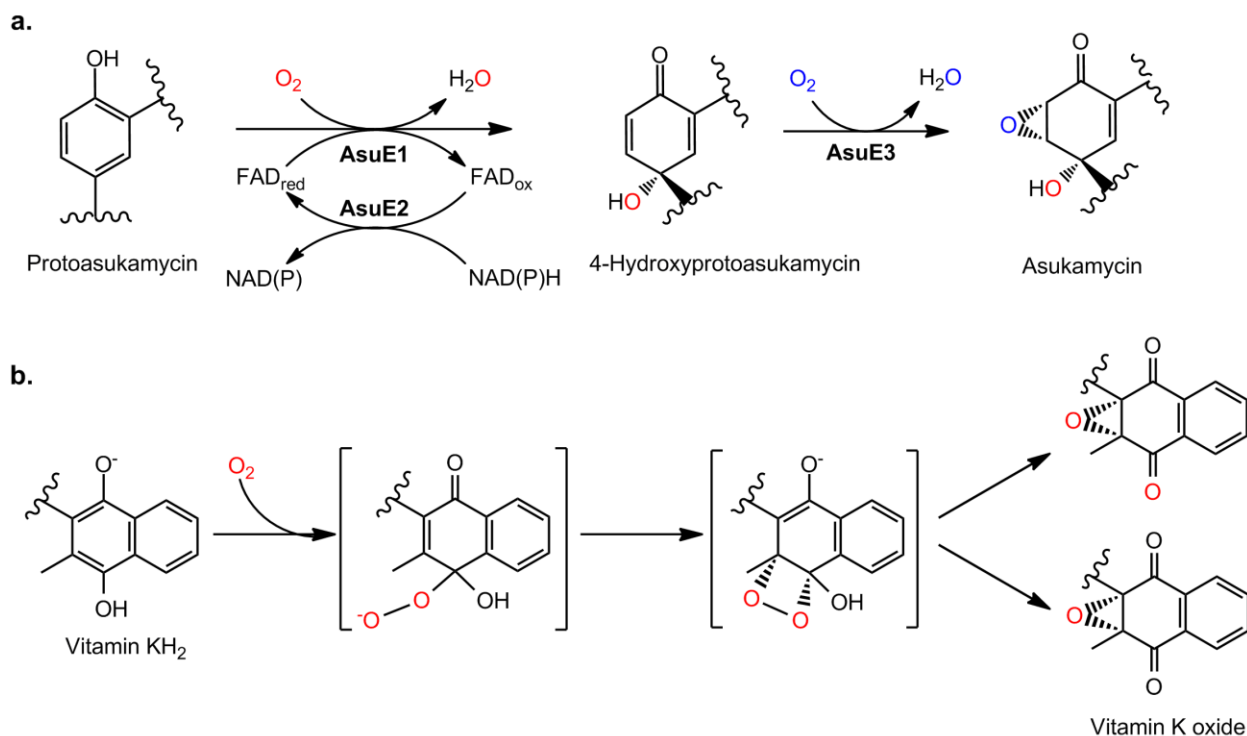


Figure 6.4 A comparison of two-step monooxygenase and one-step dioxygenase mechanisms for the respective asukamycin and vitamin K oxide biosynthesis.

As AsuE3 acts specifically on the cyclohexa-2,5-dienone moiety but not a phenol like structure, the protoasukamycin 4-hydroxylation to offer a constrained C5,6-double bond is critical for the epoxidation. Correspondingly, the *mmyO*, encoding an AsuE3-related epoxidase, was also found in the deposited methylenomycin A biosynthetic gene cluster of *Streptomyces coelicolor* A3(2) [131, 132]. MmyO could have a function in the epoxidation of the desepoxy-4,5-didehydromethylenomycin A to form methylenomycin A (Fig. 6.5). Evidently, the upper chain substituted by an acetyl group and the absence of the C₅N moiety have little impact on the catalytic function of AsuE1,E2,E3 in the epoxyquinol formation as observed for **A8** and **A1a**, respectively. Both the identified **C1** and **D1** could serve as proper substrates to address the detail catalytic aspect of the AsuE1, AsuE2 and AsuE3 enzymes for the further studies.

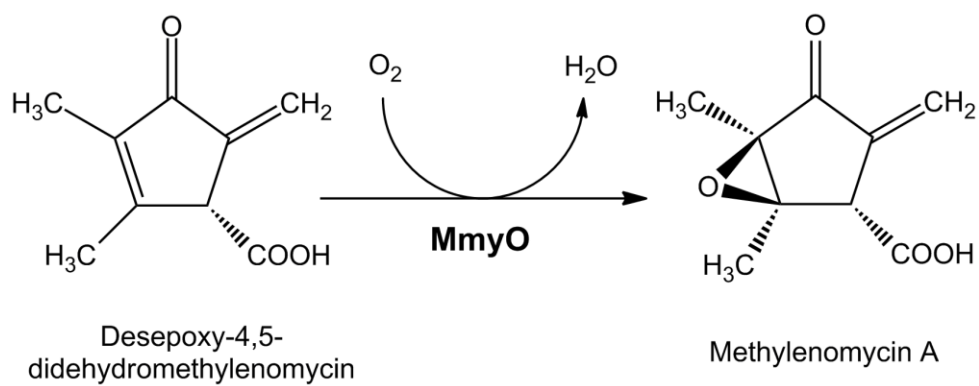


Figure 6.5 The proposed function of MmyO in methylenomycin A biosynthesis.

CHAPTER SEVEN:

A TYPE TWO THIOESTERASE AND OTHER ASUKAMYCIN BIOSYNTHETIC GENES

Background of Thioesterases

Based on the functional and structural diversity, the thioesterases in metabolic pathways are categorized into three groups, type I, type II, and the hotdog-fold thioesterases. Frequently located at the C-terminus of the polyketide synthase (PKS) or non-ribosomal polypeptide synthase (NRPS) complexes, type I thioesterase (TEI) acts to release the polyketide or polypeptide chain from the carrier protein module, either by direct hydration of the thioester linkage or by a specific intramolecular cyclization [133-135].

Distinct from TEI, the discrete type II thioesterase (TEII) mostly removes the undesirable acyl or aminoacyl residues from the catalytic enzyme complex caused by a priming or processing error, as these mischarged enzymes can hold back the entire biosynthetic progress (Fig. 7.1) [136-139]. Given a high fidelity, an error occurred in any step of the assembly line may cause the accumulation of the unprocessed molecule-enzyme complex, and severely block the entire biosynthetic process. TEII plays a surveillance role and revives the mischarged carrier protein domain, to provide the opportunity for a wanted acyl or aminoacyl unit to bind, as the yields of the polyketide and polypeptide products were often considerably impaired in the knockout mutants [138, 140-142]. For example, there is 5% of DKxanthenes accumulated in the TEII-deficient *dkxO* mutant compared with the wild type strain of *Stigmatella aurantiaca* DW4/3-1 [143]. Besides, the truncation of the McyT TEII resulted in a 95% decreased yield of microcystin in *Planktothrix agardhii* [144]. In some situation, TEII can also remove a true intermediate from the intermediate-protein complex. For example, NikP2 TEII tends to discharge β -hydroxyl-His from the peptidyl carrier protein NikP1 complex in nikkomycins X/I synthesis of *Streptomyces tendae* Tü901 [145].

The hotdog-fold thioesterases consist of a long α -helix wrapped around by five or six

anti-parallel β -sheets, reminiscent of a hotdog. They are mainly known to hydrolyze the CoA or the carrier protein-tethered acyl substrates for the breakdown of aromatic compounds [146, 147]. Not much is known for the rest of family members.

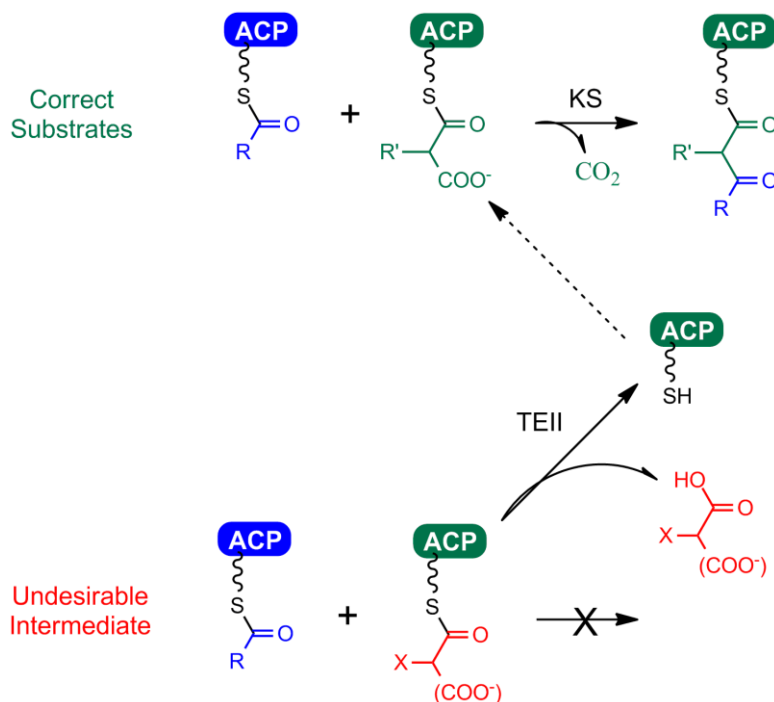


Figure 7.1 Proposed functions of type II thioesterases (TEII). The correct substrates are indicated in green; the undesirable intermediate are shown in red.

Results

Thioesterase Affects the Primed CHC

Located near the border of the *asu* cluster, the *asuC15* is closely related to a group of TEII coding genes found in the polyketide and non-ribosomal peptide biosynthetic gene clusters, including RifR and SrfD involved in the rifamycin biosynthesis of *Amycolatopsis mediterranei* and the surfactin formation of *Bacillus subtilis*, respectively [140, 148]. Mutation and biochemical studies indicated that RifR and SrfD discharge the unwanted acyl and aminoacyl residues from the carrier protein modules in the assembly lines of rifamycin and surfactin, respectively. Interestingly, the *asuC15* mutant produced a normal amount of asukamycin **A1**, yet

the yield of the congeners **A2-A7** was significantly reduced (Fig. 7.2). This incident is more evident by measuring up to 10 times higher production of the CHC-primed asukamycins than the total branched acyl-CoA initiated congeners, unlike a relatively equal distribution observed in the wild type strain. Since CHC-CoA is not only a building block of asukamycin but can also form ω -cyclohexyl fatty acids as membrane components in *S. nodosus* subsp. *asukaensis* [10], we analyzed the fatty acid compositions of the *asuC15* mutant and the wild type strain by GC-MS (Fig. 7.3, Table 7.1). Notably, 16.5% of ω -cyclohexyl-undecanoic acid (cyclohexyl-C₁₇) was detected in the *asuC15* mutant, which is at least five-fold higher than the 3.1% detected in the wild type strain. Moreover, 1.7% of ω -cyclohexyl-tridecanoic acid (cyclohexyl-C₁₉) fatty acid, which is undetectable in the wild type strain, was also found.

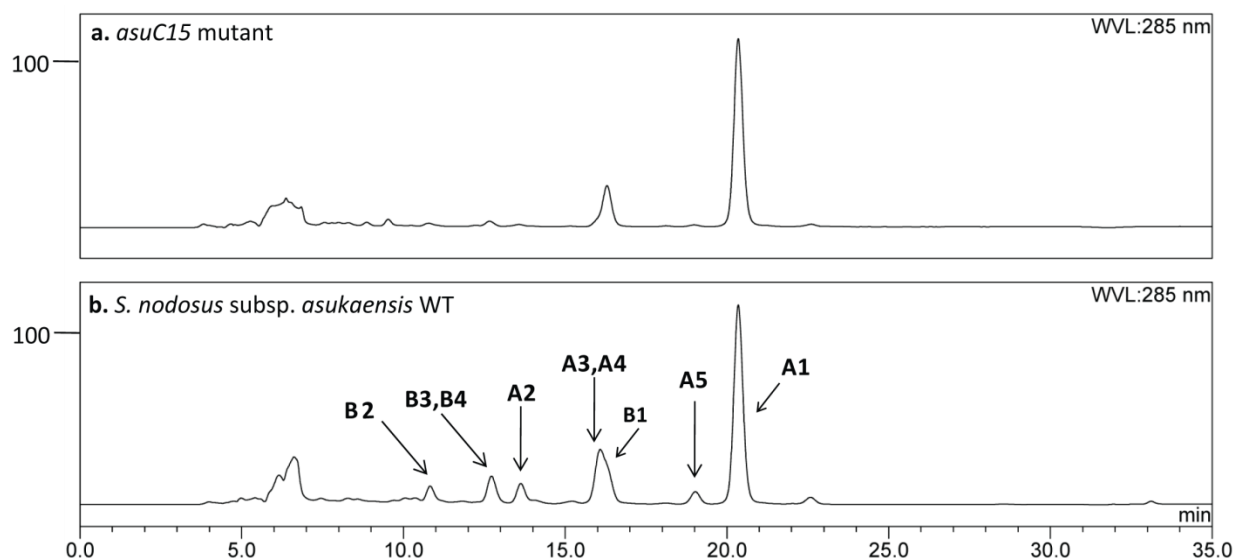
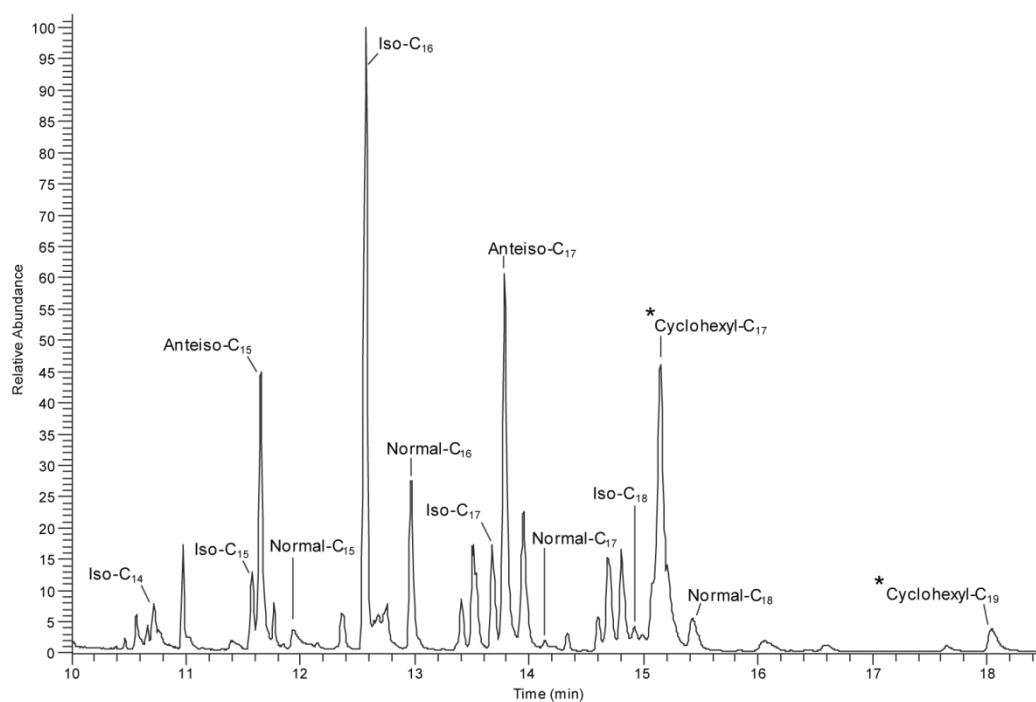
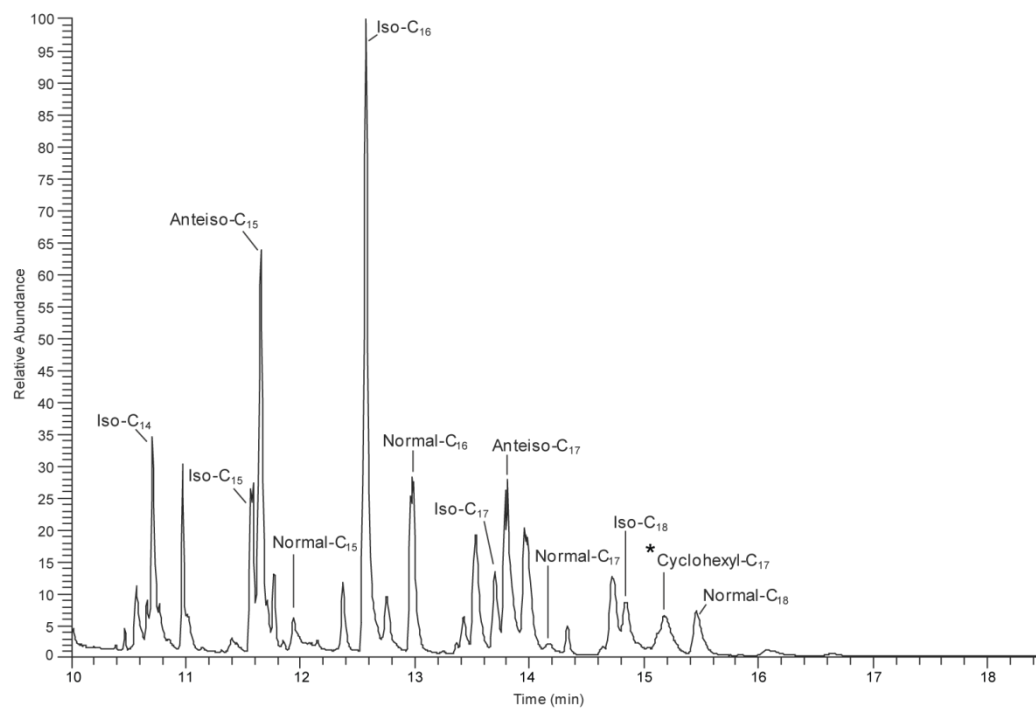


Figure 7.2 HPLC analysis of the *asuC15* mutant and the *S. nodosus* wild type strain. The arrows identify the peaks of asukamycin **A1** and related metabolites, **A2-A5**, **B1-B4**.

a. *asuC15* mutant



b. *S. nodosus* subsp. *asukaensis* wild type



* ω -cyclohexyl fatty acids

Figure 7.3 Fatty acid profiles generated by GC-MS analysis. The identified fatty acid derivatives are indicated.

Table 7.1 Fatty acid composition of *S.nodosus* wild type strain and the *asuC15* mutant.

Fatty acid	Retention time (min)	Wild type	<i>AsuC15</i> mutant
Iso-C ₁₄	10.71	10.84%	2.18%
Normal-C ₁₄	11.04	6.99%	0.00%
Iso-C ₁₅	11.57	6.20%	2.97%
Anteiso-C ₁₅	11.66	17.40%	12.22%
Normal-C ₁₅	11.93	1.52%	1.13%
Iso-C ₁₆	12.57	29.68%	28.54%
Normal-C ₁₆	12.97	9.59%	8.38%
Iso-C ₁₇	13.68	3.68%	5.09%
Anteiso-C ₁₇	13.78	7.76%	18.08%
Normal-C ₁₇	14.14	0.47%	0.59%
Iso-C ₁₈	14.92	0.07%	0.58%
Normal-C ₁₈	15.43	2.72%	2.01%
Cyclohexyl-C ₁₇	15.15	3.06%	16.52%
Cyclohexyl-C ₁₉	18.04	0.04%	1.71%

Other *asu* Gene Functions

The AsuC6, a second thioesterase-like protein, belongs to the type of hotdog-fold thioesterases, which presumably have a role to hydrolyze the thioester bond and release the acyl intermediate from the PKS enzyme complex [146, 147]. The *asuC6* mutant has not yet been constructed and the precise function of AsuC6 function remains to be clarified. Located between the *asuR* group genes and *asuE1*, *asuC1* encodes for a phosphopantetheinyl transferase (PPTase), which likely primes the apo-ACP by the covalently attaching a 4'-phosphopantetheine moiety of CoA to give a holo-ACP. Since bacteria always utilizes orthogonal carrier protein recognition as a strategy to distinguish primary metabolism from secondary metabolism [149], AsuC1 might be

a dedicated PPTase to prime the *asu* ACPs, AsuC5, C11 and C12, involved in the lower and upper chain biosynthesis.

AsuM1, a homolog of numerous antibiotic efflux exporters, could release the synthesized asukamycin products from the cells. *AsuR1-R6*, discretely detected at the two border regions of the cluster, show homology to numerous putative transcriptional regulator genes found in Gram-positive bacteria. AsuR1 and AsuR6 are closely related to the LuxR-type transcriptional regulators [150]. AsuR2 is likely a TetR-like transcriptional regulator [151]. AsuR3 is a putative integral membrane sensor protein, which could work together with the DNA binding protein AsuR4 [152]. AsuR5 belongs to the *Streptomyces* antibiotic regulatory proteins (SARP) [153]. As many antibiotic biosynthesis gene clusters contain one or multiple regulatory genes, AsuR1-R6 could have regulatory functions to control the asukamycin biosynthetic gene activities. AsuH1 is a putative ORF with an unknown function.

Discussion

CHC-CoA is not only the substrate for the PKS AsuC3,C4 in **A1** upper chain assembly, but is also recruited by the FAS complex and assembled into ω -cyclohexyl fatty acids which account for 3.1% of total cellular fatty acids in *S. nodosus* subsp. *asukaensis* [10]. The CHC-CoA utilization to form asukamycin **A1** and ω -cyclohexyl fatty acids does not occur in a fixed ratio, as **A1** was increased to more than 80% of total asukamycins, while ω -cyclohexyl fatty acids were kept under 25% of total fatty acids upon feeding excess cyclohexanecarboxylic acid [10]. For this inconsistent incorporation rate of the CHC substrate to the cellular membrane fatty acids and the asukamycin products, one explanation is the distinct substrate specificities of FabH and AsuC3,C4. While FabH prefers the branch chain acyl-CoA starters, AsuC3,C4 favors the CHC-CoA. A second reason is likely the AsuC15 TEII action to release the tethered

cyclohexylpropanoate from the FAS-ACP and allow the recruitment of more branched chain acyl-CoA starters, as the percentage of ω -cyclohexyl fatty acids was increased five-fold in the *asuC15* mutant. The cellular membrane fluidity is probably affected by variations in the content of ω -cyclohexyl fatty acids via changing the phase transition temperature, as observed for several thermo-acidophilic bacteria, which may contain up to 90% of ω -cyclohexyl fatty acids [65, 66, 154]. Thus AsuC15 could suppress excessive ω -cyclohexyl fatty acid formation, which helps to maintain the membrane homeostasis and structural integrity, particularly when the cellular level of CHC-CoA is rising. Evidently, AsuC15 can also discharge the CHC-acyl intermediate from AsuC5-ACP to enhance the production of congeners **A2-A4**, as the *asuC15* mutant predominantly accumulates **A1**, rather than an equal amount of **A1** and **A2-A4** observed in the wild type.

AsuC6, the other thioesterase in the *asu* cluster, is a hotdog-fold thioesterase. The most studied hotdog-fold thioesterase, the PaaI from *E. coli*, hydrolyzes the phenylacetyl-CoA to liberate CoA from the dead-end products [146]. Similarly, the AsuC6 could be responsible for **A1a-A5a** accumulation in the *asuD1*, *D2* and *D3* mutants, which are supposed to be tightly bound to the ACP AsuC11 in the absence of a thioesterase (Fig. 7.4). In fact, as the coronatine and aminocoumarin biosynthesis involve amide-bond formation between an amine with the free acid substrates rather than a carrier protein tethered acyl group [155, 156], the similar acylation of the C₅N moiety could require a free carboxylic acid rather than a carrier protein tethered lower chain intermediate. If so, AsuC6 could release the triene lower polyketide from the carrier protein in the wild type strain (Fig. 7.4). This seems contradictory to the previous **A1a** feeding experiments, which ruled out the lower polyketide intermediate containing free carboxylic group, [20]. However, the feeding result should be treated with caution, as the non-incorporation could result from a low permeability of the fed compound.

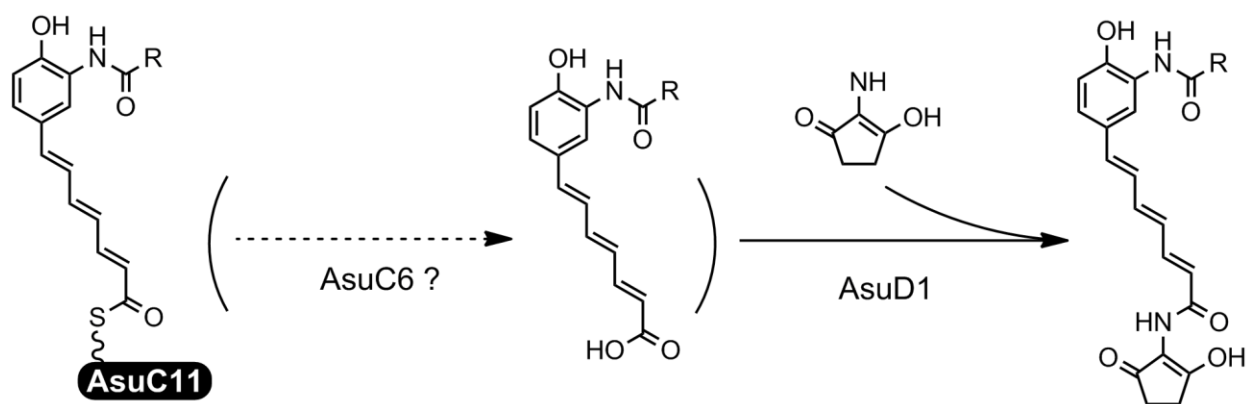


Figure 7.4 The proposed function of AsuC6.

CHAPTER EIGHT:
SUMMARY AND FUTURE PROSPECT

Summary

Prior to this study, the extensive feeding experiments have been performed to reveal the biosynthesis of manumycin A and asukamycin. The structure elements of asukamycin, including a mC₇N core, a cyclohexane moiety, and a C₅N ring, were proposed to arise from the corresponding 3,4-AHBA, shikimic acid, and 5-ALA [20, 60, 157]. The lower and upper triene polyketide chains are likely built up from 3,4-AHBA and CHC-CoA, respectively, through three steps of classical polyketide condensations. However, the biosynthetic genes involved in 3,4-AHBA, CHC-CoA, and triene chain assembly of asukamycin, have yet been uncovered. Until now, the *asuD2* (*hemA-asuA*) was the only reported gene to work on the C₅N moiety biosynthesis of asukamycin [21]. As the epoxyquinoid structure of the mC₇N core is essential for the biological activities for the manumycin metabolites, the post-assembly oxygenation of protoasukamycin also attracts massive attention [20, 38, 76].

In this study, the cloning, mutagenic analysis and characterization of the asukamycin biosynthetic genes have been carried out in *S. nodosus* subsp. *asukaensis* (Fig. 8.1). To summarize, the lower polyketide chain is initiated with 3,4-AHBA, the condensation product of ASA and DHAP through the catalytic activities of AsuA3 and A1, while the upper chain is started with the CHC-CoA, which is derived from the shikimate precursor by the action of the AsuB group enzymes. The 3,4-AHBA is adenylated by AsuA2, loaded on the ArCP AsuC12, and consecutively condensed with three malonyl extenders by PKS AsuC13,C14 and the corresponding reducing enzymes, KR AsuC7 and DH AsuC8,C9, to give a *trans* triene. Concomitantly, the CHC-CoA is primed by a set of PKSIII AsuC3,C4 and extended with two additional malonyl-CoA to form a *trans* triene upper chain. The ACP tethered lower chain intermediate is linked with the polyketide upper chain by AsuC2, and further attached with a

nascent C₅N moiety by AsuD1-D3. The resulted protoasukamycin is subsequently introduced a hydroxy and an epoxide groups by AsuE1/E2 and AsuE3, respectively, to form the final product asukamycin. Moreover, the AsuC15 type II thioesterase has a function to suppress the formation of ω -cyclohexyl fatty acid byproducts and likely maintain the homeostasis of the cellular membrane. Besides, a plausible crosstalk of the biosynthesis between the fatty acids and the asukamycin metabolites is also proposed.

Future Prospects

The manumycin metabolites hold great promise in pharmaceutical treatments due to their unique structural moieties. In this work, the genetic and biochemical results set a stage for the further work to investigate the molecular mechanism of each catalytic step, especially, the pathway-specific biosynthetic enzymes. This information not only allows us to identify and study the biosynthetic enzymes for other manumycin metabolites, but also shed lights on the further bioengineering of the manumycin family compounds.

The Uncharacterized Asukamycin Biosynthetic Genes

Although a majority of the *asu* genes have been investigated by mutagenesis or biochemical analysis, the functions of several biosynthetic genes remain elusive. To access these genes, we can take advantage of the established pART1391 to construct a gene-knockout series of the pART1391 derivatives, which can be introduced and expressed in *S. lividans*, following a similar procedure to the case for pART1361-E3 described in chapter 6. If the corresponding transformant strains display distinct metabolic profiles compared with that of the wild type, these genes could be critical for the asukamycin biosynthesis.

Located downstream of *asuC13*, the *asuC14* encodes a protein highly related to PKS AsuC13, except for a truncated N-terminus and lack of a putative catalytic triad. To address the

function role of AsuC14, we can create an *asuC14* mutant, which might fail to give any asukamycin product if AsuC14 function together with AsuC13 on the Claisen condensation. As the iterative type II PKS is frequently paired with its ortholog, a chain length factor (CLF), it is likely that AsuC14 forms a confined tunnel with AsuC13 to accommodate the growing triene polyketide. Under this assumption, the *asuC14* mutant could generate a new set of asukamycin derivatives with various lower chains, such as diene, tetraene, or pentene.

AsuC6, a hotdog-fold thioesterase, could also play a role in controlling the lower chain biosynthesis. This functional activity of AsuC6 can be verified by gene inactivation. If the majority of asukamycin production was abolished by this mutation, AsuC6 could catalyze the hydrolysis of the thioester bond to release the lower polyketide from the ACP AsuC11 (Fig. 7.4). In this case, it is worthwhile to question whether AsuC6 has a substrate preference towards the triene chain to a premature diketide or triketide intermediate. Therefore, a series of di-, tri-, and tetraaketides can be synthesized and linked to the CoA analog, *N*-acetyl cysteamine (SNAC), for a further *in vitro* enzymatic evaluation, where a significantly higher catalytic activity on the tetraaketide than the di- or triketide would suggest the participation of AsuC6 in the chain length control.

The only set of the PKS reducing enzymes in the *asu* cluster, the ketoreductase AsuC7 and the dehydratases AsuC8,C9, were proposed to function in the compilation of the triene polyketides. The *asuC7* or *asuC8,C9* mutants likely fail to produce asukamycin and congeners. These mutants may only accumulate 3,4-AHBA rather than the asukamycin derivatives containing trioxo- or trihydroxy-polyketide chains, as the downstream type II PKS AsuC13,C14 may reject the 3-oxodiketide or 3-hydroxydiketide intermediates, which seize the *asu* ACPs and block the downstream synthesis. Besides, the plausible involvement of AsuC7 and AsuC8,C9 in the upper chain biosynthesis can also be justified by checking the presence of **E1** and **E3/E4**

metabolites accumulated in the mutants. If so, the absence of these reducing enzymes should ultimately add to the production of cyclohexyl fatty acids, or even form the 3,4-AHBA initiated fatty acids. To date, there is no reported 3,4-AHBA initiated fatty acids, which might be detected in the *asuC7* mutant, *asuC8,C9* mutant, or the previously constructed *asuA2* and *asuC11C12* mutants.

Besides these structural biosynthetic genes, the resistant genes have yet been clarified in the *asu* cluster. Functional expression of the pART1391 in *S. lividans* indicated that these cloned *asu* genes are sufficient to convey the self-immunity of asukamycin. A major facilitator superfamily (MFS) transporter, AsuM1, has been found and proposed to serve as an antibiotic efflux transporter to free the nascent asukamycin products from the cells. The *asuM1* can be inactivated in pART1361 and pART1361-E3 to give the pART1361-M1 and pART1361-E3M1, respectively, which were separately introduced into *S. lividans*. Presumably, the transformant carrying a pART1361-M1 is lethal, or displays severe growth retardation, while the pART1361-E3M1 may produce 4-hydroxyprotoasukamycins, **D1-D5**, as a quinol structure of the premature **D1-D5**, unlike the expoxyquinol core of asukamycin, exhibits no cytotoxicity.

Mutation study indicated that the AsuC15 TEII suppresses the formation of the ω -cyclohexyl fatty acids and likely maintains the homeostasis of the cellular membrane. We assumed that AsuC15 releases the tethered 3-cyclohexylpropanoate from the FAS-ACP, which allows the recruitment of the branched chain acyl-CoA starters. To confirm this novel activity, the *asuC15* can be cloned into the shuttle vector pIJ622 under the control of the constitutive *ermE** promoter to generate pART1401, which is further expressed in *S. lividans*. The resulted transformant of *S. lividans*/pART1401 can be fed with cyclohexanecarboxylic acid and analyzed the cellular level of ω -cyclohexyl fatty acids, which is expected to be lower than that in the *S. lividans* carrying a control empty vector. Moreover, we can perform an enzymatic assay using

the recombinant AsuC15 to hydrolyze the 3-cyclohexylpropanyl-ACP, which could be synthesized from a 3-cyclohexylpropanyl-SNAC and a FAS-ACP by the malonyl-CoA:ACP transacylase SgFabD of *Streptomyces glaucescens* [158]. AsuC15 should display higher catalytic activity towards the 3-cyclohexylpropanyl-ACP than a butyryl-ACP or 4-methylpentanoyl-ACP, the ubiquitous intermediates for *Streptomyces* fatty acid biosynthesis.

The Biosynthesis of Other Manumycin Metabolites

Despite that the biosynthetic genes involved in the C₅N moiety and CHC-CoA assemblage are closely positioned and appears to be co-transcribed, many functionally related *asu* genes are not organized in an apparent order in the cluster (Fig. 2.1). For instance, the key genes *asuA1* and *asuA3* performing the 3,4-AHBA formation are alienated by eight unrelated ORFs and belong to two separated transcription units, whereas the equivalent *griI* and *griH* position side by side and possibly share the same transcript engaged in the grinoxone production in *S. griseus* [59]. This implies that the acquired asukamycin biosynthesis has evolved through multiple horizontal gene transfer events and possibly an extensive genomic rearrangement in *S. nodosus*, which could be further confirmed by comparison with other closely related manumycin biosynthetic gene clusters.

As the majority of other manumycin metabolites share an mC₇N core as well as a C₅N moiety, we can probe with the *asuA*, *asuD*, and *asuE* group genes to find the corresponding biosynthetic genes, such as the ones for manumycin A and colabomycin from *S. parvulus* Tü64 and *Streptomyces griseoflavus* Tü2880, respectively. Notably, *S. griseoflavus* Tü2880 produces solely colabomycins that possess a *trans* tetraene lower polyketide, while *S. nodosus* accumulates asukamycins and congeners containing an identical lower triene chain. This structural disparity of triene and tetraene suggests that these two strains employ distinct enzyme systems to control the length of the lower polyketide chain (Fig. 8.2). The colabomycin producer

might develop the specified type II PKS components to set up a larger binding pocket than that of the AsuC13,C14, to accommodate a tetraene polyketide chain. In addition, a hotdog-fold thioesterase could play a key role to release the ACP tethered tetraene rather than triene for the colabomycin lower chain assembly.

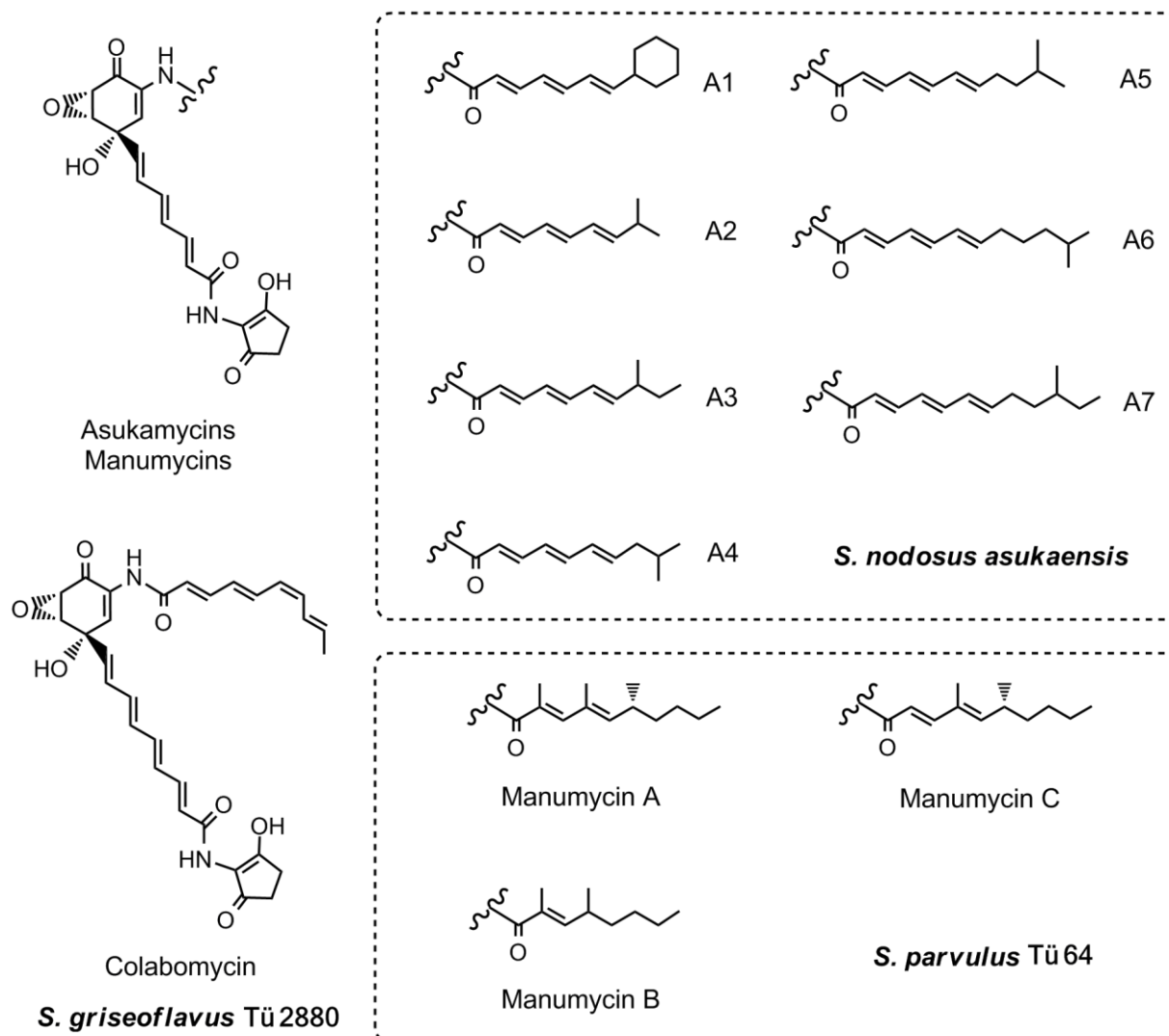


Figure 8.2 Structures of manumycin metabolites from *S. nodosus asukaensis*, *S. parvulus* Tü64, and *S. griseoflavus* Tü2880.

The most diverse building block of the manumycin metabolites is the upper polyketide chain. Instead of a CHC-primed triene chain, manumycin A-C opens the upper tetraketide assembly using an ACP-tethered butyryl substrate, likely a fully-reduced fatty acid intermediate

resulted from the action of FabH in *S. parvulus* (Fig. 8.2). Butyryl-CoA is also employed as a building starter of several polyketide products, including R1128 [159], murayaquinone [160], FD-594 [161], and sulfurmycinone [162]. After the initiation process, the nascent diketide intermediates of manumycin A and B are further extended through three and two runs of condensations using methylmalonyl-ACPs, respectively. Alternatively, manumycin C differs from manumycin A at the third extender unit, a malonyl-ACP rather than the methylmalonyl-ACP. This promiscuity could be resulted from three aspects: 1). a limited supply of the methylmalonyl substrate; 2). a low stringency of the polyketide condensation enzyme; 3). a low specificity of the downstream amide synthase, an *AsuC2* homolog. To test the first possibility, an extra amount of methylmalonate and malonate can be add to the culture of *S. parvulus*, and an increasing production ratio of manumycin A against B and C could specify the consequence due to a shortage of methylmalonyl substrate. Since the condensation enzymes involved in asukamycin upper chain formation has not been fully addressed, it is worthwhile to target other PKS genes in the manumycin gene cluster. Besides, we should be aware of the amide synthase, a *asuC2* homolog, which could process a premature triketide to form manumycin C. Furthermore, the saturated configuration on the C5,C6 position of the manumycin A upper chain is expected to arise from the action of an additional reductase, which could function independently or immediately after the formation of the diketide with a fixed stereospecificity.

Synthesis of the Unnatural Asukamycin Metabolite

To expand the diversity of the metabolites, one approach is to supplement the synthetic precursors to fermentation cultures. For example, the alicyclic carboxylates with a variable ring size has been fed and resulted in the production of the novel asukamycin analogs, containing various cyclic ring structures to substitute the cyclohexane moiety in *S. nodosus* [10]. However,

this could be ineffective due to the competition between these synthetic precursors and the natural CHC-CoA. In this study, the constructed *asuB1* mutant, which failed to form the CHC-CoA, provides a better platform for these feeding approaches mentioned above than the wild type strain.

Moreover, the constructed *asuA3* and *asuA1* mutants with the 3,4-AHBA deficiency can be used to synthesize many asukamycin analogs by feeding 3,4-AHBA analogs, such as 3,5-AHBA, 3-aminobenzoic acid (Fig. 8.3). These analogs bear a distinct core structure to replace the native mC₇N moiety, which could lead to novel biological activities, as the epoxyquinoid feature was proposed to convey the antimicrobial activities for manumycin metabolites. Besides, these feeding experiments can also justify the specificity of the AsuE1-E3 oxygenases, in which the oxidized core points toward that these oxygenases are capable of processing the corresponding 3,4-AHBA derivative.

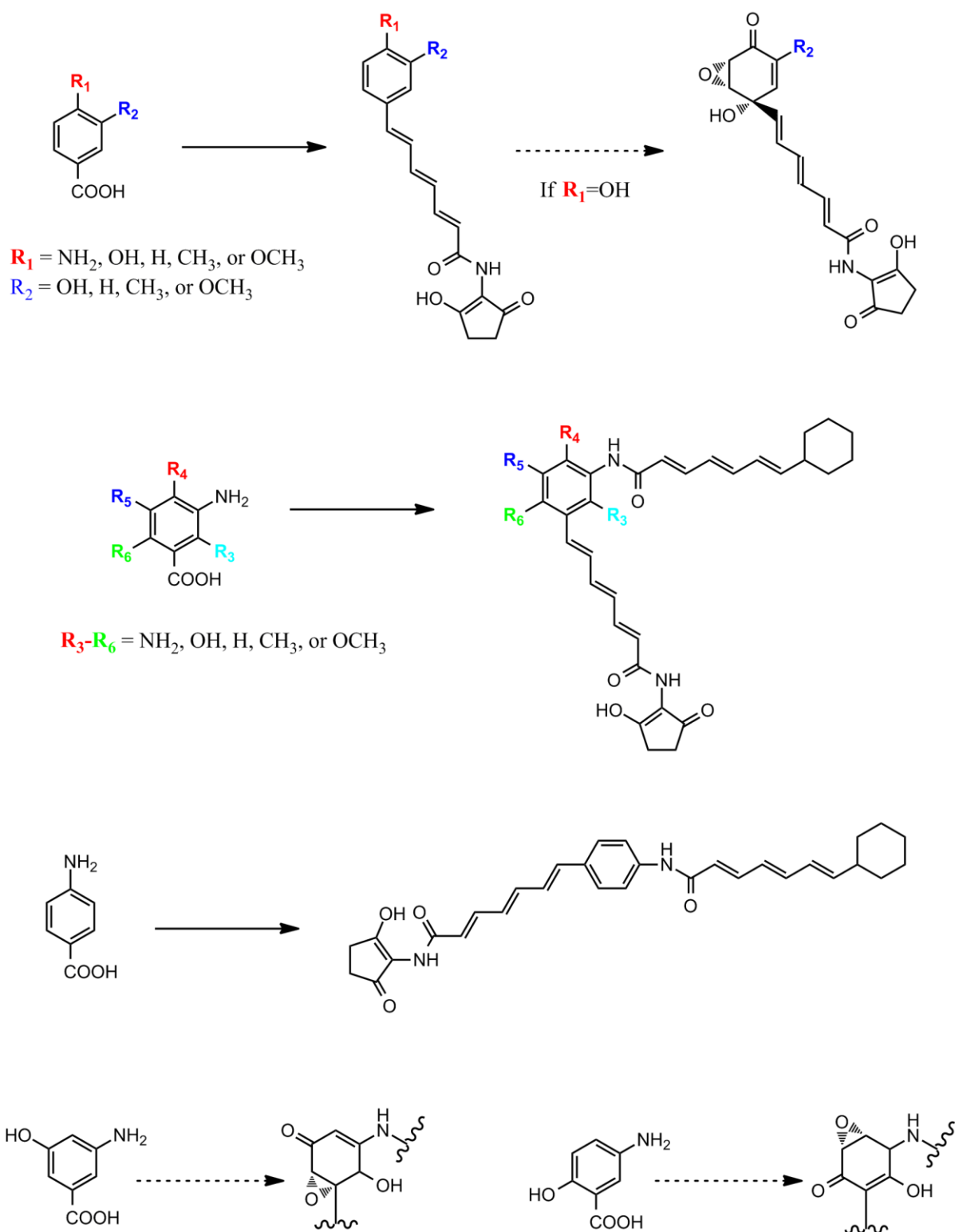


Figure 8.3 Confirmed or postulated asukamycin analogs obtained by feeding the *asuA3* or *asuA1* mutants with diverse aromatic precursor. The solid arrows indicate previously reported or partially confirmed feeding results, while the dashed arrows show the possible derivatives.

CHAPTER NINE:
MATERIALS AND METHODS

Bacterial Strains and Chemicals

S. nodosus subsp. *asukaensis* ATCC 29757 was obtained from the American Type Culture Collection. *S. lividans* K4-114 was kindly provided by Dr. C. Khosla. *E. coli* strains were obtained from the John Innes Center (Norwich, UK). Media and chemicals were purchased from Difco, Sigma Aldrich and EMD. All chemicals and solvents were of reagent or HPLC grade and were used without further purification unless otherwise mentioned.

Fermentation and Analysis of the Asukamycin Metabolites

Fermentation and Feeding Experiments

Wild type and mutant strains of *S. nodosus* subsp. *asukaensis* were cultivated with freeze storage spores in 25 mL YMG medium in 250 mL baffled flasks with coil on a rotary shaker at 250 rpm and 28 °C for 2-3 days [20, 110, 163]. The presence of the asukamycin products was confirmed by the bioassay against the growth of *Staphylococcus aureus*. *S. lividans* K4-114 recombinant strains were cultured in 25 mL R5 or MS medium for 4-5 days [163]. If required, the media were supplemented with the selective antibiotics at following the concentrations: apramycin (50 µg/mL); kanamycin (20 µg/mL); spectinomycin (50 µg/mL). Feeding experiments with 3,4-AHBA (100 µg/mL) and 4-hydroxyprotoasukamycin (20 µg/mL) were conducted by adding these compounds to one day-old cultures and harvesting one day later.

HPLC and LC-MS Analysis

Fermented cultures were mixed thoroughly with an equal volume of ethyl acetate. Separated by centrifugation, the ethyl acetate layer was collected and evaporated to near dryness. The crude extract was dissolved in an equal volume of methanol and analyzed using a P680 HPLC system (Dionex, Sunnyvale, CA USA) and an XTerra RP18 column (4.6 X 250 mm, Waters) at a flow rate of 0.5 mL/min at 25 °C. Twenty µL of crude extract were injected,

equilibrated with 65% solvent B (acetonitrile with 0.1% formic acid) in solvent A (water with 0.1% formic acid) for 5 min, developed with a gradient of 65-90% solvent B in solvent A for 20 min and washed with 90% solvent B in solvent A for 10 min. To analyze the *asuD1-D3* mutants, a gradient of 50-70% solvent B in solvent A was applied instead. The extraction and HPLC analysis of 3,4-AHBA followed the described protocol [59].

High resolution MS and LC-MS analyses were carried out on a 6210-TOF LCMS system (Agilent Technologies Inc., Santa Clara, CA USA), in which the LC was performed using a XDB C18 (4.6 X 50 mm, 1.8 micron particle size) high throughput column (Agilent technologies, Inc.) with the same elution program as the HPLC analysis mentioned above. The exact masses of the identified compounds are listed in Table 9.1.

Fatty Acid Analysis

The mycelia of the fermentation cultures were collected, washed three times with 10% glycerol and mixed with 3 mL MeOH:CHCl₃ (2:1) in a glass homogenizer. The mixture was separated by centrifugation, and the supernatant was further rinsed three times with 1 mL of water. The organic layer was extracted, hydrolyzed and the methyl esters of the fatty acids were prepared [164, 165]. The GC-MS analysis was conducted on a Trace Gas Chromatograph (Thermo Quest Inc. Schaumburg, IL, USA) using a 30 m x 0.25 mm DB-225 column with a 0.15 m film thickness (J&W Scientific, Folsom, CA). The flow rate of the carrier gas ultrapure helium was 1.5 ml/min and the GC program was as follows: 60 °C for 1 min; 15 °C/min to 200 °C; 5 °C/min to 260 °C and hold for 10min. The peak areas were recorded by XCalibur-Qual Browser software (Thermo Quest Inc. Schaumburg, IL, USA). The signals of the fatty acid methyl esters were identified by comparison with authentic samples purchased from Sigma, NuCheck Prep.

Table 9.1 Exact mass of asukamycin and its derivatives.

	Formula	Calculated Mass	Observed Mass	Mass Error (ppm)	Upper Chain Fragment
A1	$C_{31}H_{34}N_2O_7$	546.2366	546.2360	1.19	189.13
A2	$C_{28}H_{30}N_2O_7$	506.2053	506.2062	1.78	149.09
A3, A4	$C_{29}H_{32}N_2O_7$	520.2210	520.2228	3.62	163.11
A5	$C_{30}H_{34}N_2O_7$	534.2366	534.2377	2.05	177.13
A6, A7	$C_{31}H_{36}N_2O_7$	548.2523	548.2530	1.36	191.14
B1	$C_{31}H_{36}N_2O_7$	548.2523	548.2528	0.91	189.13
B2	$C_{28}H_{32}N_2O_7$	508.2210	508.2229	3.74	149.10
B3, B4	$C_{29}H_{34}N_2O_7$	522.2366	522.2382	3.06	163.11
B5	$C_{30}H_{36}N_2O_7$	536.2523	536.2517	1.02	177.13
C1	$C_{31}H_{34}N_2O_5$	514.2468	514.2477	1.73	189.13
C2	$C_{28}H_{30}N_2O_5$	474.2155	474.2163	1.68	149.10
C3, C4	$C_{29}H_{32}N_2O_5$	488.2311	488.2317	1.15	163.11
C5	$C_{30}H_{34}N_2O_5$	502.2468	502.2477	1.77	177.13
D1	$C_{31}H_{34}N_2O_6$	530.2417	530.2422	0.90	189.13
D2	$C_{29}H_{32}N_2O_6$	504.2260	504.2254	1.25	149.10
D3, D4	$C_{28}H_{30}N_2O_6$	490.2104	490.2110	1.34	163.11
D5	$C_{30}H_{34}N_2O_6$	518.2417	518.2411	1.06	177.13
A8	$C_{20}H_{20}N_2O_7$	400.1271	400.1289	4.73	---
B8	$C_{20}H_{22}N_2O_7$	402.1427	402.1444	4.19	---
C8	$C_{20}H_{20}N_2O_5$	368.1372	368.1394	6.02	---
A1a	$C_{26}H_{29}NO_6$	451.1995	451.2010	3.44	189.13
A2a	$C_{23}H_{25}NO_6$	411.1682	411.1657	6.13	149.09
A3a,A4a	$C_{24}H_{27}NO_6$	425.1838	425.1804	8.13	163.11
A5a	$C_{25}H_{29}NO_6$	439.1995	439.1990	1.09	177.12
B1a	$C_{26}H_{31}NO_6$	453.2151	453.2171	4.43	189.13
B2a	$C_{23}H_{27}NO_6$	413.1838	413.1801	8.93	149.09
B3a, B4a	$C_{24}H_{29}NO_6$	427.1995	427.1956	9.19	163.10
B5a	$C_{25}H_{31}NO_6$	441.2151	441.2120	7.05	177.12

Purification and NMR Analysis of **D1** and **B8**

A reliable yield of the novel intermediate 4-hydroxyprotoasukamycin **D1** was obtained in *S. lividans* K4-114 carrying pART1361E3, which was generated from pART1361 with the λ -Red PCR strategy by replacing *asuE3* with a spectinomycin resistance gene. *S. lividans* K4-114/pART1361E3 was inoculated into 500 mL MS medium in 2-liter flasks with a coil and fermented on a rotary shaker at 250 rpm and 28 °C for 4-5 days. One liter of harvested culture was extracted three times with an equal volume of ethyl acetate, and the combined ethyl acetate extract was dried, concentrated and purified on a silica gel column (100-200 mesh), eluting with dichloromethane/methanol (100:3). The compound **D1** fraction was collected and further purified by semi-preparative C18 reverse-phase HPLC (Dionex), eluting with 75-85% solvent C (methanol with 0.1% formic acid) in solvent A, to give 20 mg of pure compound **D1**. Its ¹H-NMR, ¹³C-NMR, HSQC and HMBC spectra were recorded in DMSO-*d*₆ on a Varian System 700 spectrometer (Table 6.1).

To purify the **B8**, the *asuC2* mutant was inoculated into 50 mL YMG medium in 250 mL flasks with coils and fermented at 250 rpm and 28 °C for 3 days. One liter of harvested culture was extracted three times with an equal volume of ethyl acetate. The combined ethyl acetate extract was dried, concentrated and purified on a silica gel column (100-200 mesh), eluting with dichloromethane/methanol (90:10). The compound **B8** fraction was further purified by semi-preparative C18 reverse-phase HPLC (Dionex), eluting with 35-50% solvent C in solvent A, and 2 mg of pure compound **B8** was obtained. Its ¹H- and ¹³C-NMR spectra were recorded in DMSO-*d*₆ on a Varian System 700 spectrometer (Table 4.1).

Genomic Library and Mutant Construction

Molecular biology procedures and DNA manipulations were carried out according to

standard protocols. The cosmid genomic library of *S. nodosus* subsp. *asukaensis* was constructed by cloning the *Sau*3AI partially digested genomic DNA into pOJ446, an *E. coli*-*Streptomyces* shuttle vector. Ligation mixtures were further packaged with the Gigapack III Gold Packaging kit (Stratagene) and transfected into *E. coli* SURE strain (Stratagene). Two ³²P-labelled DNA probes, the *chcA* and *asuD2* genes, were used for screening the constructed cosmid library.

To construct mutants by antibiotic resistance gene insertion, the target gene-containing DNA fragment was cloned into the *Bam*HI site of the pGM160 vector [163]. The internal coding region with or without the junction region were deleted or replaced with either the 1.4 kb apramycin resistance gene or the 0.8 kb kanamycin resistance gene from pOJ446 or pBluescript, respectively (Fig. 9.1) [163]. The truncated plasmid clones were delivered by polyethylene glycol-based transformation into *S. nodosus* subsp. *asukaensis*, and integrated into the chromosome forced by incubating the transformants at 39 °C with continuing selection for thiostrepton resistance. One or two rounds of streaking at 39 °C in the absence of thiostrepton allowed the identification of thiostrepton-sensitive strains, in which the targeted genes were replaced with the antibiotic resistance gene. The resulting recombinants were further confirmed by Southern hybridization analysis (Fig. 9.1), except for the mutant *asuA2*, which was verified by chromosome walking and genomic sequencing.

To construct the *asuE1* mutant, the 1.5 kb upstream and downstream regions, including 100 bp of *asuE1*, were amplified by PCR and tandem cloned in the pHGF9050 vector. The four oligonucleotide primers used, AsuE1-1 to -4, are listed in Table 9.2. The resulting pART1334 was transformed into *E. coli* ET12567/pUZ8002 and conjugated with *S. nodosus* subsp. *asukaensis* wild type [163]. The apramycin resistant recombinants resulting from the homologous recombination between the plasmid and the wild type *S. nodosus* were further selected, subcultured in MS liquid medium for 1-2 rounds, and screened for apramycin sensitive

recombinants derived from a second crossover event. The double crossover recombinant was confirmed by Southern hybridization analysis (Fig. 9.1).

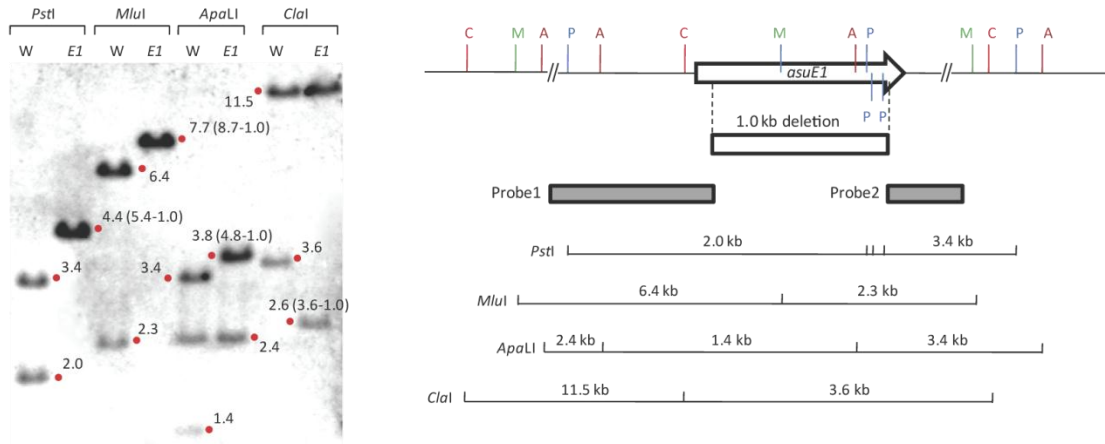
Table 9.2 Oligonucleotide primers used for the mutant constructions and λ -Red recombinations.

Primers	Sequence from 5' to 3'
AsuE1-1	CCCAAGCTTCGAAGACCCGTGGCGTGAGCC
AsuE1-2	CCCAGATCTCCGCGCGCACAGCAGCGC
AsuE1-3	CCCAGATCTCCGGCGGTGAAGGGCGCGCAC
AsuE1-4	CCCCTCGAGACCTGATGGAGGGGTCCAGTA
AsuRED-4	<u>GGTCCGGAAGCGGCCTGCGGAGCGCCCTGCGGGGCGGCTCTAGA</u> <u>GATATCATTCCGGGGATCCGTCGACC</u>
AsuRED-6	<u>AGAACCACGGCTGGACCGAGGGCTGACACCCCCGGGGCGTATCC</u> <u>GGCCGTTGTAGGCTGGAGCTGCTTC</u>
AsuRED-E3F	<u>AGTCGTCAGCCTGCCCTACCACCACCCGTTTCATGGTGGCCTCGCG</u> <u>GGCCATTCCGGGGATCCGTCGACC</u>
AsuRED-E3R	<u>AGCCGACGATCGTGCTGCGCCGGTCGATCAGCTCGGCCAGGGCCT</u> <u>TGCGTGTAGGCTGGAGCTGCTTC</u>
S83TF	AAGGATCCGGCGGCACCCGCAACATCGGTGGCACCAA
S83TR	GGGATGGAGGTGGTGAAGATGAAG

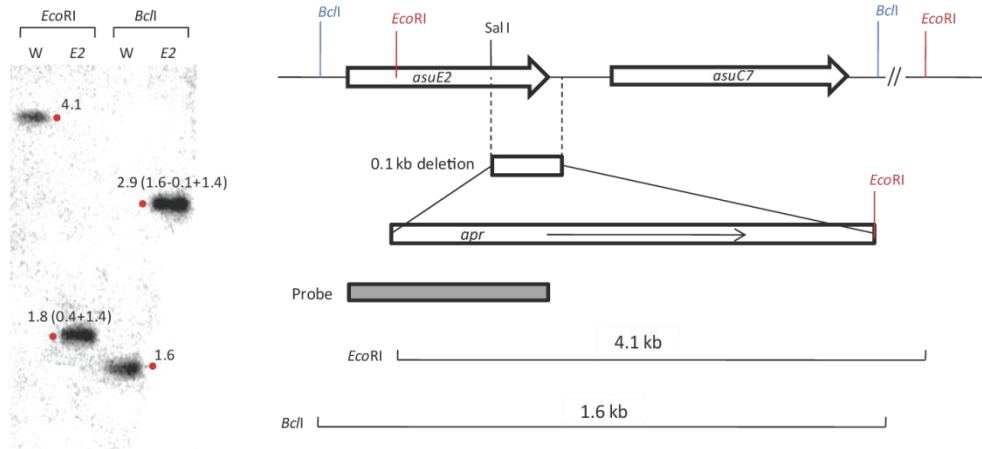
* The underlined regions indicate the DNA sequence matching pART1361.

Figure 9.1 Southern blots of thirteen constructed mutants. Hybridization probes and anticipated restriction digestion patterns are indicated.

a.



b.



c.

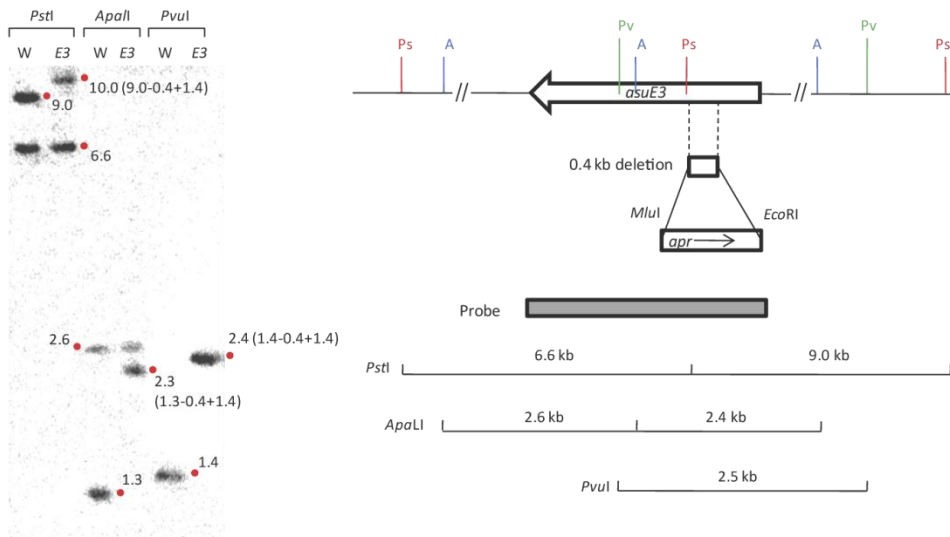
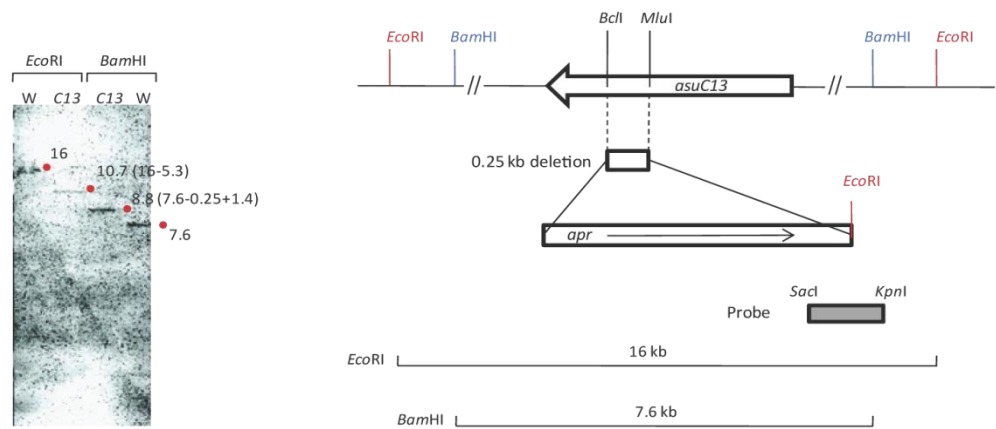
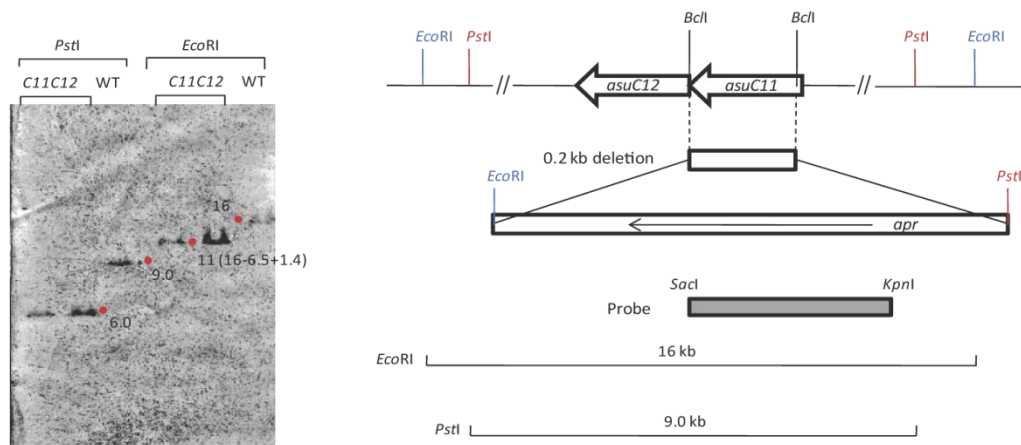


fig. cont'd

d.



e.



f.

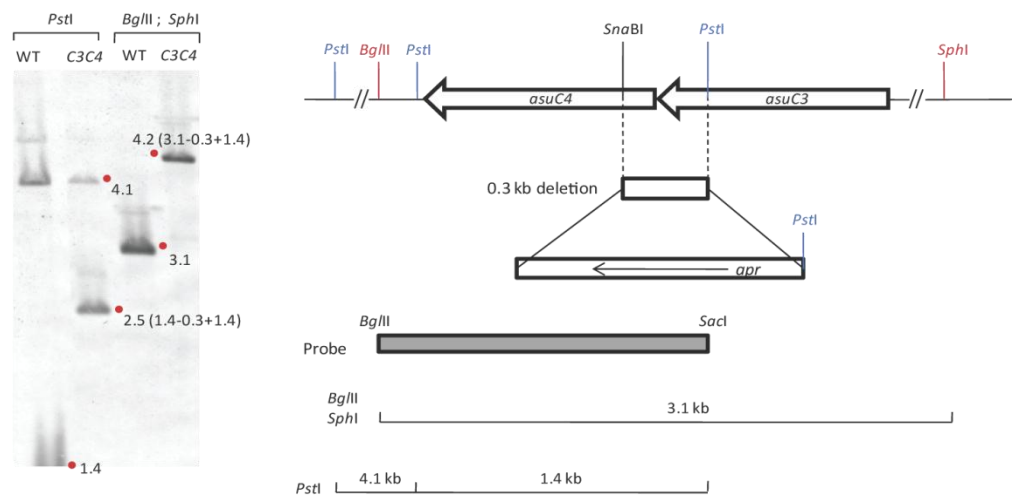
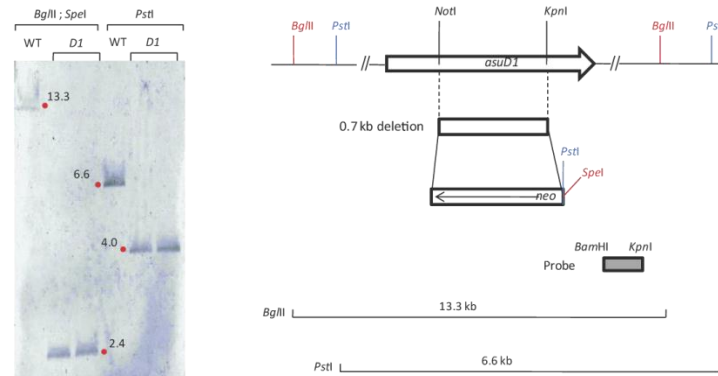
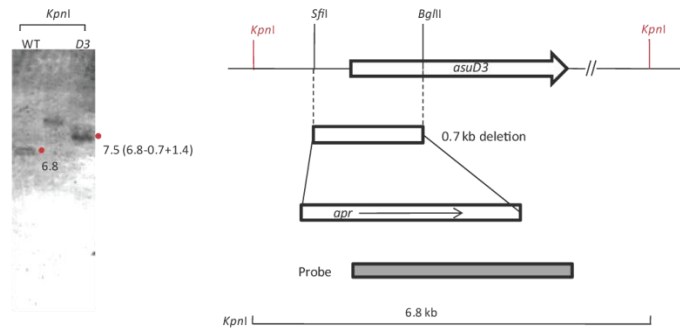


fig. cont'd

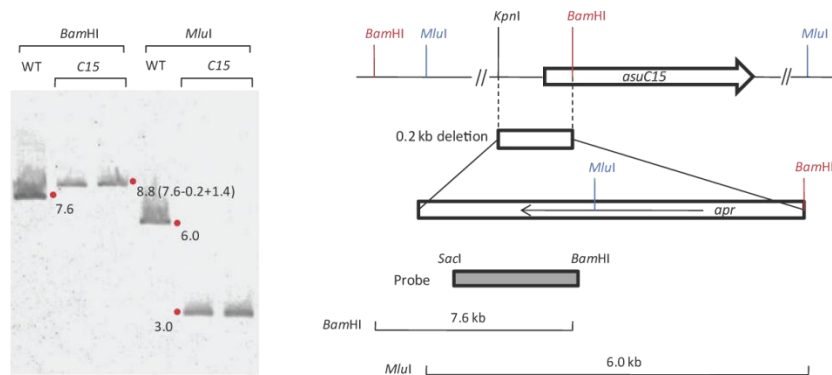
g.



h.



i.



j.

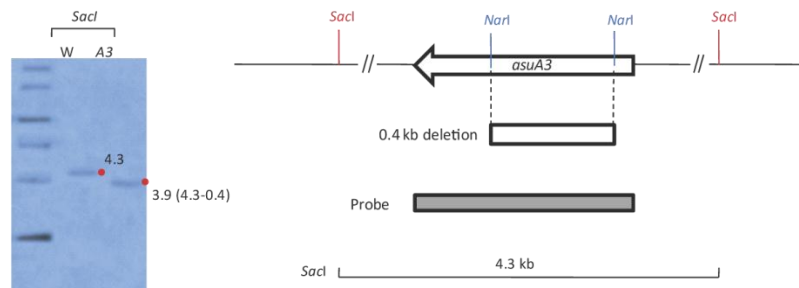
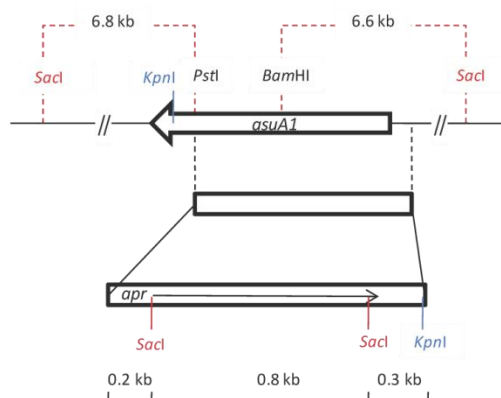
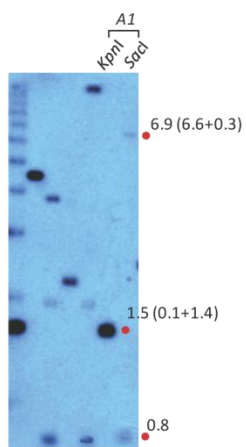


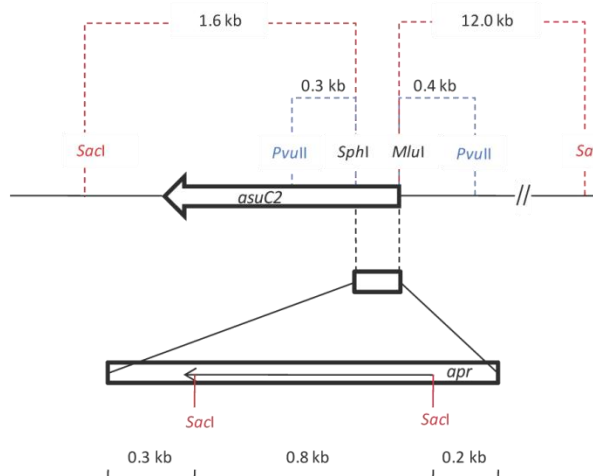
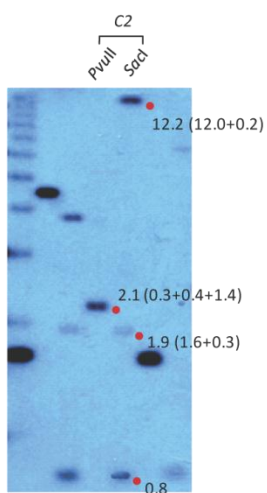
fig. cont'd

k.



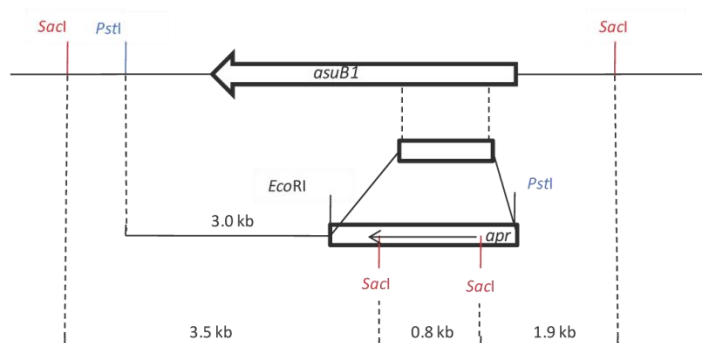
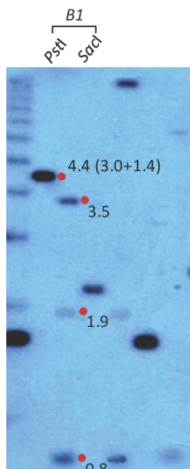
Notes: probed with apramycin resistance gene.

l.



Notes: probed with apramycin resistance gene.

m.



Notes: probed with apramycin resistance gene.

Reassembly and Heterologous Expression of the Cloned *asu* Cluster

The *E. coli* BW25113/pIJ790 was cultivated in LB medium supplemented with 25 µg/mL chloramphenicol plus 10 mM L-arabinose at 28 °C [89]. When the OD₆₀₀ reaches 0.6, the *E. coli* cells were harvested, washed with ice-cold 10% glycerol for three times, concentrated and stocked in the ice-cold GYT (10% glycerol; 0.125% yeast extract; 0.25% tryptone). The cosmid clones 2B9 and 10D6 were linearized by restriction digestion with *Spe*I and *Eco*RI, respectively, equally mixed and introduced into *E. coli* BW25113/pIJ790 by electroporation. The cells were then added to 1 mL SOC [89], recovered at 37 °C for 3 hours, and plated out onto LB agar with 100 µg/mL apramycin. For the negative control, the linearized 2B9 and 10D6 were transformed separately by the same procedure. The recombinant clone was confirmed by matching the anticipated *Eco*RI digestion pattern and named pART1361 (Fig. 2.2). Intergeneric conjugation of the recombinant cosmids from *E. coli* to *S. lividans* K4-114 followed the established protocol [163].

To construct pART1391, a 1.5 kb DNA fragment from pIJ778 was PCR-amplified using primers AsuRED-4 and -6 (Table 9.2) to carry a spectinomycin resistance gene cassette plus two 50-bp nucleotides, designed to be identical to the boundaries of the targeted region on pART1361 (Fig. 2.3) [89]. To obtain the recombinant strain, the gel-purified PCR fragment was introduced into *E. coli* BW25113/pART1361/pIJ790 by electroporation, and the transformants were screened for spectinomycin resistance. The deletion in the resulting clone was confirmed by matching up to the expected *Eco*RI digestion pattern and verified by PCR. The pART1361E3 construction followed the same strategy as described above but using primers AsuRED-E3F and -E3R (Table 9.2).

To insert the point mutation that modifies the TCC (Ser) codon into ACC (Thr) in the *asuD2* gene, the internal fragment containing the *Bam*HI-*Kpn*I sites was PCR-amplified using

primers S83TF and S83TR (Table 9.2). The *Bam*HI-*Kpn*I-cleaved fragment was then used to replace the corresponding region in the pALS3 plasmid. The further steps were identical with the pALS4 construction [21].

REFERENCES

1. Buzzetti F, Zahner H, Hutter R, Gaumann E, Neipp L, Prelog V, Kellerschierlein W: **Stoffwechselprodukte von Mikroorganismen .41. Manumycin.** *Pharm Acta Helv* 1963, **38**(12):871-874.
2. Schroder K, Zeeck A: **Manumycin.** *Tetrahedron Lett* 1973(50):4995-4998.
3. Zeeck A, Schroder K, Frobel K, Grote R, Thiericke R: **The structure of manumycin .1. characterization, structure elucidation and biological-activity.** *J Antibiot* 1987, **40**(11):1530-1540.
4. Thiericke R, Stellwaag M, Zeeck A, Snatzke G: **The structure of manumycin .3. Absolute-configuration and conformational studies.** *J Antibiot* 1987, **40**(11):1549-1554.
5. Alcaraz L, Macdonald G, Ragot JP, Lewis N, Taylor RJK: **Manumycin A: Synthesis of the (+)-enantiomer and revision of stereochemical assignment.** *J Org Chem* 1998, **63**(11):3526-3527.
6. Omura S, Kitao C, Tanaka H, Oiwa R, Takahashi Y, Nakagawa A, Shimada M, Iwai Y: **New antibiotic, asukamycin, produced by *Streptomyces*.** *J Antibiot* 1976, **29**(9):876-881.
7. Cho HG, Sattler I, Beale JM, Zeeck A, Floss HG: **Some aspects of the stereochemistry and biosynthesis of asukamycin.** *J Org Chem* 1993, **58**(27):7925-7928.
8. Kakinuma K, Ikekawa N, Nakagawa A, Omura S: **Structure of asukamycin, a possible shunt metabolite from 3-dehydroquinic acid in the shikimate pathway.** *J Am Chem Soc* 1979, **101**(12):3402-3404.
9. Hu YD, Floss HG: **New type II manumycins produced by *Streptomyces nodosus* ssp *asukaensis* and their biosynthesis.** *J Antibiot* 2001, **54**(4):340-348.
10. Hu YD, Floss HG: **Starter unit specificity of the asukamycin "upper" chain polyketide synthase and the branched-chain fatty acid synthase of *Streptomyces nodosus* subsp *asukaensis*.** *Heterocycles* 2006, **69**(1):133-149.
11. Kohno J, Nishio M, Kawano K, Nakanishi N, Suzuki S, Uchida T, Komatsubara S: **TMC-1 A, B, C and D, new antibiotics of the manumycin group produced by *Streptomyces* sp - Taxonomy, production, isolation, physico-chemical properties, structure elucidation and biological properties.** *J Antibiot* 1996, **49**(12):1212-1220.
12. Nakano H, Hara M, Saito Y, Ikuina Y, Takiguchi T, Okabe M: **UCF1 compounds derivatives thereof and processes for their preparation.** In.: KYOWA HAKKO KOGYO KK (JP); 1991.

13. Sattler I, Grone C, Zeeck A: **New compounds of the manumycin group of antibiotics and a facilitated route for their structure elucidation.** *J Org Chem* 1993, **58**(24):6583-6587.
14. Uosaki Y, Agatsuma T, Tanaka T, Saitoh Y: **EI-1511-3, -5 and EI-1625-2, novel interleukin-1 beta converting enzyme inhibitors produced by *Streptomyces* sp E-1511 and E-1625 .2. Structure determination.** *J Antibiot* 1996, **49**(11):1079-1084.
15. Tanaka T, Tsukuda E, Ochiai K, Kondo H, Teshiba S, Matsuda Y: **EI-1511-3, -5 and EI-1625-2, novel interleukin-1 beta converting enzyme inhibitors produced by *Streptomyces* sp E-1511 and E-1625 .1. Taxonomy of producing strain, fermentation and isolation.** *J Antibiot* 1996, **49**(11):1073-1078.
16. Tanaka T, Tsukuda E, Uosaki Y, Matsuda Y: **EI-1511-3, -5 and EI-1625-2, novel interleukin-1 beta converting enzyme inhibitors produced by *Streptomyces* sp E-1511 and E-1625 .3. Biochemical properties of EI-1511-3, -5 and EI-1625-2.** *J Antibiot* 1996, **49**(11):1085-1090.
17. Tanaka T, Tsukuda E, Ochiai K, Ando K, Kondo H, Uosaki Y, Saitoh Y, Matsuda Y, Koizumi F, Agatsuma T: **Interleukin-1 inhibiting manumycin derivatives and streptomyces strains for their production.** In.: KYOWA HAKKO KOGYO KK (JP); 1996.
18. Takagi I, Akashi, Satoshi, Mizogami, Kazutoshi, Hanada, Kazunori, Yamagishi, Michio: **Polyene-based compound.** In.: TAISHO PHARMACEUT CO LTD; 1994.
19. Schmidt U, Neumann K, Schumacher A, Weinbrenner S: **Synthesis of enopeptin B from *Streptomyces* sp RK-1051.** *Angew Chem Int Edit* 1997, **36**(10):1110-1112.
20. Hu YD, Floss HG: **Further studies on the biosynthesis of the manumycin-type antibiotic, asukamycin, and the chemical synthesis of protoasukamycin.** *J Am Chem Soc* 2004, **126**(12):3837-3844.
21. Petricek M, Petrickova K, Havlicek L, Felsberg J: **Occurrence of two 5-aminolevulinate biosynthetic pathways in *Streptomyces nodosus* subsp *asukaensis* is linked with the production of asukamycin.** *J Bacteriol* 2006, **188**(14):5113-5123.
22. Shu YZ, Huang S, Wang RR, Lam KS, Klohr SE, Volk KJ, Pirnik DM, Wells JS, Fernandes PB, Patel PS: **Manumycin-E, manumycin-F and manumycin-G, new members of manumycin class antibiotics, from *Streptomyces* Sp.** *J Antibiot* 1994, **47**(3):324-333.
23. Patel PS, Shu Y-z: **Manumycin compounds.** In. United States: Bristol-Myers Squibb Company (Princeton, NJ); 1995.

24. Brodasky TF, Stroman DW: **Antibiotic compound and process for recovery thereof from a fermentation broth**. In. United States: The Upjohn Company (Kalamazoo, MI); 1986.
25. Brodasky TF, Stroman DW, Dietz A, Mizesak S: **U-56,407, a new antibiotic related to asukamycin - isolation and characterization**. *J Antibiot* 1983, **36**(8):950-956.
26. Franco CMM, Maurya R, Vijayakumar EKS, Chatterjee S, Blumbach J, Ganguli BN: **Alisamycin, a new antibiotic of the manumycin group .1. Taxonomy, production, isolation and biological-activity**. *J Antibiot* 1991, **44**(12):1289-1293.
27. Franco CMM, Vijayakumar EKS, Chatterjee S, Blumbach J, Ganguli BN, N. B: **A novel antibiotic Alisamycin a process for its production and its use**. In.: HOECHST AG (DE); 1991.
28. Chatterjee S, Vijayakumar EKS, Franco CMM, Blumbach J, Ganguli BN: **On the structure of alisamycin, a new member of the manumycin class of antibiotics**. *J Antibiot* 1993, **46**(6):1027-1030.
29. Hayashi K, Nakagawa M, Fujita T, Nakayama M: **Absolute stereochemistry of alisamycin**. *Biosci Biotech Bioch* 1994, **58**(7):1332-1333.
30. Nakayama M, Nakagawa, Shohei, Fujita, Tomoyuki, Hayashi, Kenichiro: **Antibiotic substance 106-B, its production, antimicrobial agent and antitumor agent comprising antibiotic substance 106-B as active ingredient**. In.: TEIKA CORP; 1993.
31. Hayashi K, Nakagawa M, Fujita T, Tanimori S, Nakayama M: **Nisamycin, a new manumycin group antibiotic from *Streptomyces* Sp K106**. *J Antibiot* 1993, **46**(12):1904-1907.
32. Hayashi K, Nakagawa M, Nakayama M: **Nisamycin, a New manumycin group antibiotic from *Streptomyces* Sp K106 .1. Taxonomy, fermentation, isolation, physicochemical and biological properties**. *J Antibiot* 1994, **47**(10):1104-1109.
33. Hayashi K, Nakagawa M, Fujita T, Tanimori S, Nakayama M: **Nisamycin, a new manumycin group antibiotic from *Streptomyces* Sp K106 .2. Structure determination and structure-activity-relationships**. *J Antibiot* 1994, **47**(10):1110-1115.
34. Grote R, Zeeck A, Drautz H, Zahner H: **Metabolic products of microorganisms .244. Colabomycins, new antibiotics of the manumycin group from *Streptomyces Griseoflavus* .1. Isolation, characterization and biological properties**. *J Antibiot* 1988, **41**(9):1178-1185.
35. Grote R, Zeeck A, Beale JM: **Metabolic products of microorganisms .245. colabomycins, new antibiotics of the manumycin group from *Streptomyces Griseoflavus* .2. Structure of colabomycin-A**. *J Antibiot* 1988, **41**(9):1186-1195.

36. Dick O, Onken U, Sattler I, Zeeck A: **Influence of increased dissolved-oxygen concentration on productivity and selectivity in cultures of a colabomycin-producing strain of *Streptomyces Griseoflavus*.** *Appl Microbiol Biot* 1994, **41**(4):373-377.
37. Slechta L, Cialdella JJ, Mizesak SA, Hoeksema H: **Isolation and characterization of a new antibiotic U-62162.** *J Antibiot* 1982, **35**(5):556-560.
38. Sattler I, Thiericke R, Zeeck A: **The manumycin-group metabolites.** *Nat Prod Rep* 1998, **15**(3):221-240.
39. Hara M, Han M: **Ras farnesyltransferase inhibitors suppress the phenotype resulting from an activated Ras mutation in *Caenorhabditis Elegans*.** *P Natl Acad Sci USA* 1995, **92**(8):3333-3337.
40. Hara M, Akasaka K, Akinaga S, Okabe M, Nakano H, Gomez R, Wood D, Uh M, Tamanoi F: **Identification of Ras farnesyltransferase inhibitors by microbial screening.** *P Natl Acad Sci USA* 1993, **90**(6):2281-2285.
41. Ito T, Kawata S, Tamura S, Igura T, Nagase T, Miyagawa J, Yamazaki E, Ishiguro H, Matsuzawa Y: **Suppression of human pancreatic cancer growth in BALB/c nude mice by manumycin, a farnesyl:protein transferase inhibitor.** *Jpn J Cancer Res* 1996, **87**(2):113-116.
42. Kainuma O, Asano T, Hasegawa M, Kenmochi T, Nakagohri T, Tokoro Y, Isono K: **Inhibition of growth and invasive activity of human pancreatic cancer cells by a farnesyltransferase inhibitor, manumycin.** *Pancreas* 1997, **15**(4):379-383.
43. Xu GP, Pan JX, Martin C, Yeung SCJ: **Angiogenesis inhibition in the in vivo antineoplastic effect of manumycin and paclitaxel against anaplastic thyroid carcinoma.** *J Clin Endocr Metab* 2001, **86**(4):1769-1777.
44. Pan JX, Yeung SCJ: **Recent advances in understanding the antineoplastic mechanisms of farnesyltransferase inhibitors.** *Cancer Research* 2005, **65**(20):9109-9112.
45. Yeung SCJ, Xu GP, Pan JX, Christgen M, Bamiagis A: **Manumycin enhances the cytotoxic effect of paclitaxel on anaplastic thyroid carcinoma cells.** *Cancer Research* 2000, **60**(3):650-656.
46. Yeung SCJ, She MR, Yang HL, Pan JX, Sun LL, Chaplin D: **Combination chemotherapy including combretastatin A4 phosphate and paclitaxel is effective against anaplastic thyroid cancer in a nude mouse xenograft model.** *J Clin Endocr Metab* 2007, **92**(8):2902-2909.

47. Downward J: **Targeting ras signalling pathways in cancer therapy.** *Nature Reviews Cancer* 2003, **3**(1):11-22.
48. Nagase T, Kawata S, Tamura S, Masuda Y, Inui Y, Yamasaki E, Ishiguro H, Ito T, Matsuzawa Y: **Inhibition of cell growth of human hepatoma cell line (Hep G2) by a farnesyl protein transferase inhibitor: A preferential suppression of ras farnesylation.** *Int J Cancer* 1996, **65**(5):620-626.
49. Finegold AA, Schafer WR, Rine J, Whiteway M, Tamanoi F: **Common modifications of trimeric-G proteins and Ras protein - Involvement of polyisoprenylation.** *Science* 1990, **249**(4965):165-169.
50. Pan JX, She MR, Xu ZX, Sun L, Yeung SCJ: **Farnesyltransferase inhibitors induce DNA damage via reactive oxygen species in human cancer cells.** *Cancer Research* 2005, **65**(9):3671-3681.
51. Sears KT, Daino H, Carey GB: **Reactive oxygen species-dependent destruction of MEK and Akt in Manumycin stimulated death of lymphoid tumor and myeloma cell lines.** *Int J Cancer* 2008, **122**(7):1496-1505.
52. Bernier M, Kwon YK, Pandey SK, Zhu TN, Zhao RJ, Maciuk A, He HJ, DeCabo R, Kole S: **Binding of manumycin A inhibits I kappa B kinase beta activity.** *J Biol Chem* 2006, **281**(5):2551-2561.
53. Striz I, Krasna E, Petrickova K, Brabcova E, Kolesar L, Slavcev A, Jaresova M, Petricek M: **Manumycin and asukamycin inhibition of IL-1beta and IL-18 release from human macrophages by caspase-1 blocking.** *Allergy* 2008, **63**:142-143.
54. Zheng ZH, Dong YS, Zhang H, Lu XH, Ren X, Zhao GY, He JG, Si SY: **Isolation and characterization of N98-1272 A, B and C, selective acetylcholinesterase inhibitors from metabolites of an actinomycete strain.** *J Enzym Inhib Med Ch* 2007, **22**(1):43-49.
55. Kim CG, Kirschning A, Bergon P, Zhou P, Su E, Sauerbrei B, Ning S, Ahn Y, Breuer M, Leistner E *et al*: **Biosynthesis of 3-amino-5-hydroxybenzoic acid, the precursor of mC₇N units in ansamycin antibiotics.** *J Am Chem Soc* 1996, **118**(32):7486-7491.
56. Thiericke R, Zeeck A: **Studies of precursor-directed biosynthesis with *Streptomyces* Sp .1. Isolation of manumycin analogs by feeding of aminobenzoic acids as C₇N starter units.** *J Chem Soc Perk T 1* 1988(8):2123-2127.
57. Thiericke R, Langer HJ, Zeeck A: **Studies of precursor-directed biosynthesis with *Streptomyces* .2. New and unusual manumycin analogs produced by *Streptomyces Parvulus*.** *J Chem Soc Perk T 1* 1989(5):851-855.
58. Gould SJ, Melville CR, Cone MC: **3-Amino-4-hydroxybenzoic acid is derived from the tricarboxylic acid cycle rather than the shikimic acid pathway.** *J Am Chem Soc* 1996, **118**(39):9228-9232.

59. Suzuki H, Ohnishi Y, Furusho Y, Sakuda S, Horinouchi S: **Novel benzene ring biosynthesis from C-3 and C-4 primary metabolites by two enzymes.** *J Biol Chem* 2006, **281**(48):36944-36951.
60. Thiericke R, Zeeck A, Nakagawa A, Omura S, Herrold RE, Wu STS, Beale JM, Floss HG: **Biosynthesis of the manumycin group antibiotics.** *J Am Chem Soc* 1990, **112**(10):3979-3987.
61. Moore BS, Cho HJ, Casati R, Kennedy E, Reynolds KA, Mocek U, Beale JM, Floss HG: **Biosynthetic-studies on ansatrienin-A - Formation of the cyclohexanecarboxylic acid moiety.** *J Am Chem Soc* 1993, **115**(12):5254-5266.
62. Cropp TA, Wilson DJ, Reynolds KA: **Identification of a cyclohexylcarbonyl CoA biosynthetic gene cluster and application in the production of doramectin.** *Nature Biotechnology* 2000, **18**(9):980-983.
63. Sekiyama Y, Palaniappan N, Reynolds KA, Osada H: **Biosynthesis of phoslactomycins: cyclohexanecarboxylic acid as the starter unit.** *Tetrahedron* 2003, **59**(38):7465-7471.
64. Moore BS, Poralla K, Floss HG: **Biosynthesis of the cyclohexanecarboxylic acid starter unit of omega-cyclohexyl fatty-acids in *Alicyclobacillus Acidocaldarius*.** *J Am Chem Soc* 1993, **115**(12):5267-5274.
65. Kaneda T: **Iso-fatty and anteiso-fatty acids in bacteria - Biosynthesis, function, and taxonomic significance.** *Microbiological Reviews* 1991, **55**(2):288-302.
66. Zhang YM, Rock CO: **Membrane lipid homeostasis in bacteria.** *Nature Reviews Microbiology* 2008, **6**(3):222-233.
67. Beale JM, Lee JP, Nakagawa A, Omura S, Floss HG: **Biosynthesis of the antibiotic reductionmycin.** *J Am Chem Soc* 1986, **108**(2):331-332.
68. Endler K, Schuricht U, Hennig L, Welzel P: **Exploratory investigations into the biosynthesis of the antibiotic moenomycin A.** *Tetrahedron Lett* 1998, **39**(1-2):13-16.
69. McAlpine JB, Bachmann BO, Pirae M, Tremblay S, Alarco AM, Zazopoulos E, Farnet CM: **Microbial Genomics as a guide to drug discovery and structural elucidation: ECO-02301, a novel antifungal agent, as an example.** *Journal of Natural Products* 2005, **68**(4):493-496.
70. Banskota AH, McAlpine JB, Sorensen D, Ibrahim A, Aouidate M, Pirae M, Alarco AM, Farnet CM, Zazopoulos E: **Genomic analyses lead to novel secondary metabolites.** *J Antibiot* 2006, **59**(9):533-542.

71. Omura S, Imamura N, Hinotozawa K, Otoguro K, Lukacs G, Faghiih R, Tolmann R, Arison BH, Smith JL: **The structure of virustomycin-A.** *J Antibiot* 1983, **36**(12):1783-1786.
72. Werner G, Hagenmaier H, Drautz H, Baumgartner A, Zahner H: **Metabolic products of microorganisms. 224. Bafilomycins, a new group of macrolide antibiotics. Production, isolation, chemical structure and biological activity.** *J Antibiot (Tokyo)* 1984, **37**(2):110-117.
73. Nakagawa A, Wu TS, Keller PJ, Lee JP, Omura S, Floss HG: **Biosynthesis of asukamycin - formation of the 2-amino-3-hydroxycyclopent-2-enone moiety.** *Journal of the Chemical Society-Chemical Communications* 1985(8):519-521.
74. Jaffe EK: **The porphobilinogen synthase catalyzed reaction mechanism.** *Bioorg Chem* 2004, **32**(5):316-325.
75. Avissar YJ, Ormerod JG, Beale SI: **Distribution of delta-aminolevulinic acid biosynthetic pathways among phototrophic bacterial groups.** *Arch Microbiol* 1989, **151**(6):513-519.
76. Thiericke R, Zeeck A, Robinson JA, Beale JM, Floss HG: **The biosynthesis of manumycin - origin of the oxygen and nitrogen-atoms.** *Journal of the Chemical Society-Chemical Communications* 1989(7):402-403.
77. Kuliopulos A, Hubbard BR, Lam Z, Koski IJ, Furie B, Furie BC, Walsh CT: **Dioxygen transfer during vitamin-K dependent carboxylase catalysis.** *Biochemistry* 1992, **31**(33):7722-7728.
78. Naganathan S, Hershline R, Ham SW, Dowd P: **The active-site of vitamin-K and the role of the vitamin-K-dependent carboxylase.** *J Am Chem Soc* 1994, **116**(22):9831-9839.
79. Dowd P, Hershline R, Ham SW, Naganathan S: **Vitamin-K and energy transduction - a base strength amplification mechanism.** *Science* 1995, **269**(5231):1684-1691.
80. Gould SJ, Kirchmeier MJ, LaFever RE: **Incorporation of two oxygens from $^{18}\text{O}_2$ in the epoxyquinone from the dihydroxyacetanilide epoxidase reaction: Evidence for a dioxygenase mechanism.** *J Am Chem Soc* 1996, **118**(33):7663-7666.
81. Fujimori DG, Hrvatin S, Neumann CS, Strieker M, Marahiel MA, Walsh CT: **Cloning and characterization of the biosynthetic gene cluster for kutznerides.** *P Natl Acad Sci USA* 2007, **104**(42):16498-16503.
82. Yanai K, Murakami T: **The kanamycin biosynthetic gene cluster from *Streptomyces kanamyceticus*.** *J Antibiot (Tokyo)* 2004, **57**(5):351-354.

83. Wenzel SC, Muller R: **Recent developments towards the heterologous expression of complex bacterial natural product biosynthetic pathways.** *Current Opinion in Biotechnology* 2005, **16**(6):594-606.
84. Binz TM, Wenzel SC, Schnell HJ, Bechthold A, Muller R: **Heterologous expression and genetic engineering of the phenalinolactone biosynthetic gene cluster by using Red/ET recombineering.** *Chembiochem* 2008, **9**(3):447-454.
85. Hu YF, Phelan VV, Farnet CM, Zazopoulos E, Bachmann BO: **Reassembly of anthramycin biosynthetic gene cluster by using recombinogenic cassettes.** *Chembiochem* 2008, **9**(10):1603-1608.
86. Wolpert M, Heide L, Kammerer B, Gust B: **Assembly and heterologous expression of the coumermycin A(1) gene cluster and production of new derivatives by genetic engineering.** *Chembiochem* 2008, **9**(4):603-612.
87. Gust B, Challis GL, Fowler K, Kieser T, Chater KF: **PCR-targeted *Streptomyces* gene replacement identifies a protein domain needed for biosynthesis of the sesquiterpene soil odor geosmin.** *P Natl Acad Sci USA* 2003, **100**(4):1541-1546.
88. Murphy KC: **Use of bacteriophage lambda recombination functions to promote gene replacement in *Escherichia coli*.** *J Bacteriol* 1998, **180**(8):2063-2071.
89. Datsenko KA, Wanner BL: **One-step inactivation of chromosomal genes in *Escherichia coli* K-12 using PCR products.** *P Natl Acad Sci USA* 2000, **97**(12):6640-6645.
90. Pfennig F, Schauwecker F, Keller U: **Molecular characterization of the genes of actinomycin synthetase I and of a 4-methyl-3-hydroxyanthranilic acid carrier protein involved in the assembly of the acylpeptide chain of actinomycin in *Streptomyces*.** *J Biol Chem* 1999, **274**(18):12508-12516.
91. Zhou Z, Lai JR, Walsh CT: **Directed evolution of aryl carrier proteins in the enterobactin synthetase.** *P Natl Acad Sci USA* 2007, **104**(28):11621-11626.
92. Ferreras JA, Stirrett KL, Lu XQ, Ryu JS, Soll CE, Tan DS, Quadri LEN: **Mycobacterial phenolic glycolipid virulence factor biosynthesis: Mechanism and small-molecule inhibition of polyketide chain initiation.** *Chem Biol* 2008, **15**(1):51-61.
93. Hertweck C: **The biosynthetic logic of polyketide diversity.** *Angewandte Chemie-International Edition* 2009, **48**(26):4688-4716.
94. Sattely ES, Fischbach MA, Walsh CT: **Total biosynthesis: in vitro reconstitution of polyketide and nonribosomal peptide pathways.** *Nat Prod Rep* 2008, **25**(4):757-793.

95. Olsen JG, Kadziola A, von Wettstein-Knowles P, Siggaard-Andersen M, Lindquist Y, Larsen S: **The X-ray crystal structure of beta-ketoacyl [acyl carrier protein] synthase I.** *FEBS Letters* 1999, **460**(1):46-52.
96. Price AC, Choi KH, Heath RJ, Li ZM, White SW, Rock CO: **Inhibition of beta-ketoacyl-acyl carrier protein syntheses by thiolactomycin and cerulenin - Structure and mechanism.** *J Biol Chem* 2001, **276**(9):6551-6559.
97. Huang WJ, Jia J, Edwards P, Dehesh K, Schneider G, Lindqvist Y: **Crystal structure of beta-ketoacyl-acyl carrier protein synthase II from *E. coli* reveals the molecular architecture of condensing enzymes.** *EMBO Journal* 1998, **17**(5):1183-1191.
98. Tang YY, Lee HY, Tang Y, Kim CY, Mathews I, Khosla C: **Structural and functional studies on SCO1815: A beta-ketoacyl-acyl carrier protein reductase from *Streptomyces coelicolor* A3(2).** *Biochemistry* 2006, **45**(47):14085-14093.
99. Cohen-Gonsaud M, Ducasse S, Hoh F, Zerbib D, Labesse G, Quemard A: **Crystal structure of MabA from *Mycobacterium tuberculosis*, a reductase involved in long-chain fatty acid biosynthesis.** *Journal of Molecular Biology* 2002, **320**(2):249-261.
100. Qin YM, Haapalainen AM, Kilpelainen SH, Marttila MS, Koski MK, Glumoff T, Novikov DK, Hiltunen JK: **Human peroxisomal multifunctional enzyme type 2 - Site-directed mutagenesis studies show the importance of two protic residues for 2-enoyl-CoA hydratase 2 activity.** *J Biol Chem* 2000, **275**(7):4965-4972.
101. Castell A, Johansson P, Unge T, Jones TA, Backbro K: **Rv0216, a conserved hypothetical protein from *Mycobacterium tuberculosis* that is essential for bacterial survival during infection, has a double hotdog fold.** *Protein Science* 2005, **14**(10):2764-2764.
102. Sacco E, Covarrubias AS, O'Hare HM, Carroll P, Eynard N, Jones TA, Parish T, Daffe M, Backbro K, Quemard A: **The missing piece of the type II fatty acid synthase system from *Mycobacterium tuberculosis*.** *P Natl Acad Sci USA* 2007, **104**(37):14628-14633.
103. Brown AK, Bhatt A, Singh A, Saparia E, Evans AF, Besra GS: **Identification of the dehydratase component of the mycobacterial mycolic acid-synthesizing fatty acid synthase-II complex.** *Microbiology-Sgm* 2007, **153**:4166-4173.
104. Noguchi A, Kitamura T, Onaka H, Horinouchi S, Ohnishi Y: **A copper-containing oxidase catalyzes C-nitrosation in nitrosobenzamide biosynthesis.** *Nature Chemical Biology* 2010, **6**(9):641-643.
105. Palaniaappan N, Kim BS, Sekiyama Y, Osada H, Reynolds KA: **Enhancement and selective production of phoslactomycin B, a protein phosphatase IIa inhibitor, through identification and engineering of the corresponding biosynthetic gene cluster.** *J Biol Chem* 2003, **278**(37):35552-35557.

106. Pan H, Tsai SC, Meadows ES, Miercke LJW, Keatinge-Clay AT, O'Connell J, Khosla C, Stroud RM: **Crystal structure of the priming beta-ketosynthase from the R1128 polyketide biosynthetic pathway.** *Structure* 2002, **10**(11):1559-1568.
107. Davies C, Heath RJ, White SW, Rock CO: **The 1.8 angstrom crystal structure and active-site architecture of beta-ketoacyl-acyl carrier protein synthase III (FabH) from *Escherichia coli*.** *Structure* 2000, **8**(2):185-195.
108. Tang Y, Lee TS, Kobayashi S, Khosla C: **Ketosynthases in the initiation and elongation modules of aromatic polyketide synthases have orthogonal acyl carrier protein specificity.** *Biochemistry* 2003, **42**(21):6588-6595.
109. Holton SJ, Dairou J, Sandy J, Rodrigues-Lima F, Dupret JM, Noble MEM, Sim E: **Structure of *Mesorhizobium loti* arylamine N-acetyltransferase 1.** *Acta Crystallographica Section F-Structural Biology and Crystallization Communications* 2005, **61**:14-16.
110. Yu TW, Bai LQ, Clade D, Hoffmann D, Toelzer S, Trinh KQ, Xu J, Moss SJ, Leistner E, Floss HG: **The biosynthetic gene cluster of the maytansinoid antitumor agent ansamitocin from *Actinosynnema pretiosum*.** *P Natl Acad Sci USA* 2002, **99**(12):7968-7973.
111. August PR, Tang L, Yoon YJ, Ning S, Muller R, Yu TW, Taylor M, Hoffmann D, Kim CG, Zhang XH *et al*: **Biosynthesis of the ansamycin antibiotic rifamycin: deductions from the molecular analysis of the rif biosynthetic gene cluster of *Amycolatopsis mediterranei* S699.** *Chem Biol* 1998, **5**(2):69-79.
112. Yu TW, Muller R, Muller M, Zhang XH, Draeger G, Kim CG, Leistner E, Floss HG: **Mutational analysis and reconstituted expression of the biosynthetic genes involved in the formation of 3-amino-5-hydroxybenzoic acid, the starter unit of rifamycin biosynthesis in *Amycolatopsis mediterranei* S699.** *J Biol Chem* 2001, **276**(16):12546-12555.
113. Hein DW, Rustan TD, Martin WJ, Bucher KD, Miller LS, Furman EJ: **Acetylator genotype-dependent N-acetylation of arylamines *in vivo* and *in vitro* by hepatic and extrahepatic organ cytosols of syrian-hamsters congeneric at the polymorphic acetyltransferase locus.** *Archives of Toxicology* 1992, **66**(2):112-117.
114. Vineis P, Bartsch H, Caporaso N, Harrington AM, Kadlubar FF, Landi MT, Malaveille C, Shields PG, Skipper P, Talaska G *et al*: **Genetically based N-acetyltransferase metabolic polymorphism and low-level environmental exposure to carcinogens.** *Nature* 1994, **369**(6476):154-156.
115. Wang P, Denoya CD, Morgenstern MR, Skinner DD, Wallace KK, Digate R, Patton S, Banavali N, Schuler G, Speedie MK *et al*: **Cloning and characterization of the gene**

- encoding 1-cyclohexenylcarbonyl coenzyme A reductase from *Streptomyces collinus*.** *J Bacteriol* 1996, **178**(23):6873-6881.
116. Chen S, von Bamberg D, Hale V, Breuer M, Hardt B, Muller R, Floss HG, Reynolds KA, Leistner E: **Biosynthesis of ansatrienin (mycotrienin) and naphthomycin - Identification and analysis of two separate biosynthetic gene clusters in *Streptomyces collinus* Tu 1892.** *European Journal of Biochemistry* 1999, **261**(1):98-107.
 117. Ostash B, Saghatelian A, Walker S: **A streamlined metabolic pathway for the biosynthesis of moenomycin A.** *Chem Biol* 2007, **14**(3):257-267.
 118. Astner I, Schulze JO, van den Heuvel J, Jahn D, Schubert WD, Heinz DW: **Crystal structure of 5-aminolevulinate synthase, the first enzyme of heme biosynthesis, and its link to XLSA in humans.** *EMBO Journal* 2005, **24**(18):3166-3177.
 119. Gerber R, Lou LL, Du LC: **A PLP-dependent polyketide chain releasing mechanism in the biosynthesis of mycotoxin fumonisins in *Fusarium verticillioides*.** *J Am Chem Soc* 2009, **131**(9):3148-3149.
 120. Hanada K: **Serine palmitoyltransferase, a key enzyme of sphingolipid metabolism.** *Biochimica Et Biophysica Acta-Molecular and Cell Biology of Lipids* 2003, **1632**(1-2):16-30.
 121. Webster SP, Alexeev D, Campodiano DJ, Watt RM, Alexeeva M, Sawyer L, Baxter RL: **Mechanism of 8-amino-7-oxononanoate synthase: Spectroscopic, kinetic, and crystallographic studies.** *Biochemistry* 2000, **39**(3):516-528.
 122. Galm U, Schimana J, Fiedler HP, Schmidt J, Li SM, Heide L: **Cloning and analysis of the simocyclinone biosynthetic gene cluster of *Streptomyces antibioticus* TO 6040.** *Archives of Microbiology* 2002, **178**(2):102-114.
 123. Pacholec M, Meyers CLF, Oberthur M, Kahne D, Walsh CT: **Characterization of the aminocoumarin ligase SimL from the simocyclinone pathway and tandem incubation with NovM,P,N from the novobiocin pathway.** *Biochemistry* 2005, **44**(12):4949-4956.
 124. Steffensky M, Li SM, Heide L: **Cloning, overexpression, and purification of novobiocic acid synthetase from *Streptomyces spheroides* NCIMB 11891.** *J Biol Chem* 2000, **275**(28):21754-21760.
 125. Grote R, Zeeck A, Drautz H, Zahner H: **Metabolic products of microorganisms .246. 2880-II, a metabolite related to ferulic acid from *Streptomyces Griseoflavus*.** *J Antibiot* 1988, **41**(9):1275-1276.
 126. Cole LJ, Gatti DL, Entsch B, Ballou DP: **Removal of a methyl group causes global changes in *p*-hydroxybenzoate hydroxylase.** *Biochemistry* 2005, **44**(22):8047-8058.

127. Entsch B, Vanberkel WJH: **Flavoprotein structure and mechanism .1. Structure and mechanism of para-hydroxybenzoate hydroxylase.** *FASEB Journal* 1995, **9**(7):476-483.
128. Entsch B, Cole LJ, Ballou DP: **Protein dynamics and electrostatics in the function of p-hydroxybenzoate hydroxylase.** *Archives of Biochemistry and Biophysics* 2005, **433**(1):297-311.
129. Kirchner U, Westphal AH, Muller R, van Berkel WJH: **Phenol hydroxylase from *Bacillus thermoglucosidasius* A7, a two-protein component monooxygenase with a dual role for FAD.** *J Biol Chem* 2003, **278**(48):47545-47553.
130. van der Werf MJ, Swarts HJ, de Bont JAM: ***Rhodococcus erythropolis* DCL14 contains a novel degradation pathway for limonene.** *Applied and Environmental Microbiology* 1999, **65**(5):2092-2102.
131. Redenbach M, Ikeda K, Yamasaki M, Kinashi H: **Cloning and physical mapping of the EcoRI fragments of the giant linear plasmid SCP1.** *J Bacteriol* 1998, **180**(10):2796-2799.
132. Hornemann U, Hopwood DA: **Isolation and characterization of desepoxy-4,5-didehydro-methylenomycin-A, precursor of antibiotic methylenomycin-A in Scp1+ strains of *Streptomyces Coelicolor* A3(2).** *Tetrahedron Lett* 1978(33):2977-2978.
133. Weissman KJ: **Polyketide biosynthesis: understanding and exploiting modularity.** *Philos Transact A Math Phys Eng Sci* 2004, **362**(1825):2671-2690.
134. Roongsawang N, Washio K, Morikawa M: **In vivo characterization of tandem C-terminal thioesterase domains in arthrofactin synthetase.** *Chembiochem* 2007, **8**(5):501-512.
135. Hutchinson CR: **Polyketide and non-ribosomal peptide synthases: falling together by coming apart.** *Proc Natl Acad Sci U S A* 2003, **100**(6):3010-3012.
136. Heathcote ML, Staunton J, Leadlay PF: **Role of type II thioesterases: evidence for removal of short acyl chains produced by aberrant decarboxylation of chain extender units.** *Chem Biol* 2001, **8**(2):207-220.
137. Schwarzer D, Mootz HD, Linne U, Marahiel MA: **Regeneration of misprimed nonribosomal peptide synthetases by type II thioesterases.** *Proc Natl Acad Sci U S A* 2002, **99**(22):14083-14088.
138. Yeh E, Kohli RM, Bruner SD, Walsh CT: **Type II thioesterase restores activity of a NRPS module stalled with an aminoacyl-S-enzyme that cannot be elongated.** *Chembiochem* 2004, **5**(9):1290-1293.

139. Linne U, Schwarzer D, Schroeder GN, Marahiel MA: **Mutational analysis of a type II thioesterase associated with nonribosomal peptide synthesis.** *Eur J Biochem* 2004, **271**(8):1536-1545.
140. Koglin A, Lohr F, Bernhard F, Rogov VV, Frueh DP, Strieter ER, Mofid MR, Guntert P, Wagner G, Walsh CT *et al*: **Structural basis for the selectivity of the external thioesterase of the surfactin synthetase.** *Nature* 2008, **454**(7206):907-911.
141. Kotowska M, Pawlik K, Smulczyk-Krawczyszyn A, Bartosz-Bechowski H, Kuczek K: **Type II Thioesterase ScoT, Associated with Streptomyces coelicolor A3(2) Modular Polyketide Synthase Cpk, Hydrolyzes Acyl Residues and Has a Preference for Propionate.** *Applied and Environmental Microbiology* 2009, **75**(4):887-896.
142. Kim BS, Cropp TA, Beck BJ, Sherman DH, Reynolds KA: **Biochemical evidence for an editing role of thioesterase II in the biosynthesis of the polyketide pikromycin.** *J Biol Chem* 2002, **277**(50):48028-48034.
143. Meiser P, Weissman KJ, Bode HB, Krug D, Dickschat JS, Sandmann A, Muller R: **DKxanthene biosynthesis - Understanding the basis for diversity-oriented secondary metabolism.** *Chem Biol* 2008, **15**(8):771-781.
144. Christiansen G, Molitor C, Philmus B, Kurmayer R: **Nontoxic strains of cyanobacteria are the result of major gene deletion events induced by a transposable element.** *Molecular Biology and Evolution* 2008, **25**(8):1695-1704.
145. Chen H, Hubbard BK, O'Connor SE, Walsh CT: **Formation of beta-hydroxy histidine in the biosynthesis of nikkomycin antibiotics.** *Chem Biol* 2002, **9**(1):103-112.
146. Song F, Zhuang ZH, Finci L, Dunaway-Mariano D, Kniewel R, Buglino JA, Solorzano V, Wu J, Lima CD: **Structure, function, and mechanism of the phenylacetate pathway hot dog-fold thioesterase PaaI.** *J Biol Chem* 2006, **281**(16):11028-11038.
147. Kotaka M, Kong R, Qureshi I, Ho QS, Sun HH, Liew CW, Goh LP, Cheung P, Mu YG, Lescar J *et al*: **Structure and catalytic mechanism of the thioesterase CalE7 in enediynes biosynthesis.** *J Biol Chem* 2009, **284**(23):15739-15749.
148. Claxton HB, Akey DL, Silver MK, Admiraal SJ, Smith JL: **Structure and functional analysis of RifR, the type II thioesterase from the rifamycin biosynthetic pathway.** *J Biol Chem* 2009, **284**(8):5021-5029.
149. Lai JR, Koglin A, Walsh CT: **Carrier protein structure and recognition in polyketide and nonribosomal peptide biosynthesis.** *Biochemistry* 2006, **45**(50):14869-14879.
150. Nasser W, Reverchon S: **New insights into the regulatory mechanisms of the LuxR family of quorum sensing regulators.** *Analytical and Bioanalytical Chemistry* 2007, **387**(2):381-390.

151. Ramos JL, Martinez-Bueno M, Molina-Henares AJ, Teran W, Watanabe K, Zhang XD, Gallegos MT, Brennan R, Tobes R: **The TetR family of transcriptional repressors.** *Microbiology and Molecular Biology Reviews* 2005, **69**(2):326-356.
152. Groban ES, Clarke EJ, Salis HM, Miller SM, Voigt CA: **Kinetic buffering of cross talk between bacterial two-component sensors.** *Journal of Molecular Biology* 2009, **390**(3):380-393.
153. Kitani S, Iida A, Izumi TA, Maeda A, Yamada Y, Nihira T: **Identification of genes involved in the butyrolactone autoregulator cascade that modulates secondary metabolism in *Streptomyces lavendulae* FRI-5.** *Gene* 2008, **425**(1-2):9-16.
154. Simbahan J, Drijber R, Blum P: ***Alicyclobacillus vulcanalis* sp nov., a thermophilic, acidophilic bacterium isolated from Coso Hot Springs, California, USA.** *International Journal of Systematic and Evolutionary Microbiology* 2004, **54**:1703-1707.
155. Galm U, Dessoy MA, Schmidt J, Wessjohann LA, Heide L: **In vitro and in vivo production of new aminocoumarins by a combined biochemical, genetic, and synthetic approach.** *Chem Biol* 2004, **11**(2):173-183.
156. Liyanage H, Penfold C, Turner J, Bender CL: **Sequence, expression and transcriptional analysis of the coronafacate ligase-encoding gene required for coronatine biosynthesis by *Pseudomonas syringae*.** *Gene* 1995, **153**(1):17-23.
157. Hu YD, Melville CR, Gould SJ, Floss HG: **3-Amino-4-hydroxybenzoic acid: The precursor of the C₇N unit in asukamycin and manumycin.** *J Am Chem Soc* 1997, **119**(18):4301-4302.
158. Florova G, Kazanina G, Reynolds KA: **Enzymes involved in fatty acid and polyketide biosynthesis in *Streptomyces glaucescens*: Role of FabH and FabD and their acyl carrier protein specificity.** *Biochemistry* 2002, **41**(33):10462-10471.
159. Marti T, Hu ZH, Pohl NL, Shah AN, Khosla C: **Cloning, nucleotide sequence, and heterologous expression of the biosynthetic gene cluster for R1128, a non-steroidal estrogen receptor antagonist - Insights into an unusual priming mechanism.** *J Biol Chem* 2000, **275**(43):33443-33448.
160. Gould SJ, Melville CR, Chen J: **The biosynthesis of murayaquinone, a rearranged polyketide.** *Tetrahedron* 1997, **53**(13):4561-4568.
161. Kondo K, Eguchi T, Kakinuma K, Mizoue K, Qiao YF: **Structure and biosynthesis of FD-594; a new antitumor antibiotic.** *J Antibiot (Tokyo)* 1998, **51**(3):288-295.
162. Fujiwara A, Hoshino T, Tazoe M, Fujiwara M: **Auramycins and sulfurmycins, new anthracycline antibiotics: characterization of aglycones, auramycinone and sulfurmycinone.** *J Antibiot (Tokyo)* 1981, **34**(5):608-610.

163. Kieser T, Bibb MJ, Buttner MJ, Chater KF, Hopwood DA: **Practical *Streptomyces* Genetics**. Norwich: The John Innes Foundation; 2000.
164. Shipley MM, Dillwith JW, Bowman AS, Essenberg RC, Sauer JR: **Changes in lipids of the salivary-glands of the lone star tick, *Amblyomma-Americanum* during feeding.** *Journal of Parasitology* 1993, **79**(6):834-842.
165. Chen Z, Madden RD, Dillwith JW: **Effect of precocene II on fatty acid metabolism in the pea aphid, *Acyrtosiphon pisum*, under cold stress.** *Journal of Insect Physiology* 2005, **51**(4):411-416.

APPENDIX: PERMISSIONS


**THE JOURNAL OF
BIOLOGICAL CHEMISTRY**

Institution: LOUISIANA STATE UNIV Sign In

QUICK SEARCH | Author: Keyword: Year: Vol: Page: Go [Advanced Search] [Browse the Archive]

Home | Current issue | Archive | Papers in Press | Minireviews | Classics | Reflections | Papers of the Week

Copyright Permission Policy

These guidelines apply to the reuse of articles, figures, charts and photos in the *Journal of Biological Chemistry*, *Molecular & Cellular Proteomics* and the *Journal of Lipid Research*.

For authors reusing their own material:

Authors need **NOT** contact the journal to obtain rights to reuse their own material. They are automatically granted permission to do the following:

- Reuse the article in print collections of their own writing.
- Present a work orally in its entirety.
- Use an article in a thesis and/or dissertation.
- Reproduce an article for use in the author's courses. (If the author is employed by an academic institution, that institution also may reproduce the article for teaching purposes.)
- Reuse a figure, photo and/or table in future commercial and noncommercial works.
- Post a copy of the paper in PDF that you submitted via BenchPress.
 - Only authors who published their papers under the "Author's Choice" option may post the final edited PDFs created by the publisher to their own/departmental/university Web sites.
 - All authors may link to the journal site containing the final edited PDFs created by the publisher.

Please note that authors must include the following citation when using material that appeared in an ASBMB journal:

"This research was originally published in Journal Name. Author(s). Title. *Journal Name*. Year; Vol:pp-pp. © the American Society for Biochemistry and Molecular Biology."

For other parties using material for noncommercial use:

Other parties are welcome to copy, distribute, transmit and adapt the work — at no cost and without permission — for noncommercial use as long as they attribute the work to the original source using the citation above.

Examples of noncommercial use include:

- Reproducing a figure for educational purposes, such as schoolwork or lecture presentations, with attribution.
- Appending a reprinted article to a Ph.D. dissertation, with attribution.

For other parties using material for commercial use:

Navigate to the article of interest and click the "Request Permissions" button on the middle navigation bar. (See diagram at right.) It will walk you through the steps for obtaining permission for reuse.

Services

- Email this article to a friend
- Alert me when this article is cited

This Week's Issue
 April 1, 2011, 286 (13)

 Alert me to new issues of JBC

Authors

Submit

Subscribers

Editorial Board

RSS and Email Alerts

Article Statistics

Teaching Tools

Copyright Permissions

Advertise

Contact JBC

Advertisement



JBC on the go.
 Access articles with the iPhone app.

Advertisement



VITA

Zhe Rui is the son of Guohua Bao and Burinuo Ao. He was born in Hohhot, Inner Mongolia, China, in 1984. He received his Bachelor of Science degree in biological sciences from Zhejiang University in Hangzhou, China, in July of 2006. He started his doctoral work at Louisiana State University in Baton Rouge, Louisiana, in August of 2006. Zhe Rui will graduate with the degree of Doctor of Philosophy in May, 2011.